universität
wien

# DISSERTATION

Titel der Dissertation

## Preclinical tools in PET-tracer development:

Automatisation and biopharmaceutical evaluation with special

emphasis on the adenosine $A_3$ receptor

angestrebter akademischer Grad

## Doktor der Naturwissenschaften (Dr. rer. nat.)

Verfasser:                  Mag. pharm. Daniela Ingeborg Barbara Häusler

Matrikel-Nummer:            0009336

Dissertationsgebiet:        Pharmazie (A091-449)

Betreuer:                   o.Univ.-Prof. Mag. Dr. Helmut Viernstein

Wien, am 31.03.2010

# FÜR MEINE FAMILIE

**Für meine Eltern Ingrid und Hermann, und für meine Schwester Katharina.**

Liebe Mama, lieber Papa, liebe Kathi,

danke, dass ihr immer für mich da wart und seid!

Danke, dass wir eine Familie sind!

Dank Eurer Liebe bin ich zu der geworden, die ich heute bin.

**In Liebe, eure Tochter/ deine Schwester,**

**Dani(ela)**

# DIE KUNST DER KLEINEN SCHRITTE

Ich bitte nicht um Wunder und Visionen Herr, sondern um Kraft für den Alltag.

Lehre mich die Kunst der kleinen Schritte.

Mach mich erfinderisch, um im täglichen Vielerlei rechtzeitig meine Erkenntnisse und Erfahrungen ernst zu nehmen, damit sie mir nutzen.

Schenke mir das Fingerspitzengefühl, um herauszufinden, was erstrangig und was zweitrangig ist (das Wichtigste zuerst).

Ich bitte um Kraft für Zucht und Maß, dass ich nicht durchs Leben rutsche, sondern den Tag vernünftig einteile, auf Lichtblicke und Höhepunkte achte, und wenigstens hin und wieder Zeit finde für einen kulturellen Genuss.

Lass mich erkennen, dass Träume nicht weiterhelfen, weder über die Vergangenheit noch über die Zukunft.

Hilf mir das Nächste so gut wie möglich zu tun und die jetzige Stunde als die wichtigste zu erkennen.

Bewahre mich vor dem naiven Glauben, es müsste im Leben alles glatt gehen.

Schenke mir die nüchterne Erkenntnis, dass Schwierigkeiten, Niederlagen, Misserfolge, Rückschläge eine selbstverständliche Zugabe zum Leben sind, durch die wir wachsen und reifen.

Erinnere mich daran, dass das Herz oft gegen den Verstand streikt.

Schick mir im rechten Augenblick jemand, der den Mut hat, mir die Wahrheit in Liebe zu sagen.

Ich möchte dich und die anderen immer aussprechen lassen.

Die Wahrheit sagt man sich nicht selbst, sie wird einem gesagt.

Ich weiß, dass sich viele Probleme dadurch lösen, dass man nichts tut.

Gib, dass ich warten kann.

Du weißt, wie sehr wir die Freundschaft brauchen.

Gib, dass ich diesem schönsten, schwierigsten, riskantesten und zartesten Geschenk des Lebens gewachsen bin.

Verleihe mir die nötige Phantasie, im rechten Augenblick ein Päckchen Güte, mit oder ohne Worte, an der richtigen Stelle abzugeben.

Mach aus mir einen Menschen, der einem Schiff mit Tiefgang gleicht, um auch die zu erreichen, die unten sind.

Bewahre mich vor der Angst, ich könnte das Leben versäumen.

Gib mir nicht, was ich wünsche, sondern was ich brauche.

Lehre mich die Kunst der kleinen Schritte.

*Antoine de St. Exupery (1900-1944)*

# DANKSAGUNG

Lieber **Lukas**, danke für deine Hilfsbereitschaft, die über die Grenzen eines Arbeitskollegen weit hinausgehen! Du bist nicht nur ein wunderbarer Arbeitskollege, sondern auch ein Freund für mich geworden. Ich genieße unsere Gespräche über Gott und die Welt sehr! Danke für die Ruhe, die du ausstrahlst, und, dass du mir oftmals mit kleinen Randbemerkungen so viel bewusst machst! Danke, dass ich immer zu dir kommen kann, wenn ich etwas brauche!

Liebe **Cécile**, ich danke dir dafür, dass du jeden Tag da bist und wir über alles reden, plaudern und lachen können. Danke dir für deine Unterstützung bei der neuen [$^{11}$C]DASB Studie (und der Kalibrationsgerade).Es fühlt sich gut an dich als Freundin zu haben! Danke, dass es dich gibt. Danke ganz besonders für alle spontanen Kinobesuche, lustige Aktionen (z.B.: „Gefühl des dreidimensionalen Raumes" auf der lustigen Schaukel vorm AKH erkunden usw.) und Treffen!

Liebe **Steffi**, du hast sowohl mein Arbeitsleben, als auch mein sonstiges Leben mit deinem Sein und Wesen bereichert, und bringst mich mit deiner lustigen und liebevollen Art immer wieder (ständig) zum Lachen. Es macht mir Spaß mit dir zu Plaudern, egal worüber. Danke, dass du so unglaublichen Einsatz zeigst und auch abseits deiner Diplomarbeit als Freundin (und Engel) für mich da warst und bist!

Lieber **Fritz** (Flitsch), danke für deine Hilfe bei den verschiedensten Internet-Recherchen am Anfang meiner Diss, für dein Hilfe beim „Schneiden", in der Borschkegasse und bei den Autoradiographien.

Lieber **Rupert**, danke für deine Unterstützung und für dein Interesse an dieser Arbeit!

Liebe **Lisi**, liebe **Kathi**, liebe **Sabine**, lieber **Michi**, lieber **Markus**, danke euch allen für eure Unterstützung und für euer Dasein!

Lieber **Gregor**, danke, dass du immer an mich geglaubt hast -so viel mehr als ich je an mich selbst geglaubt hab! Danke dir für deine Liebe und unermüdliche Unterstützung während der Zeit der Dissertation, in der wir zusammen waren!

-------------------------------------------------------------------------------------------------------------------

**Ich danke euch allen, dass jeder von euch auf seine Weise für mich da war und ist.**

**Danke, dass ich durch euch erkennen durfte/darf wer ich bin und wer ich sein kann.**

-------------------------------------------------------------------------------------------------------------------

# ABSTRACT

**ABSTRACT** (english)

Preclinical tools in PET-tracer development:

Automatisation and biopharmaceutical evaluation with special emphasis on the adenosine $A_3$ receptor

Positron Emission Tomography (PET) is the first choice technology for the visualization and quantification of receptors and transporters, enabling examination of e.g. neurological, psychiatric and oncological diseases on a molecular level. Therefore, new and innovative PET-radiopharmaceuticals need to be developed to get further insights into the biochemical mechanisms involved in pathological changes. PET-tracer development starts with the idea or modelling of the chemical structure of a (new) molecule with (hopefully) good binding characteristics to the desired target site. As next steps, the compound needs to be synthesized and radiolabelled with a suitable PET-nuclide. Then it has to be evaluated regarding its parameters in various preclinical experimental settings. Hence, two major tools are crucial in the development-process of new PET-tracers:

1) a fast and reliable production method –most desirable and optimal in an automated set-up, and

2) proof of tracer suitability (high affinity, high selectivity and specificity, beside low unspecific binding) through preclinical evaluation in an animal model, prior to human application.

Both aspects, the radiochemical preparation and automatisation, as well as the biopharmaceutical evaluation are presented in the thesis in 5 different manuscripts. In detail, the development and preclinical evaluation of 4 different PET-tracers ([$^{11}$C]DASB, [$^{18}$F]FE@SUPPY, [$^{18}$F]FE@SUPPY:2, and [$^{18}$F]FE@CIT) for 3 targets, the serotonin transporter (SERT), the adenosine $A_3$ receptor (A3R) and the dopamine transporter (DAT), respectively, are covered in the present thesis.

The first manuscript presents a method for a fast, reliable and fully-automated radiosynthesis of [$^{11}$C]DASB (a tracer for the imaging of the SERT in human brain in e.g. depression patients) will facilitate further clinical investigations (e.g. for the department of psychiatry and psychotherapy of the medical university of Vienna) with this tracer.

[$^{18}$F]FE@SUPPY was introduced as the first A3R PET-tracer recently. The adenosine $A_3$ receptor is expressed in high levels in tumor cells, but not in the majority of normal cells. Potential application of a tracer for the A3R will be inflammation processes, oncological diseases as solid tumors; breast-, colon-, lung-, pancreas-, prostate-, melanoma- and brain metastases, as well as ischemia (brain and heart) and neurological pathologies as glaucoma and epilepsy.

[$^{18}$F]FE@SUPPY:2, a completely new potential $^{18}$F-fluoroethylated radiotracer for the A3R, is presented in the thesis. The thesis covers the radiochemical preparation of [$^{18}$F]FE@SUPPY:2 and the automation of the radiosyntheses of both radiotracers in manuscript 2 and 3. Moreover, preclinical evaluations (affinity, selectivity, unspecific binding, biodistribution, logP, autoradiography and in-vitro and ex-vivo metabolic stability) of the two tracers were conducted, and also a comparison of these parameters are given in manuscripts 3 and 4. [$^{18}$F]FE@CIT, a potential new tracer for imaging of the DAT for e.g. Parkinson patients, was successfully further evaluated in terms of metabolic stability against CES and autoradiographic distribution on rat brain slices. The high selectivity of [$^{18}$F]FE@CIT over SERT and NET was confirmed in this study, and furthermore, it was even significantly higher than the selectivity of the well known tracers [$^{123}$I]ß-CIT and [$^{123}$I]FP-CIT. Based on these results, we aim for the future diagnostic application of [$^{18}$F]FE@CIT in humans with neurological and psychiatric diseases caused by changes in the dopaminergic system (e.g. Parkinson's disease, depression, drug abuse).

**ABSTRACT** (deutsch)

## Präklinische Aspekte in der Entwicklung von PET-Tracern:

## Automatisierung und biopharmazeutische Evaluierung mit

## Schwerpunkt auf dem Adenosin $A_3$ Rezeptor

PET (Positronen Emmissions Tomographie) ist eine innovative Technik zur Visualisierung und Quantifizierung von Rezeptoren und Transportern in-vivo und erlaubt dadurch die Untersuchung von z.B. neurologischen, psychiatrischen und onkologischen Erkrankungen auf molekularem Level. Daher ist es notwendig, (neue) PET-Radiopharmaka zu entwickeln, um nähere Einblicke in die biochemischen Mechanismen pathologischer Veränderungen zu bekommen. Die Entwicklung eines PET-Tracers beginnt mit der Idee für ein Molekül mit geeigneter chemischer Struktur und mit guten Bindungseigenschaften zum gewünschten Target. Wenn das Molekül diese Voraussetzungen erfüllt, wird es synthetisiert, und mit einem PET-Nuklid radioaktiv markiert. Dann folgen verschiedene Untersuchungen zur Evaluierung der präklinischen Parameter des Radiopharmakons. Zwei Hauptaspekte im Entwicklungsprozess von neuen Radiopharmaka sind:

1) eine einfache und verlässliche Produktionsmethode für den PET-Tracer -im Optimalfall automatisiert- als Voraussetzung für alle weiteren Schritte

2) die präklinischen Evaluierungsparameter des Tracers zur Untersuchung auf dessen Eignung für eine gewünschte humane Applikation in der Zukunft.

Beide Aspekte, die radiochemische Herstellung bzw. Automatisierung und die biopharmazeutische Evaluierung, werden im Rahmen von 5 verschiedenen Studien in dieser Doktorarbeit präsentiert. Die Entwicklung und präklinische Evaluierung von 4 verschiedenen PET-Tracern ($[^{11}C]$DASB, $[^{18}F]$FE@SUPPY, $[^{18}F]$FE@SUPPY:2, und $[^{18}F]$FE@CIT) für 3 unterschiedeliche Zielregionen: den Serontonintransporter (SERT), den Adenosin $A_3$ Rezeptor (A3R) und den Dopamintransporter (DAT), sind wie folgt beschrieben:

Die erste Studie präsentiert eine schnelle und voll-automatisierte Methode, die die verlässliche radiochemische Herstellung von $[^{11}C]$DASB (ein Tracer für das Imaging des SERT z.B. bei Depressionspatienten) für klinische Untersuchungen (z.B. für die Universitätsklinik

für Psychiatrie, Arbeitsgruppe Neuroimaging, der MedUni Wien) mit diesem Tracer in Zukunft vereinfachen wird.

[$^{18}$F]FE@SUPPY wurde kürzlich von der Arbeitsgruppe Radiopharmazeutische Wissenschaften als der erste PET-Tracer für den A3R vorgestellt. Der Adenosin A$_3$ Rezeptor, der erst vor kurzem entdeckt worden ist, wird besonders hoch in verschiedenen pathologischen Prozessen, jedoch fast nicht in Zellen von gesunden Geweben exprimiert. Mögliche Einsatzgebiete von Tracern des A3R umfassen somit Entzündungsprozesse, onkologische Gegebenheiten wie solide Tumore und Brust-, Dickdarm-, Lungen-, Pankreas-, Prostata-, Melanom- und Hirnmetastasen; Herzkrankheiten wie Ischämie, und neurologische Erkrankungen wie zerebrale Ischämie, Glaukom und Epilepsie.

[$^{18}$F]FE@SUPPY:2 ist ein ganz neues $^{18}$F-radiomarkiertes Molekül, das als zusätzlicher potentieller Radiotracer für den A3R im Rahmen der These vorgestellt wird.  In der Arbeit (in den Manuskripten 2 & 3) ist sowohl die radiochemische Herstellung von [$^{18}$F]FE@SUPPY:2, die Optimierung der Radiosynthese von [$^{18}$F]FE@SUPPY, und die Automatisierung von beiden A3R-Tracern enthalten. Weiters werden auch die präklinischen Parameter wie Affinität, Selektivität, unspezifische Bindung, Biodistribution, logP, Autoradiographien, in-vitro und ex-vivo Metabolitenstudien dieser neuen Radiopharmaka in der Arbeit (Manuskripten 3 und 4) untersucht.

Der Tracer [$^{18}$F]FE@CIT (ein potentieller Tracer für den DAT zum Imaging von z.B. Parkinson) wurde erfolgreich bezüglich seiner metabolischen Stabilität und autaradiographischen Verteilung in einem Tiermodell im Rahmen der fünften Studie evaluiert. Die hohe Selektivität von [$^{18}$F]FE@CIT gegenüber dem SERT und dem NET (Norepinephrintransporter) konnte bewiesen werden und war sogar signifikant höher als die Selektivität der etablierten Radiopharmaka [$^{123}$I]ß-CIT and [$^{123}$I]FP-CIT. Basierend auf diesen Daten, soll [$^{18}$F]FE@CIT in Zukunft zur Diagnose von neurologischen und psychiatrischen Erkrankungen des Menschen (z.B. Parkinson, Depression, Drogenmissbrauch, etc.) angewendet werden.

# TABLE OF CONTENTS

# PART 1

# INTRODUCTION

# 1. INTRODUCTION

# 1.1. RECEPTOR AND TRANSPORTER TARGETS

## 1.1.1. GENERAL ON ADENOSINE AND ITS RECEPTORS

Adenosine is an ubiquitous nucleoside consisting of the purinebase adenine and the monosaccharide ß-D-ribose (see figure 1). It is an essential component of biological molecules, as for example $NAD^+$, ATP, ADP, AMP, cAMP, Coenzyme A and nucleic acids. Therefore, adenosine and these related compounds are important for the regulation of many aspects of cellular metabolism and energy supply[1].
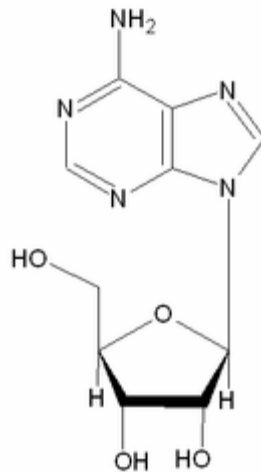


**Figure 1: Chemical structure of adenosine**

Adenosine is present in all cells and body fluids and acts on four well defined receptors, called $A_1$, $A_{2A}$, $A_{2B}$ and $A_3$, respectively (A1R, A2AR, A2B, A3R). These receptors differ in their affinity concerning adenosine, their tissure distribution and their pharmacological skills. Adenosine itself displays high affinity towards the $A_1$ and $A_{2A}$ recptors ($K_i$=10-30nM), whereas it shows only low affinity towards the $A_{2B}$ and $A_3$ receptors ($K_i$=~1µM)[2].

The adenosine receptors belong to the superfamily of G protein-coupled receptors (GPCR´s), and are located at the surface of the external cell membrane. As stated by Susan R. George in 2004, "GPCR´s are the largest family of cell-surface receptors, and transduce their signals mediated by a diverse range of signalling molecules, including ions, biogenic amines, peptides and lipids, as well as photons, to mediate alterations of intracellular function"[3].

## SIGNALTRANSDUCTION

Generally, GPCR´s can be divided into different families based on their structural and genetic characteristics. The adenosine receptors belong to the family 1, the largest subgroup within the GPCR´s, also called rhodopsin-like family.

GPCR´s induce their signals according to different G proteins, $G_s$ (stimulates the adenylatcyclasis), $G_i$ (inhibits the adenylatcyclasis), $G_q$ (activates the phospholipase C) and $G_{12/13}$ (influences ionchannels e.g. of Cl⁻), respectively[4]. Signaltransduction of GPCRs can be very complex; as shown in figure 2.
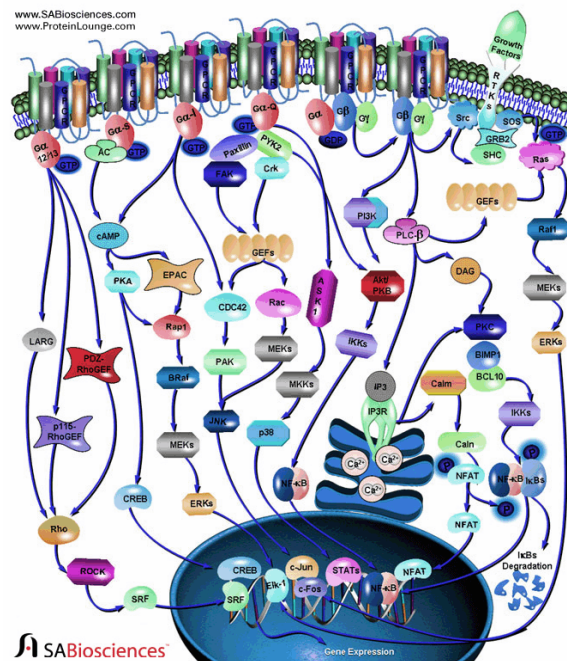


**Figure 2: Signaltransduction pathways of GPCRs**

All four adenosine receptors are monomeric proteins with seven transmembrane domains (see figure 3) and alpha helical secondary structure with approximately 21-28 amino acids in each. The extracellular domains of the receptor proteins comprise the N-terminus and three extra-cellular loops. The intracellular domains of the receptor proteins comprise a C-terminus with a palmitoylation site near the C-terminus (except of the $A_{2A}$ subtype) and three intracellular loops[5].
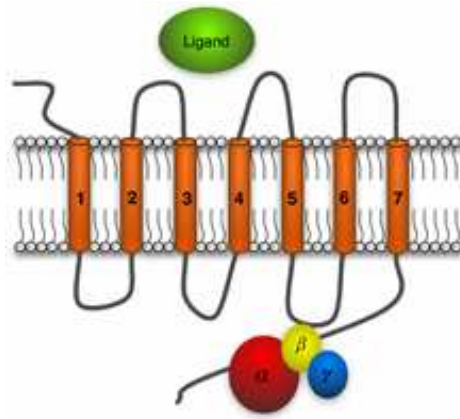


**Figure 3: Typical scheme of a GPCR with 7 transmembrane domains [6]**

As shown in figure 4, activation of the $G_i$ proteins via $A_1$ and $A_3$ receptors causes classical second-messenger pathways, such as inhibition of adenylatecyclase, resulting in inhibition of neurotransmission. Activation of the $G_s$ proteins via $A_{2A}$ and $A_{2B}$ receptors causes stimulation of adenylatecyclase activity, resulting in the stimulation of neurotransmission.



Stefano Moro[1], Giampiero Spalluto[2] and Kenneth A. Jacobson[3] *TRENDS in Pharmacological Sciences* Vol.26 No.1 January 2005
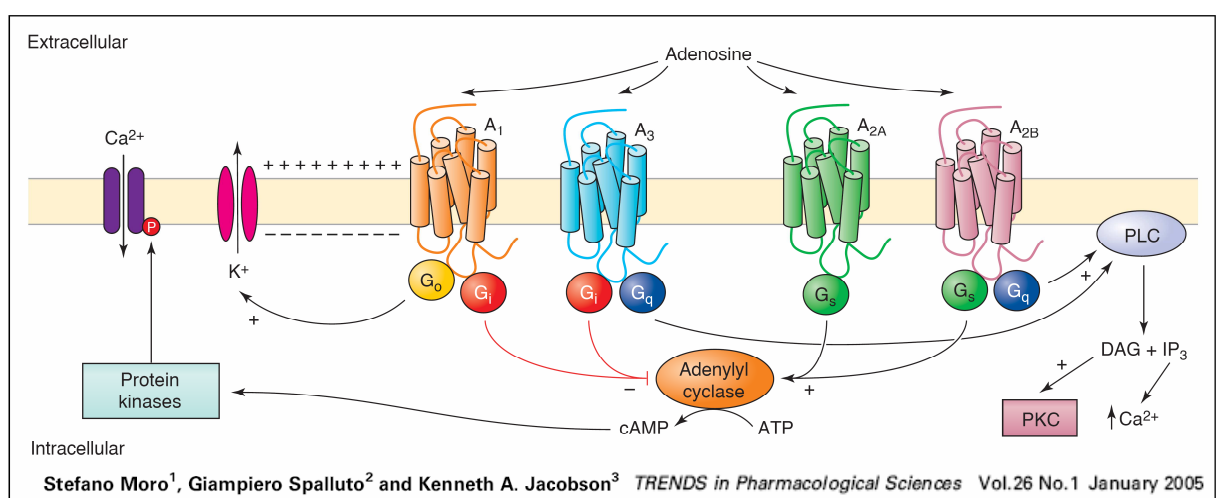
**Figure 4: Scheme of the 4 adenosine receptor subtypes ($A_1$, $A_{2A}$, $A_{2B}$, $A_3$)**

The two main sources of extracellular adenosine are its transport from the intracellular compartment via the equilibrative nucleoside transporter (ENT) and the extracellular conversion of adenosine triphosphate (ATP) by action of ectonucleotidases (EctoN) (see figure 5)[7].
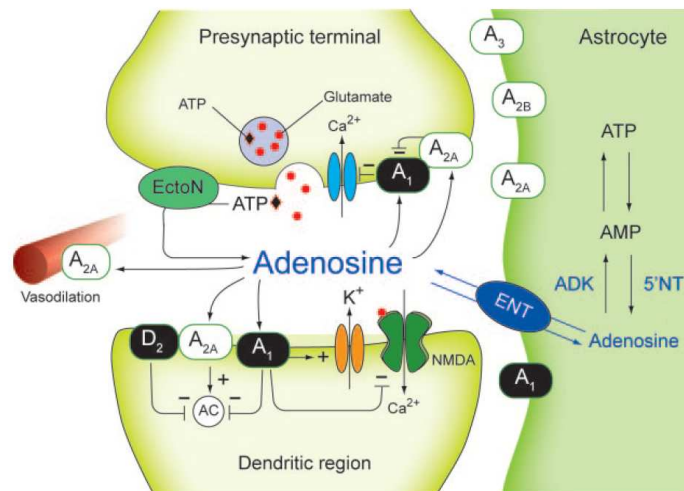


**Figure 5: Main features of adenosine signalling in the CNS**

## CLONING AND CLASSIFICATION OF THE ADENOSINE RECEPTORS

So far, all four adenosine subtypes, have been cloned from several mammalian species - including human- and some non-mammalian species (see figure 6)[8].
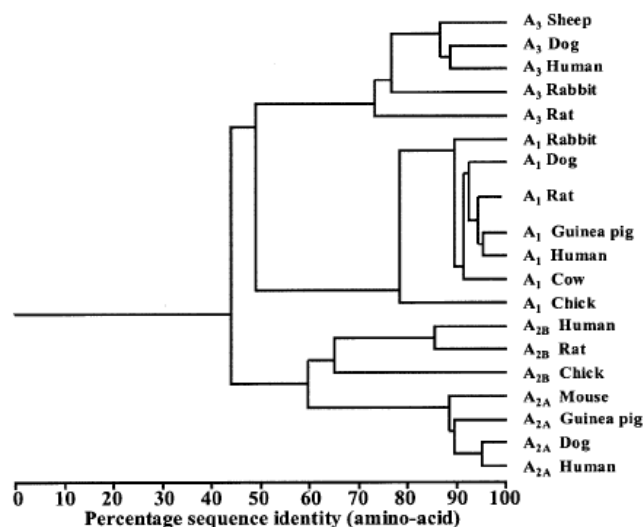


**Figure 6: Subtype based structural sequence similarity between cloned adenosine receptors[8]**

As shown in the dendrogram in figure 6, in mammals, there is a very close similarity in structure between the adenosine receptors within each sub-type. Only the adenosine $A_3$ receptor showed a large variability between the species: there is almost 30% difference of the amino acid level between the human and the rabbit A3R. This difference is in fact larger than the one between human and chick for the $A_1$ subtype[8]. Furthermore, there is also a large difference between $A_3$ receptors from different species with regard to ligand specificity[9]. Even the distribution of the $A_3$ subtype is different in man and rodents[10].

The concept of the nomenclature and classification as "adenosine receptors" precedes the later concept of purinoceptors[11,12] by Burnstock in 1978 (see figure 7). As stated and recommended by the NC-IUPHAR (=International Union of Basic and Clinical Pharmacology Committee on Receptor Nomenclature and Drug Classification) subcommittee on adenosine receptors, these receptors are nowadays named after their unique physiological ligand and agonist adenosine[13].
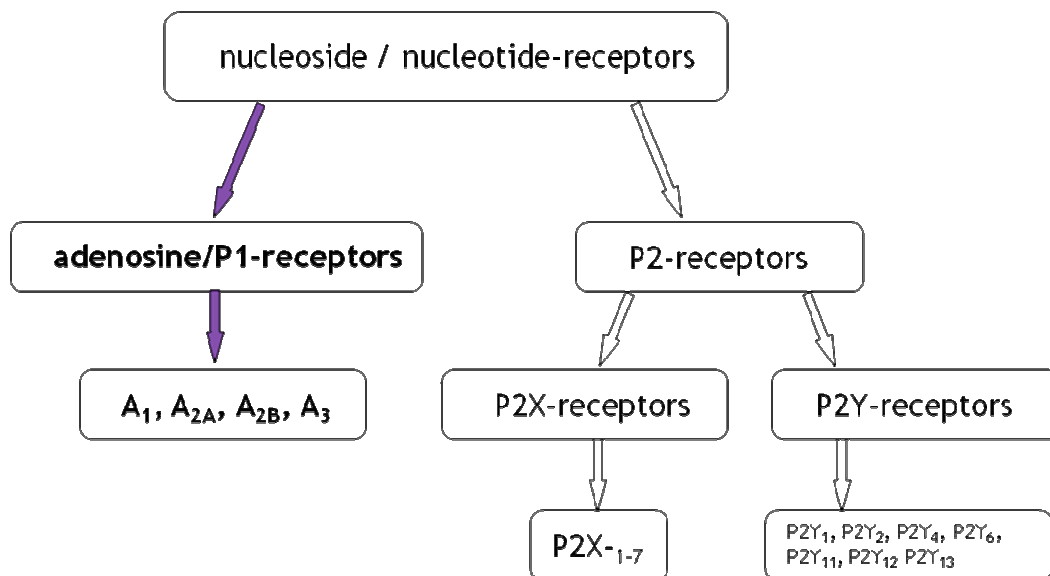


**Figure 7: Classification of the nucleoside and nucleotide receptors by G. Burnstock**

Adenosine, although often referred to as a neurotransmitter, is not a classical neurotransmitter, because it is not principally produced and released vesicularly in response of neuronal firing. Generally, it modulates many important physiologic functions within the human body, involving the heart[14] and the cardiovascular system, brain[15], kidneys, gastrointestinal-tract, lungs, inflammation and the immune system[16].

Adenosine can be found in basal levels of 100nM in the heart and of 20nM in the brain, whereas in severe ischemic stress situations it can rise to levels of a micromolar range. In detail, adenosine acts as a cytoprotective modulator in response to stress in organs or tissues, both under physiological and pathophysiological conditions[17]:

it increases the blood supply (e.g. by vasodilatation and angiogenesis), contributes to ischemic preconditioning (in the heart, brain and skeletal muscle) and suppresses inflammation (through activation and infiltration of inflammatory cells and furthermore through production of cytokines and free radicals). As a consequence, it promotes wound healing and protects tissues against ischemic damage. Moreover, it suppresses cytotoxic processes and acts as a local modulator of other neurotransmitters as glutamate and dopamine. Interestingly, the stimulating effect of the methylxanthine caffeine, which is the most widely used psychoactive drug in the world, is mainly due to its activity as an adenosine receptor antagonist[18] (see figure 8).
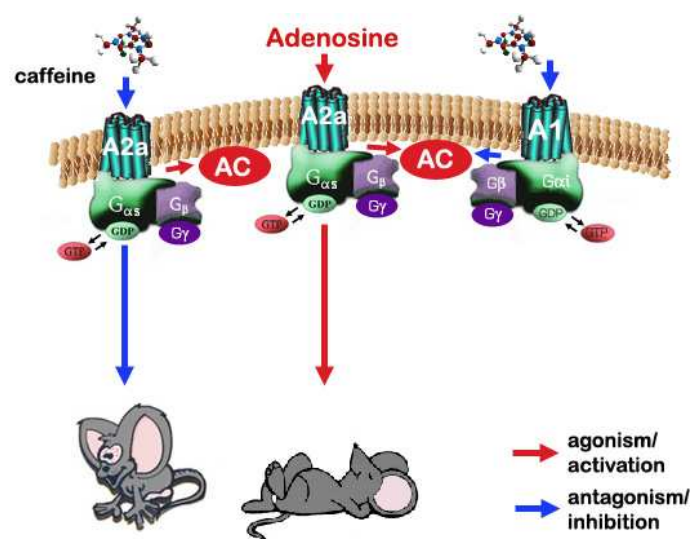


**Figure 8: Stimulating effect of caffeine[19]**

All in all, adenosine is involved in many different functions of the nervous system, e.g. it acts as an endogenous anticonvulsant, neuroprotectant and sleep-inducing factor. Adenosine is therefore one of the most important neuromodulators in the central and peripheral nervous system[20]. Therefore, therapeutic applications, both, in the central nervous system and in the periphery, are being explored for selective and affine adenosine receptor ligands.

The clinical relevance of adenosine receptor agonists and antagonists, which were already tested in humans in clinical trails, are given in the following section[17]:

Agonists for the A1R were tested in humans for cardiac arrhythmias, type 2 diabetes and angina. Antagonists of this subtype were tested in clinical trials for acute decompensated heart failure with renal impairment, cystic fibrosis and asthma. Positron emission tomography (PET)-ligands ([$^{18}$F]CPFPX and [$^{11}$C]MPDX) for the A1R are used for brain visualization to gain insights into sleeping disorders and neurodegenerative disorders as Parkinsons disease (PD). Agonists for the A2AR were tested in clinical trials for myocardial perfusion imaging and wound healing; antagonists are in phase 2 testing for PD. PET-ligands for the visualization of the $A_{2A}$ receptors in brain ([$^{11}$C]TMSX and [$^{11}$C]KW-6002) were used to gain insights in PD, psychiatric disorders and (maybe) drug addiction. An antagonist for the A2BR was tested in humans with asthma. A3R agonists were in clinical trials for rheumatoid arthritis, dry eye syndrome, psoriasis, liver cancer, hepatitis and liver regeneration. A3R antagonists were tested for glaucoma treatment, cancer, stroke and inflammation. Some A3R antagonists are in biological testing as therapeutic targets for asthma, COPD, glaucoma, cancer and stroke treatment. The first PET-ligand of the A3R ([$^{18}$F]FE@SUPPY) will be presented more detailed in the following chapter and in the scientific topic section in paper 2, 3 and 4. Adenosine itself, which is quite short-lived in circulation, is used in clinical treatment of paroxysmal supraventricular tachycardia and in radionuclide myocardial perfusion imaging[21].

Figure 9 summarizes the most important –so far known- pharmacological effects of the 4 adenosine receptor subtypes in the human body.

In conclusion, adenosine receptors are widespread on virtually every organ and tissue and according to all the mentioned actions of them, they represent promising drug targets for pharmacological intervention in many patho-physiological conditions that are believed to be

associated with changes of adenosine levels such as asthma, neurodegenerative disorders, psychosis and anxiety, chronic inflammatory diseases, and cancer[22].

This short overview shows the need for suitable pharmacological substances for the further exploration in the field of adenosine and its receptors.



**Antagonists**

$A_1AR$ — cognitive disease
$A_{2A}AR$ — neurodegeneration, Parkinson's disease, Huntington's disease, migraine
$A_3AR$ — glaucoma

$A_{2B}AR$ and $A_3AR$ — asthma

$A_{2B}AR$ — diabetes
$A_1AR$ — oedema
$A_3AR$ — renal failure
$A_{2B}AR$ — diarrhoea

**Agonists**

$A_{2A}AR$ — sleep disorder
$A_1AR$ — stroke, epilepsy, migraine
$A_3AR$ — stroke

$A_1AR$ — pain

$A_{2A}AR$ — respiratory disorders
$A_3AR$ — lung injury

$A_1AR$ — cardiac ischaemia, arrhythmia
$A_{2A}AR$ — diagnostic, reperfusion injury, thrombosis, hypertension
$A_3AR$ — cardiac ischaemia

$A_{2A}AR$ — kidney ischaemia

$A_3AR$ — cancer

$A_{2A}AR$ and $A_3AR$ — rheumatoid arthritis

$A_{2A}AR$ — inflammation

$A_{2A}AR$ — wound healing, sepsis, sepsis syndrome

**Figure 9: Overview over the pharmacological relevance of the adenosine receptors[22].**

K.A. Jacobson stated pointedly "It is hoped that new agents in development will avoid the undesirable sideffects that have impeded the clinical development of adenosine receptor ligands in the past. Selective agonists are well advanced in clinical trials for the treatment of atrial fibrillation, pain, neuropathy, pulmonary and other inflammatory conditions, and cancer. Selective antagonists have entered clinical trials for the treatment of Parkinson´s disease and congestive heart failure. Both, in the case of diseases such as stroke, where there is an unmet need, and for diseases that already have pharmacological intervention options, the introduction of adenosine-based drug therapy will provide novel mechanisms for therapy"[22].

# 1.1.2. ADENOSINE A$_3$ RECEPTOR

## CLONING, DISTRIBUTION AND GENOMIC STRUCTURE

The adenosine A$_1$ and A$_{2A}$ receptors have been known for a very long time, whereas the adenosine A$_3$ receptor was discovered recently. It was originally isolated as an orphan receptor from rat testis in 1991[23]. Further clones were obtained from rat striata, sheep hypophysial pars tuberalis and human striatum and heart[24,25,26]. cDNA sequences of the other adenosine receptor subtypes are highly similar between rat and human. As mentioned before, the A3R shows large interspecies differences in its structure. Rat A3Rs reveal only 72% sequence homology with that of human and sheep. Interestingly, between sheep and human there is 85% homology. Therefore, different pharmacological profiles, especially in antagonist binding have to be expected and kept in mind. Furthermore, peripheral A3R mRNA expression is similar between human and sheep, but not between human and rat. Generally, A$_3$ receptors have been identified and sequenced in testes, brain, lung, liver, kidney, and heart of various species, including mouse, rat and human[27].

In detail, distribution patterns of the A3R mRNA were found as following: in rat (testes, lung, kidneys, heart and brain), sheep (lung, spleen, pars tuberalis, pineal gland) and human (high amounts in lung and liver, moderate amounts in heart, kidney, placenta and brain).

The gene which encodes the human A$_3$ subtype is called ADORA3 and is located on the chromosome 1 in the location 1p13.3[27,28] (see figures 10 and 11) and constists of 318 amino acid residues. The genomic structure seems to be similar for all human adenosine receptors.
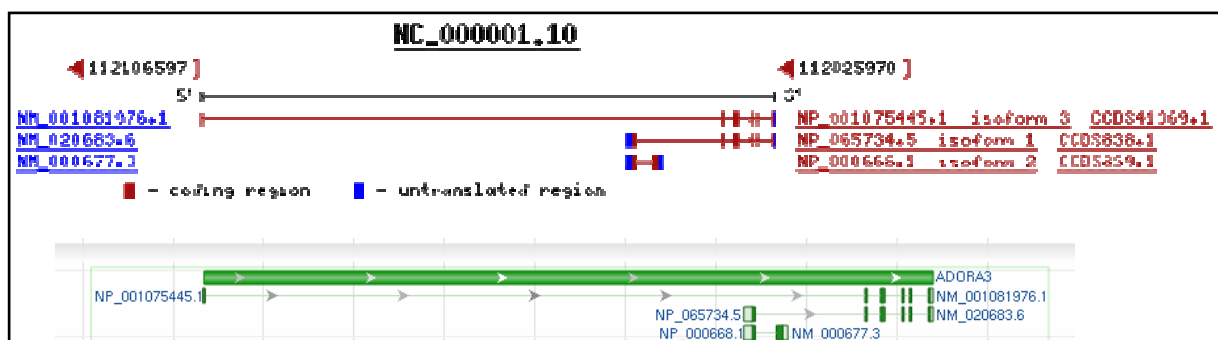


**Figure 10: Genomic regions of the human A$_3$ receptor: Homo sapiens chromosome 1, GRCh37 primary reference assembly[29]**
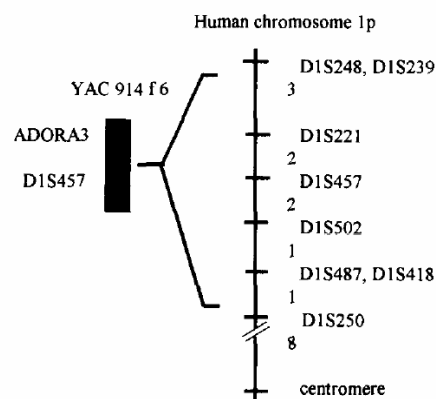
**Figure 11: Genetic linkage map of part of human chromosome 1p from 8 to 17 cM distal from centromere**[27]


## PHARMACOLOGICAL AND THERAPEUTIC RELEVANCE

Signalling pathways of the A3R include, for example, inhibition of adenylatsyclasis and PKA, and, stimulation of PLC, $IP_3$, $Ca^{++}$, $K_{ATP}$ (heart), RhoA, PLD, MAK-activity, ERK1/2. Therefore, it is important to be aware of the fact, that several intracellular mechanisms are involved in the A3R stimulation, which is important for explaining all the different aspects of its actions and functions:

The A3R is highly expressed on the cell surface of tumor cells[30, 31, 32, 33, 34, 35] and in human enteric neurons[36], but not in the majority of normal tissues[37]. In addition, A3R protein expression was studied in fresh tumors and was correlated with that of the adjacent normal tissue. The authors concluded, that primary and metastatic tumor tissues highly express A3R indicating that high receptor expression is a characteristic of solid tumors. These findings suggest the A3R as a potential target for tumor growth inhibition and imaging.

The A3Rs are known to be involved in many other diseases, such as cardiac[38] and cerebral ischemia[39], glaucoma[40], stroke[41] and epilepsy[42]. Western blot analysis showed that $A_3$ receptors are present in rat hippocampal nerve terminal membranes[43] and it has been shown, that the A3R plays a role in the brain neurotransmitter system by directly influencing for instance serotonin[44, 45, 46], dopamine[47] or glutamate[48].

Furthermore, the A3R plays a critical role in the modulation of inflammatory and autoimmune pathologies. At the present, A3R compounds are used in brain and heart

23

ischemia, asthma, sepsis, glaucoma and rheumatoid arthritis. An overview of the various different roles of the A3R in the human body is given in figure 12.
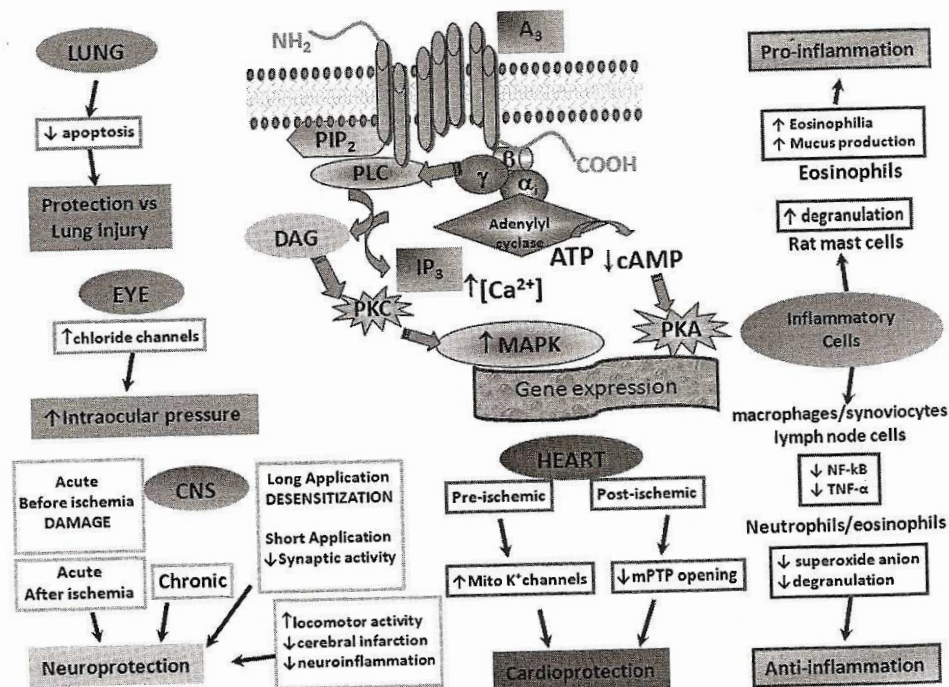


**Figure 12: Synopsis of the different actions of the A3R in the human body**

In conclusion, molecular in-vivo visualization and quantification of the A3R in the human brain, as well as in periphery, would be very attractive and important according to all the above mentioned roles of the A3R in disease conditions and its therapeutic potential.

Interestingly, some A3R antagonists have been patented concerning tumor growth, treatment of cardiac hypoxia, allergic diseases, cerebral ischemia, cancers with high concentrations of the A3R. Other papants concern their use for cognitive disorders, multiple sclerosis, neurodegeneration, PD, stroke, traumatic brain injury, asthma, COPD, glaucoma and arthritis[49].

## RADIOLABELLED LIGANDS FOR THE A3R

Although the number of synthesized A3R ligands, both, agonists and antagonists with different pharmacological characteristics is increasing, the availability of highly potent and selective ligands is not yet satisfactory. In addition, regarding radiolabelled ligands for the A3R, there is still a great need for further investigations.

### Radiolabelled agonists for the A3R

The main number of agonist radioligands for the adenosine $A_3$ receptors are tritiated compounds, which are used for preclinical testings in cell-lines or animal models. The two commercially available agonist radioligands for the A3R are [$^3$H]-NECA and [$^{125}$I]AB-MECA. [$^3$H]-NECA is quite unspecific and only useful if no other subtypes of the adenosine receptors are present. The second radiolabeled agonist, [$^{125}$I]AB-MECA, displays high affinity towards the A3R and its high specific radioactivity allows the detection of even low levels of the adenosine $A_3$ receptors. However, the latter mentioned radioligand displays also significant affninity at the adenosine $A_1$ receptors[50], which makes it only useful for imaging of the $A_3$ receptor in experiments when the other subtypes (especially the $A_1$) are blocked or not available.

### Radiolabelled antagonists for the A3R

The advantage of antagonist radioligands over agonist radioligands is, that they label all receptors present in the cell membrane, independently of the activation state and the coupling to G-proteins. Therefore, they are preferable for the use of the determination of receptor density and other information about the target receptor. One major drawback concerning most of the so far available and developed antagonists for the adenosine $A_3$ receptors is their high lipophilicity and, thus, tendency for nonspecific binding. Natural antagonists such as the methylxanthines caffeine and theophylline show generally low affnitiy for the A3 subtype. Concerning the chemistry of A3R antagonists, xanthines, 1,4-dihydropyridines, pyridines, pyrazolo-triazolo-pyrimidines, isoquinoline and quinazoline urea analogues have been developed. For a long time, there was no antagonist radioligand available for the A3R at all. In 2000, the compound MRE3008F20 was introduced as a tritiated compound[51].

The Jacobson group published a series of A3R antagonists[52], one amongst them was compound Nr. 7, displaying high affinity (Ki=4.2nM) and selectivity (rA1/hA3= 2700) towards the human A3R. Since this compound comprised a fluoroethylester function, it was obvious that our group chose this compound for radiolabelling with F-18. Hence, in 2008, the first PET-tracer for the A3R, [$^{18}$F]FE@SUPPY, was introduced by our group[53].

In the meantime, [76Br]-4´truncated nucleoside compounds were developed as A3R PET-tracers by Dale Kisewetter and his coworkers. Compound Nr. 4 (MRS 3581) was introduced as an A3R agonist and compound Nr. 6 (MRS 5147) was introduced as an A3R antagonist. Binding studies were conducted, and, as the authors state, 60-70% of total binding was A3 specific. Furthermore, in-vitro metabolism in hepatocytes, in vitro tissue binding (on rat brain and testis slices) and biodistribution in rats has been conducted.

## [18F]FE@SUPPY

[18F]FE@SUPPY, (5-(2-[18F]fluoroethyl)2,4-diethyl-3-(ethylsulfanylcarbonyl)-6-phenylpyridine-5-carboxylate), is a pentasubstituted pyridine-derivative comprising two ester functions (one carboxylic and one thiocarboxylic), with the F-18 label on the carboxylic ester function (see figure 13).
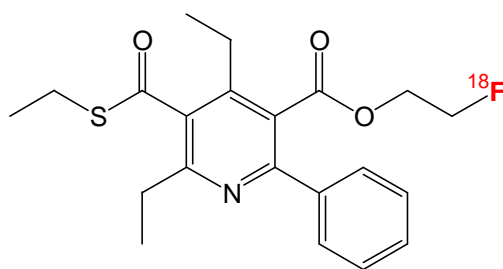


**Figure 13: Chemical structure of [18F]FE@SUPPY**

Since, the radiochemical preparation of [18F]FE@SUPPY was introduced in 2008, first bioevaluation studies have been conducted with this molecule[54]. Prior to the potential future application of [18F]FE@SUPPY in humans, further preclinical evaluations have to be performed to prove tracer safety. Moreover, the automatisation of the radiochemical preparation, to guarantee routine preparation of this tracer for these evaluations was conducted. Both, the automation and further preclinical evaluations are presented in detail in the papers 3 and 4 in the scientific topic section.

Based on the high affinity of [$^{18}$F]FE@SUPPY for the A3R, and the knowledge, that pharmaceuticals often improve their chemical characteristics through allosteric changes, we developed the counterpart [$^{18}$F]FE@SUPPY:2 (5-ethyl 2,4-diethyl-3-((2-[$^{18}$F]flourethyl)sulfanylcarbonyl)-6-phenylpyridine-5-carboxylate) as an additional potential ligand for the A3R. [$^{18}$F]FE@SUPPY:2 is a pyridine-derivative with the F-18 label on the thioester moiety (see figure 14), and should also display characteristics as an A3R antagonist. It could therefore display a comparable or even improved affinity, blood-brain-barrier permeability, selectivity and/or stability.
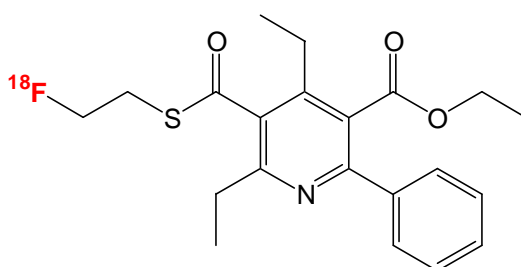


**Figure 14: Chemical structure of [$^{18}$F]FE@SUPPY:2**

The radiosynthesis of [$^{18}$F]FE@SUPPY:2 is described in detail in paper 2, and the automatisation of the radiochemical preparation is presented in paper 3 in the specific topic section. Results concerning first preclinical evaluations of [$^{18}$F]FE@SUPPY:2 are given in papers 3 and 4.

# 1.1.3. DOPAMINE TRANSPORTER

## GENERAL

Dopamine (see figure 15) is biosynthesized from tyrosine with the rate-limiting step, being catalysed by tyrosine hydroxylase. Then, it is packaged into synaptic vesicels, and released into the synaptic space on nerve firing. There, it can activate postsynaptic receptors ($D_{1-5}$) or presynaptic dopamine autoreceptors. Dopamine receptors are GPCR´s that either increase ($D_1$, $D_5$) or inhibit ($D_{2,3,4}$) the activity of adenylyl cyclase. The dopamine transporter (DAT) regulates the dopamine concentration in the synaptic cleft through reuptake of dopamine into presynaptic neurons. Therefore, it plays a central role in the spatial and temporal buffering of the released dopamine.
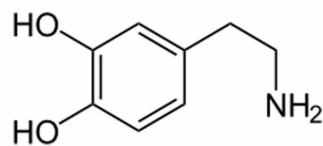


**Figure 15: Chemical structure of dopamine**

The DAT was first described more than 30 years ago, and is composed of 12 transmembrane spanning regions with the carboxyl and amino termini residing intracellularly (see figure 16). The gene of the human DAT is located on chromosome 5 at the region 5p15.3. The DAT belongs to the neurotransmitter/sodium symporter family (NSS, solute carrier 6) together with the closely related monoamine transporters SERT (serotonin transporter) and NET (norepinephrin transporter)[55]. The DAT is located on the plasma membrane of nerve terminals in a small number of neurons in the brain, especially in the axonal membranes of nigrostriatal dopaminergic neurons and nucleus accumbens, but can also be found in the globus pallidus, cingulate cortex, olfactory tubercle, amygdale and midbrain.
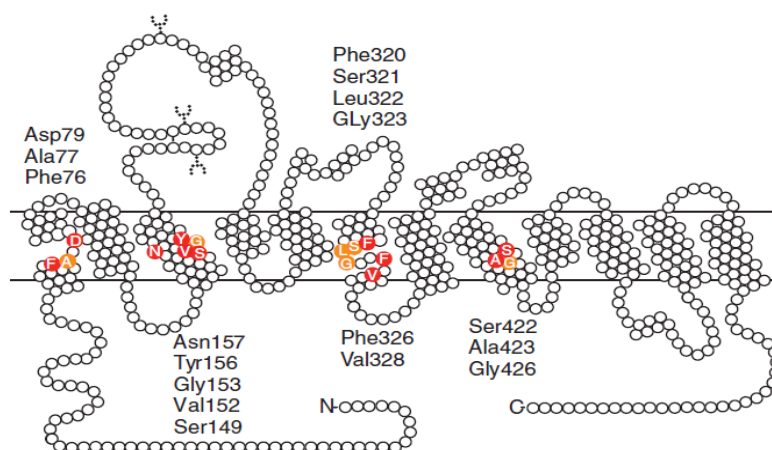
**Figure 16: schematic representation of the human dopamine transporter[55]**

Physiologically, the DAT displays vital influence on dopamine function by modulating locomotor activity, cognition and the reward system. From a pharmacological point of view, is serves as a binding site of stimulants and drugs (e.g. amphetamine and cocaine). Hence, the density of this transporter can be used as a marker for dopamine terminal innervation[56].

In contrast to the early developing status of the A3R-concept, great efforts have been taken over the past decades, towards the investigation of suitable DAT imaging agents and radiotracers:

Quantitative neuroimaging of the dopamine transporter is a state-of-the-art method to evaluate changes of presynaptic DAT expression and occupancy in neurological and psychiatric diseases using SPECT or PET. Striatal dopamine transporter density is frequently used as a specific marker of dopaminergic degeneration in patients suffering from Parkinson's disease[57,58,59]. Changes of DAT binding potential have been found in depression [60] and drug abuse including cocaine[61,62,63,64], alcohol[65] and methylphenidate[66]. Therefore, the measurement of DAT binding potential has been used in various fields of drug research[67,68]. In addition, alterations of the DAT can be associated with neurodegenerative and neuropsychiatric disorders, including attention deficit-hyperactivity disorder, Huntington´s chorea and schizophrenia. Therefore, the development and evaluation of ameliorated DAT ligands is of great practical relevance for neuroimaging of neurological and psychiatric disorders.

Radiolabelled cocaine analogues based on ß-CIT have proven undisputable for the imaging of the dopamine transporter[69,70,71,72,73,74,75]. Among these, the so called WIN-compounds exhibit a 2-200-fold higher affinity for the DAT than cocaine. Some of these compounds have been labeled with carbon-11 or fluorine-18, and were used for positron emission tomography. However, further improvements in their pharmacodynamic and pharmacokinetic features were aimed for. An important improvement, yielding in a 1.5 times higher affinity to the dopamine transporter, a 10 fold increased selectivity DAT over SERT and a 59 times increased selectivity DAT over NET[72], was achieved by a simple replacement of the carboxylic methyl ester group in ß-CIT by a fluoroethyl ester[73].

Looking at the metabolic pattern of ß-CIT and methylester-analogues, enzymatic ester cleavage appears to be the major degradation route[76,77,78]. There is evidence for a higher metabolic stability of esters when the alkyl-rest was replaced by a fluoroalkyl-chain[79,80]. Furthermore, ester cleavage results in a non-radioactive tropane acid compound and 2-[$^{18}$F]fluoroethanol as the only labelled metabolite, which is washed out of the brain and cleared hepatobiliary. Therefore, no disturbing interaction of radioactive metabolites is concluded in neuroimaging with the compound called [$^{18}$F]FE@CIT (2-[$^{18}$F]fluoroethyl 3ß-(4-iodophenyl)tropane 2ß-carboxylate) (see figure 17).

The successful radiochemical preparation and biodistribution of this tracer was presented by our group in 2005[81]. Since the results of the first studies with this tracer were successfull and promising, further evaluations were performed, and will be given in detail in paper 5 in the scientific topic section.
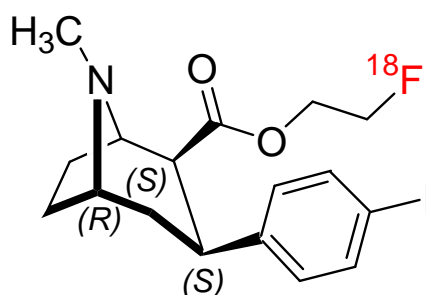


**Figure 17: Chemical structure of [$^{18}$F]FE@CIT**

A further cocaine-derivative, N-(3-iodopro-2E-enyl)-2-beta-carbomethoxy-3beta-(4`-methylphenyl)nortropane (PE2I) has been proved to be a very potent radiopharmaceutical

to image the DAT. Therefore, this compound has been labelled with iodine -123 or -125, as well as with tritium and carbon-11[82]. DAT radiotracers, which are already widely used in humans, (some of them even have reached phase III or IV of clinical applications), are [$^{11}$C]cocaine, [$^{123}$I]ß-CIT, [$^{123}$I]FE-CIT, [$^{123}$I]/[$^{18}$F]/[$^{11}$C]FP-CIT, [$^{18}$F]/[$^{11}$C]CFT, [$^{123}$I]/[$^{11}$C]altropane, [$^{123}$I]/[$^{11}$C]PE2I, [$^{11}$C]methylphenidate and [$^{99m}$Tc]TRODAT-1[83],[84]. A recently presented compound [$^{123}$I]-4-(2-(bis(4-fluorophenyl)methoxy)ethyl)-1-(4-iodobenzyl)piperidine proved selective for imaging the DAT, but didn´t show sufficient brain uptake in rats due to P-gp washout, and is therefore not suitbable for in vivo DAT imaging[85].

# 1.1.4. SEROTONIN TRANSPORTER

## GENERAL

Serotonin (5-hydroxy-tryptamine, 5-HT, see figure 18) is an important modulatory neurotransmitter, and, although only about 1% of the body's serotonin is localized in the brain, serotonin has profound effects on brain function.
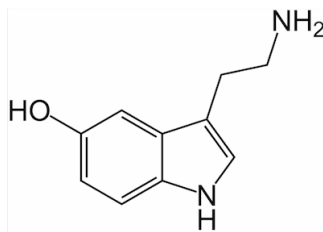


**Figure 18: Chemical structure of serotonin**

Despite serotonin's effects are complex and yet incompletely understood, alterations of the serotonergic expression have been frequently shown in psychiatric and neurological diseases such as depression, anxiety disorders, attention deficit hyperactivity disorder (ADHD), Alzheimer's disease (AD) and epilepsy. Following the release of 5-HT, a portion is re-uptaken by the presynaptic serotonergic neuron in a manner similar to that of the reuptake of dopamine or norepinephrine: it makes use of a specific transporter protein, called serotonin transporter (SERT, 5-HTT). The function of serotonin is exerted upon its interaction with specific receptors. More than 20 serotonin receptor subtypes have been identified as $5HT_{1A}$-$5HT_7$. Most of these receptors are coupled to G-proteins that affect the activities of either adenylate cyclase or phospholipase C, while the $5HT_3$ belongs to the class of ion-channels. Some serotonin receptors are predominantly expressed presynaptically and others postsynaptically[86].

The serotonin transporter is a monoamine transporter protein with 12 transmembrane segments, 5 extracellular and 5 intracellular loops. As evident from figure 19, both, the amino, and the carboxyterminal tail are located intracellularly.
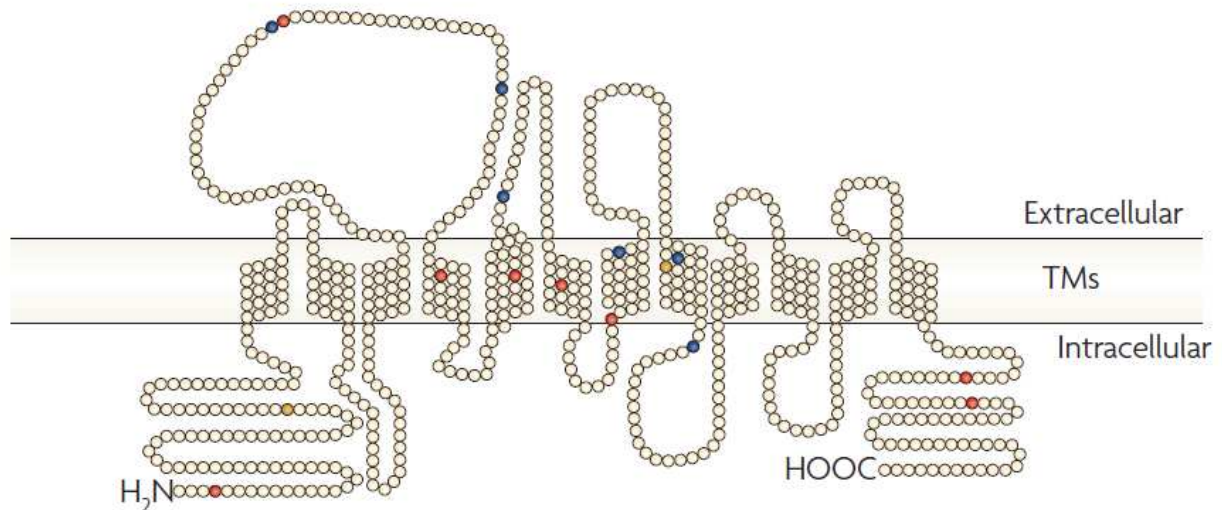
**Figure 19: Schematic picture of the SERT protein[87].**

The serotonergic neurotransmission is mainly regulated by the major inhibitory (5-HT$_{1A}$) and excitatory (5-HT$_{2A}$) serotonergic receptor subtypes and the serotonin transporter, which transports the neurotransmitter serotonin from synaptic spaces into presynaptic neurons. The transport of serotonin terminates the action of serotonin and recycles it in a sodium dependant manner.

The gene that encodes the serotonin transporter (see figure 20) is called solute carrier family 6 member 4 (SLC6A4). In humans, this gene is located on chromosome 17 in the area 17q11.1-q12. The structure of the SLC6A4 gene includes the sites of the major functional variants: the serotonin-transporter-gene-linked polymorphic region (5-HTTLPR), the variable number of tandem repeats (VNTR) (between 9 and 12 repeats can be found in intron 2 (STin2)) and the single nucleotide polymorphisms (SNPs).
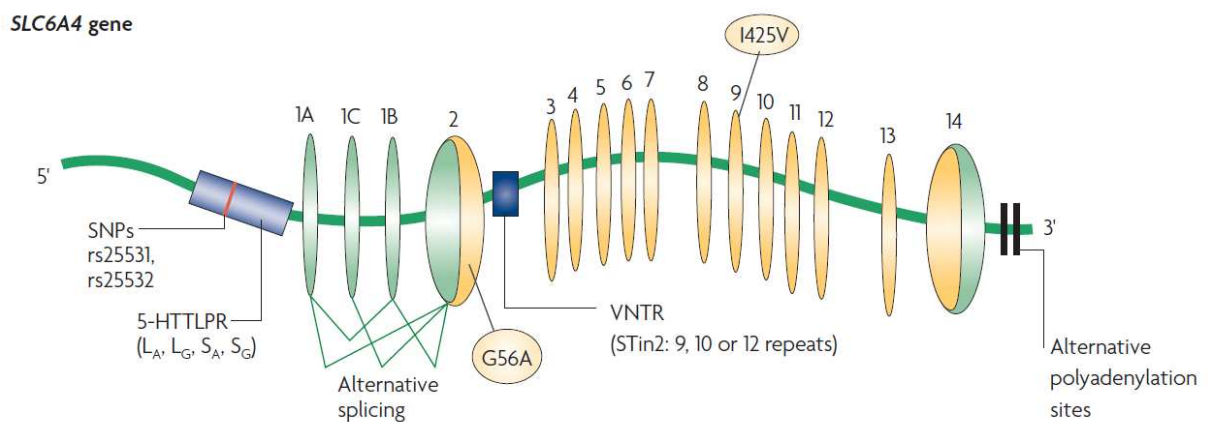


**Figure 20: Organization of the human serotonin transporter gene (*SLC6A4*)[87]**

33

Mutations associated with this gene may result in changes in the function of the 5-HTT. Based on evidences in molecular neuroimaging, postmortem and genetic studies, the serotonin transporter plays a pivotal role in the treatment of affective disorders[88,89]. The serotonin transporter is involved in the pathophysiology of psychiatric disorders, e.g. schizophrenia[90], mood disorders[91], depression[92,93,94,95,96] and anxiety disorders[97]. Hence, the SERT is an important site for the so called selective serotonin reuptake inhibitors (SSRIs), which reduce the activity of 5-HTT, therefore increase the serotonin level in extracellular space, and decrease binding of specific displaceable radioligands to 5-HTT. For the visualisation and quantification of the SERT, highly selective carbon-11 (and fluorine-18 labelled) PET-tracers have been developed and synthesised.

The most prominent and clinically used 11C-tracers are: [11C]McN5256[98], [11C]DASB[99], [11C]MADAM[100], [11C]DAPP[99] (see figure 21).
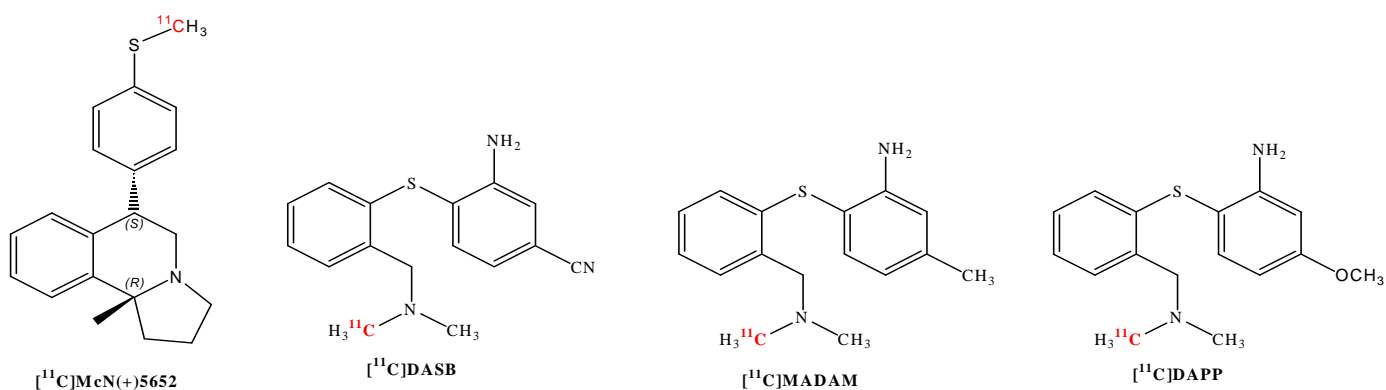


**Figure 21: Chemical structure of a selection of clinically used 11C-SERT tracers.**

## [11C]DASB

The best established and explored SERT ligand for PET-imaging in the brain is, so far, [11C]DASB (3-amino-4-[N-methyl-N-[11C]methyl-amino-methylphenylsulfanyl]-benzonitrile) (see figure 21). Its promising properties ($K_i$= 1.1nM, high specific binding; reversible, high brain uptake, signal/noise ratio 7.9; cerebellar clearance 15.6min; logP[7.4] 2.7, excellent selectivity (NET/SERT= 1230 and DAT/SERT= 1300) make it a suitable PET-tracer[99].

Since, [11C]DASB provides all the prerequisites for a reliable quantification of the SERT binding potential in-vivo, there is a great need for this specific SERT-tracer. The radiosynthesis of [11C]DASB was described already in 2000, converting the secondary amine

precursor (MASB = desmethyl-DASB) with freshly prepared [$^{11}$C]methyliodide into the derived dipenyl-sulfid-molecule[99]. Later, an evaluation of the reaction parameters was performed[101]. Several PET-studies have demonstrated the excellent imaging quality of this radioligand, suggesting [$^{11}$C]DASB as the first choice for measurement of SERT binding in studies focused on SSRI-dependent changes in SERT binding in patients in-vivo[102,103,104,105,106]. Therefore, the development of the radiochemical preparation of this tracer into a rapid fully-automated set-up was conducted by our group. Details are given in paper 1 in the scientific topic section.

# 1.2. PET-TRACER DEVELOPMENT

PET is the first choice technology for the visualization and quantification of receptors and transporters enabling examination of e.g. neurological, psychiatric and oncological diseases on a molecular level. New and innovative PET-radiopharmaceuticals need to be developed to get further insights into the biochemical mechanisms involved in pathological changes.

At the very beginning, PET-tracer development starts with the idea or modelling of the chemical structure of a (new) molecule with (hopefully) good binding characteristics to the desired target site. Then, as next steps, the compound needs to be radiolabelled with a suitable PET-nuclide, and then, it has to be evaluated regarding its parameters in various preclinical experiment settings.

Hence, two major tools are crucial in the development process of new PET-tracers:

1) a reliable production method –most desireable and optimal in an automated set-up, and

2) proof of tracer suitability (high affinity, high selectivity and specificity, beside low unspecific binding) through preclinical evaluation in an animal model prior to human application.

In the next chapters these tools (both: the reliable radiochemical preparation/ automatisation, and the preclinical evaluation) are described in detail theoretically, whereas the results of 5 different investigations with respect to this focus are given in the scientific topic section (manuscripts 1-3 deal with the radiochemical preparation and automatisation, manuscripts 3-5 deal with the preclinical evaluation).

## 1.2.1. RADIOCHEMICAL ASPECTS

Positron emitters can be found throughout the entire chart of nuclides, but only few display suitable physical properties combined with the possibility of being produced under simple conditions. The most important PET-nuclides for clinical applications are summarized in table 1. The two most widely used PET radoinuclides are $^{11}$C and $^{18}$F, and the focus of the thesis lies upon this two nuclides.

| nuclide | production | | half-life |
|---|---|---|---|
| F-18 (F⁻) | $^{18}O$ | (p,n) $^{18}F$ | 109.7 min |
| F-18 (F$_2$) | $^{20}Ne$ | (d,α) $^{18}F$ | 109.7 min |
| C-11 | $^{14}N$ | (p, α) $^{11}C$ | 20.4 min |
| N-13 | $^{16}O$ | (p, α) $^{13}N$ | 10.0 min |
| O-15 | $^{14}N$ | (d,n) $^{15}O$ | 2.0 min |
| Cu-64 | $^{64}Ni$ | (p,n) $^{64}Cu$ | 12,7 h |
| Y-86 | $^{86}Sr$ | (p,n) $^{86}Y$ | 14,7 h |
| Br-76 | $^{76}Se$ | (p,n) $^{76}Br$ | 16,0 h |
| Ga-68 | $^{68}Ge$ / $^{68}Ga$ generator | | 67.6 min |

**Table 1: Important PET-nuclides for clinical application**

# [¹¹C]RADIOCHEMISTRY

Carbon-11 is commonly prepared as carbon dioxide in the cyclotron. Subsequently, this active precursor is converted either into [¹¹C]CH$_3$I for methylations, into [¹¹C]HCN, [¹¹C]COCl$_2$ or [¹¹C]CHO for special applications, or it is used directly for the synthesis of carbonyls or carboxyls via corresponding Grignard reactions. The major radiosynthetic pathways are illustrated in figure 22.
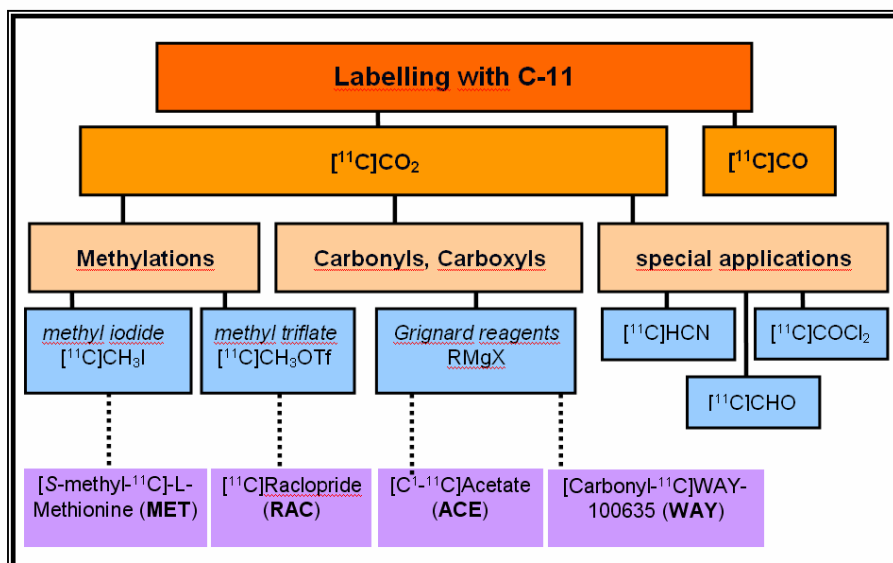
**Figure 22: Labelling techniques with C-11**

*Methylations*

[$^{11}$C]Methyl iodide may be prepared from [$^{11}$C]carbon dioxide by reduction to [$^{11}$C]methanol and then treatment with a source of HI. The reduction is carried out either by catalytic hydrogenation, or more often, by lithium aluminium hydride (LiAlH$_4$). As the carbon dioxide, methanol, and methyl halide are all volatile, separation from non-volatile impurities is easily achieved by distillation or gas chromatography. [$^{11}$C]CH$_3$I has also been prepared from [$^{11}$C]methane through substitution by iodine[107]. Larsen et al[108] have reported the automated on-line preparation of [$^{11}$C]methyl iodide in 1.0 Ci quantities. [$^{11}$C]methane and iodine in helium were recirculated through a tube at 700–750°C, removing the iodomethane being formed. Methyl triflate has been introduced as an even faster methylating agent[109,110]. Radiolabelled methyl triflate is generally obtained by the reaction of methyl halide with silver triflate; for example, a gas stream containing [$^{11}$C]methyl iodide impinges upon silver triflate absorbed upon graphite at loadings as high as 50% at 170–200°C. An excellent review on this topic was presented by R. Bolton[72]. In table 2 an overview of the most commonly used [$^{11}$C]methylated PET-radiopharmaceuticals is given, including [$^{11}$C]DASB. In the scientific topic section, in paper 1, a detailed description about an automated method for the rapid and reliable preparation of this tracer via [$^{11}$C]methyl iodide is given.

| PET-tracer | Abbrevation | Target |
|---|---|---|
| [*S*-methyl-$^{11}$C]-L-methionine | MET | Brain tumours |
| [$^{11}$C]metomidate | MTO | 11ß-hydroxylase (adrenal cortex) |
| [$^{11}$C]flumazenil | FMZ, Ro 15-1788 | central benzodiazepine receptors (GABA$_A$) |
| [$^{11}$C]Patrick-Emond-substance 2I | PE2I | Dopamine transporter |
| [$^{11}$C]raclopride | RAC | D$_2$ receptor |
| [$^{11}$C]*N,N*-Dimethyl-2-(2-amino-4-cyanophenylthio)-benzylamine | DASB | Serotonin transporter |
| [$^{11}$C]carfentanyl | CFN | µ-opioid receptor |
| [*N*-Methyl-$^{11}$C]-6-OH-BTA-1 | PIB | ß-amyloid plaques (AD) |

**Table 2: Important [$^{11}$C]methylated PET-radiopharmaceuticals**


# [$^{18}$F]RADIOCHEMISTRY

Figure 23 illustrates possible labelling techniques with F-18. Depending on the starting material, e.g. [$^{18}$F]fluoride or [$^{18}$F]F$_2$-gas, respectively, nucleophilic and electrophilic reactions are possible. Complementary to the direct radiofluorination reactions, fluorinated synthons can be produced, which are subsequently bound to the target molecules. Fluoroalkylations – and especially fluoroethylations – represent the most important class for this indirect labelling technique.
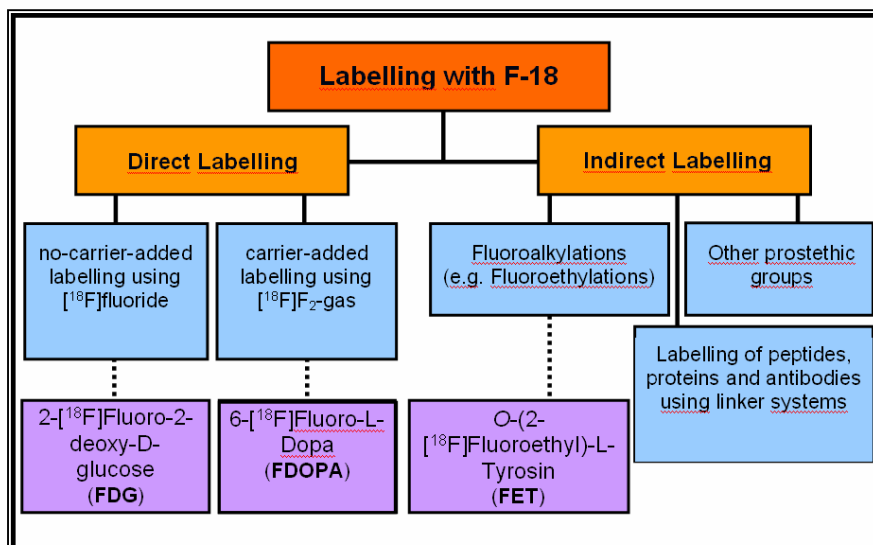
**Figure 23: Labelling techniques with F-18**

### *Fluoroalkylations*

Since many biologically active compounds contain alkylic side chains, e.g. methyl- and ethyl-groups, these structural units may be targets for the affixation of a radiolabel. In fact, many compounds have been labelled with a [$^{11}$C]methyl-group for PET. Thus, the development of [$^{18}$F]fluoroalkylated tracers was the logical consequence. A variety of different fluoroalkylating agents have been developed so far:

[$^{18}$F]bromofluoromethane[111,112], [$^{18}$F]fluoroiodomethane[113], 2-[$^{18}$F]bromofluoroethane[114,69], 2-[$^{18}$F]tosyloxyfluoroethane[115,116], 3-[$^{18}$F]bromofluoropropane[117,118,119], 3-[$^{18}$F]fluoroiodo-propane[120] and 3-[$^{18}$F]tosyloxyfluoropropane[121]. The thus labelled synthons are restricted to small alkyl-chains to avoid too large structural differences.

### *Fluoroethylations*

Fluoroethylations represent the most important class amongst the fluoroalkylations, since fluoroethylating agents can be easily produced from commercially available substances, and the fluoroethyl-group is sterically close to methyl- and ethyl-groups. Targets for fluoroethylations are amine[122,123,124,125,126,127], hydroxylic[128,129], mercapto[130,131] and carboxylic moieties. 2-[$^{18}$F]Tosyloxyfluoroethane is widely used, since it is easy to prepare, very stable and suitable for a variety of compounds[132].

On the other hand, it is not as reactive as 2-[18F]fluoroethyltriflate[133,134]; sensitive to some solvents and bases[133]; not a selective agent[135] and intricate to purify – a semi preparative HPLC is unavoidable. Hence, microwave enhanced conditions were proposed that increased the selectivity and the radiochemical yields[136].

2-[18F]Bromofluoroethane can also be produced rapidly, because no preparative HPLC is necessary, but the distillation is very tricky. Thus, a lot of effort was put into investigations to optimize yields and quality of this intermediate compound by addition of sodium iodide and application of solid phase extraction for purification[137,138].

Three of the introduced tracers in this thesis, [18F]FE@SUPPY, [18F]FE@SUPPY:2 and [18F]FE@CIT, respectively, are fluoroethylated tracers, and, therefore, prepared via this kind of synthetic route. The explanation of their similar and special sounding names ([18F]FE@...) lies partly in their preparation methods: the [18F]FE refers to the fluorine-18 **f**luoro**e**thylation method, and the @ is a trademark for the newly developed tracers by our group.

## ADVANTAGES OF [18F]LABELLED PET-TRACERS

Rationales for the development of [18F]labelled radiotracers bear the advantages of the 18F nuclide: the relatively long half-life of fluorine-18 (109.7min) as compared to carbon-11 (20.3min), and a hypothesised higher stability of the [18F]fluoroethyl-esters as compared to their parent C-11 methyl or ethylesters.

The longer half-life leads to the advantage of longer patient protocols, especially necessary for radiopharmaceuticals reaching late equilibriums at the receptors or enzymes, or enables the imaging of sore consecutive patients. A longer half-life also supports the concept of distribution of these valuable radiopharmaceuticals to PET-centres without on-site cyclotron (satellite principle) and commercial exploitation. The the higher stability reduces the demanded amount of applied radiotracer (to bring intact radiotracer to the bindingsite/target), thus, reduces the radiation burden for the patients and simplifies kinetic models for the quantification of receptor or enzyme binding of the tracers. Therefore, our group introduced a method for the development of [11C]-tracers into their respective [18F]-tracers[139].

In the following chapter, details about the so called "cold" chemistry (precursor and reference standard preparation) of the radiotracers described and presented in this thesis ([$^{11}$C]DASB, [$^{18}$F]FE@SUPPY, [$^{18}$F]FE@SUPPY:2 and [$^{18}$F]FE@CIT) are given.

## "COLD" CHEMISTRY

### *Precuror Chemistry*

As a prerequisite for a successful radiochemical preparation, a suitable precursor molecule with an efficient leaving group has to be prepared. Due to the short halflife of F-18, saving time for this [$^{18}$F]fluorination steps, is essential for effective radiolabelling. It is better to spend time for suitable precursors than waste time and yield in the subsequent labeling step. In this thesis, for the [$^{18}$F]flouroethylated radiotracers, the widely used leaving group p-toluene-solfonate (=tosylate, =OTs) was used for aliphatic nucleophilic displacement.

### *A) [$^{18}$F]FE@SUPPY-Derivatives*

The precursors of the two A3R tracers, are called Tos@SUPPY (5-(2-tosyloxyethyl)2,4-diethyl-3-(ethylsulfanylcarbonyl)-6-phenylpyridine-5-carboxylate) and Tos@SUPPY:2 (5-ethyl2,4-diethyl-3-((2-tosyloxyethyl)sulfanylcarbonyl)-6-phenylpyridine-5-carboxylate). The reaction scheme for the preparation of both precursor molecules is presented in figure 24.
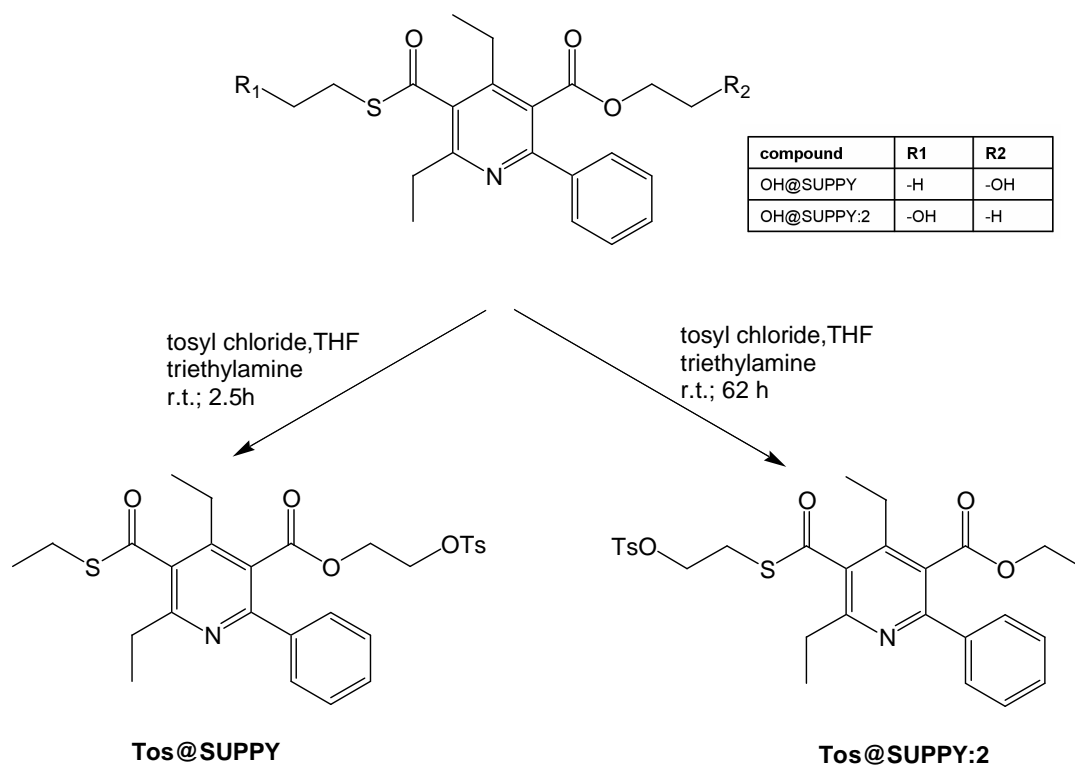
**Figure 24: Preparation scheme of Tos@SUPPY and Tos@SUPPY:2 starting from OH@SUPPY and OH@SUPPY:2, respectively.**

*B) [$^{18}$F]FE@CIT*

ß-CIT (3-ß-(4-idophenyl)tropane-2-ß-carboxylic acid) (see figure 25), the precursor for the preparation of [$^{18}$F]FE@CIT, was prepared as described elsewhere, yielding in about 61% of ß-CIT[81].
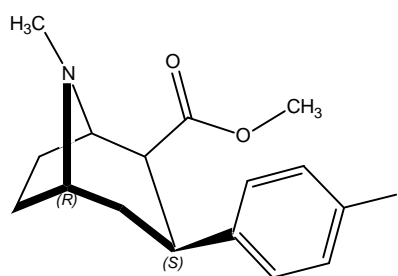


**Figure 25: Chemical structure of ß-CIT**

*C) [^{11}C]DASB*

MASB (=desmethyl-DASB=N-Methyl-2-(2-amino-4-cyanophenylthio)-benzylamine) (see figure 26), the precursor for the preparation of [^{11}C]DASB, is a commercially available compound, and was therefore purchased from the company ABX, in Germany[140].
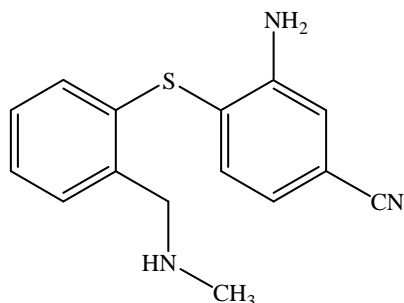


**Figure 26: Chemical structure of MASB**

*Reference Standards*

*A) [^{18}F]FE@SUPPY-Derivatives*

The reference standards FE@SUPPY (5-(2-fluoroethyl) 2,4-diethyl-3-(ethylsulfanylcarbonyl)-6-phenyl-pyridine-5-carboxylate) and FE@SUPPY:2 (5-ethyl 2,4-diethyl-3-((2-fluoroethyl)sulfanylcarbonyl)-6-phenyl-pyridine-5-carboxylate) were prepared as shown in figure 27.



| compound | R1 | R2 |
|----------|-----|-----|
| OH@SUPPY | -H | -OH |
| OH@SUPPY:2 | -OH | -H |
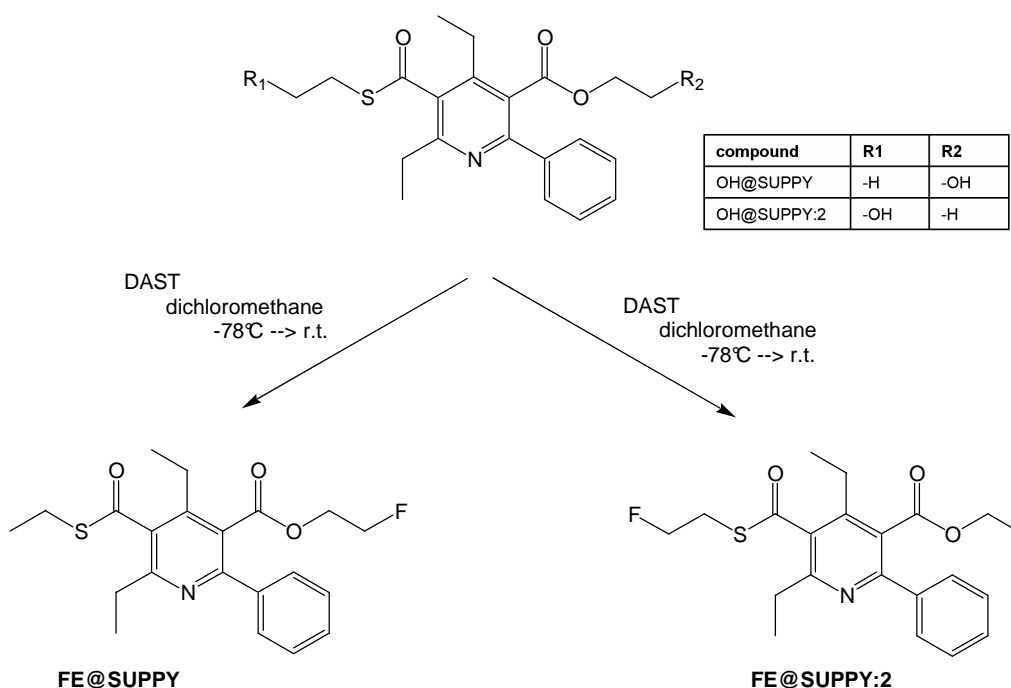
**Figure 27: Reaction scheme for the preparation of the standard compounds FE@SUPPY and FE@SUPPY:2.**

Briefly, OH@SUPPY or OH@SUPPY:2, respectively, was dissolved in water-free dichloromethane at -78°C under inert gas. Then, diethylaminosulfur trifluoride (DAST) was slowly added dropwise to obtain crude FE@SUPPY or FE@SUPPY:2. The reaction was kept at -78°C for half an hour and then slowly heated to room temperature. After completion of the reaction, the mixture was cooled to 0°C and hydrolysis was performed by addition of 10mL of water. The organic phase was separated and the aqueous phase was extracted 3-times with diethylether. The combined organic phases were dried over magnesium sulphate and the solvent was evaporated under reduced pressure. Subsequent purification was performed using again combined straight phase and reversed-phase column chromatography. The method is described in detail elsewhere [141].

*B) [$^{18}$F]FE@CIT*

*FE@CIT* (3-ß-(4-idophenyl)tropane-2-ß-carboxylic acid 2-fluoroethylester) was prepared from ß-CIT and analyzed by spectroscopic methods, resulting in 42% yield[81] (see figure 28).
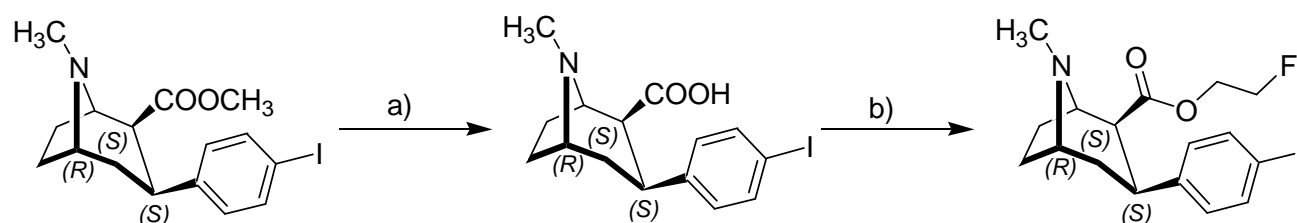


**Figure 28: Scheme of the synthesis of FE@CIT**

**Reagents and conditions:**

**a) 6N HCl, reflux for 24 hours**

**b) standard synthesis: 2-fluoroethanol, DMAP, EDCI and dichloromethane**

*C) [$^{11}$C]DASB*

DASB reference standard (see figure 31) was obtained from the company ABX, in Germany[142].

<div align="center">RADIOSYNTHESES</div>

For the radiochemical preparation of the radiotracers, described in this thesis, three different routes of radiolabelling were selected: a direct radiolabelling method

([*$^{18}$F]FE@SUPPY-Derivatives*), an indirect radiolabelling method via synthon ([*$^{18}$F]FE@CIT*) and a C11-methylation method ([*$^{11}$C]DASB*).

*A) Radiochemical preparation via direct radiolabelling: [$^{18}$F]FE@SUPPY-Derivatives*

Radiosyntheses of [$^{18}$F]FE@SUPPY and [$^{18}$F]FE@SUPPY:2 were performed in simple and straight forward one-step, one-pot procedures, each. The radiosynthesis of [$^{18}$F]FE@SUPPY was presented recently by our group[143]. The radiosynthesis of [$^{18}$F]FE@SUPPY:2 will be explained in detail in the scientific topic section in paper 2.

Briefly, preparation for both tracers started from cyclotron-produced [$^{18}$F]fluoride. After addition of potassium carbonate and aminopolyether (Kryprofix 2.2.2.), aceotropic drying assisted by repeated addition of acetonitrile was performed at 100°C. The activated, dried [$^{18}$F]fluoride-aminopolyether complex was converted to [$^{18}$F]FE@SUPPY by addition of Tos@SUPPY, or to [$^{18}$F]FE@SUPPY:2 by addition of Tos@SUPPY:2, in acetonitrile at elevated temperature (see figure 29).



| compound | R1 | R2 |
| --- | --- | --- |
| Tos@SUPPY | -H | -OTos |
| Tos@SUPPY:2 | -OTos | -H |
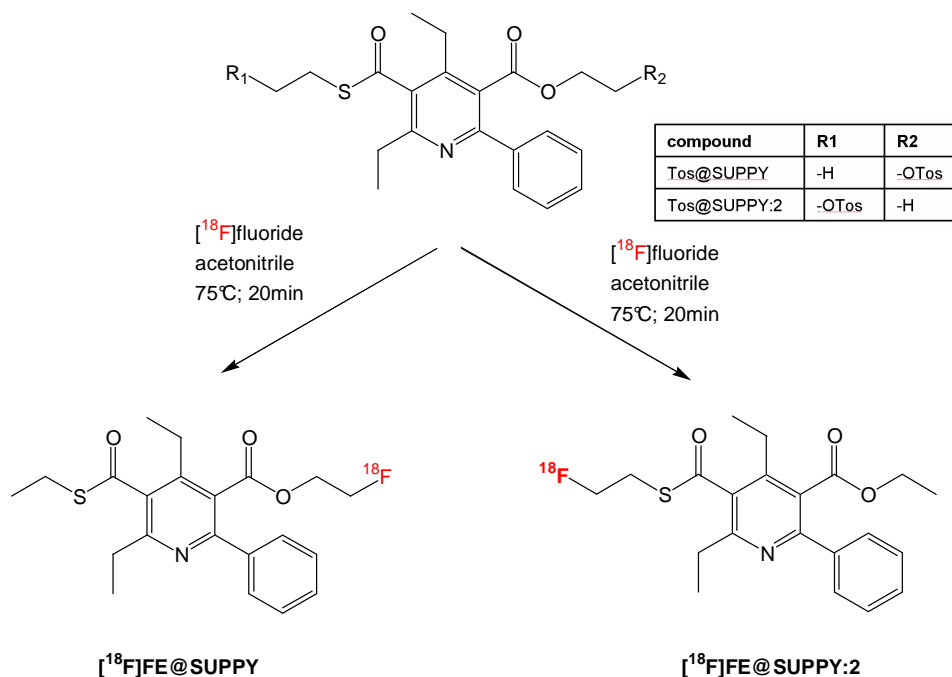
**Figure 29: Reaction scheme for the radiochemical preparation of [$^{18}$F]FE@SUPPY and [$^{18}$F]FE@SUPPY:2.**

The crude reaction mixture was passed online over two consecutive anion-exchange cartridges (PS-HCO3), thereby reducing the amount of unreacted [$^{18}$F]fluoride. Thereafter, purification was conducted by using semi-preparative RP-HPLC and subsequent solid phase

extraction to separate residual solvents. Then, the respective product ([$^{18}$F]FE@SUPPY or [$^{18}$F]FE@SUPPY:2) was eluated with 2mL ethanol and formulated with saline and phosphate buffer. Finally, sterile filtration (0.22μm) under aseptic conditions (laminar air flow hot cell, class A) was performed to avoid microbial contamination.

*B) Indirect radiolabelling method via synthon: [$^{18}$F]FE@CIT*

Radiochemical preparation of [$^{18}$F]FE@CIT (see figure 30) was conducted via destillation of [$^{18}$F]bromofluoroethane ([$^{18}$F]BFE) and reaction with (1R-2-exo-3-exo)8-methyl-3-(4-iodo-phenyl)-8-azabicyclo[3.2.1]octane-2-carboxylic acid. After 10 minutes at 150°C the product was purified using a C-18 SepPak. The radiosynthesis evinced radiochemical yields of >90% (based on [$^{18}$F]BFE), the specific radioactivity was >416 GBq/μmol. An average 30μAh cyclotron irradiation yielded in more than 2.5GBq [$^{18}$F]FE@CIT[81].
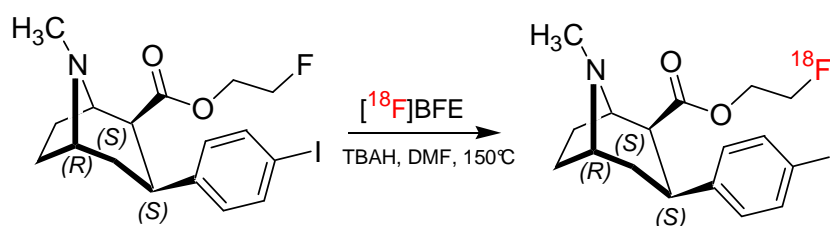


**Figure 30: Scheme of the synthesis of [$^{18}$F]FE@CIT.**

*C) C11-metylation method: [$^{11}$C]DASB*

Radiosynthesis of [$^{11}$C]DASB via [$^{11}$C]methyl iodide (see figure 31) was first described in 2000 by Wilson and his co-workers[99]. Details about the developmemt into a fully-autpmated set-up are given in paper 1 in the specific topic section. Briefly, freshly prepared [$^{11}$C]methyl iodide was trapped online in the reaction mixture containing 1 mg of precursor (MASB; desmethyl-DASB) in 500 μL of DMSO. The reaction mixture was heated at 100°C for 2min, diluted with 1 mL of mobile phase and subsequently transferred to the semi-preparative HPLC system. Purification was achieved using RP-HPLC with a mobile phase consisting of 40% acetonitrile and 60% 0.1 mol/L ammonium acetate at a flow rate of 8mL/min. Then, the product fraction was diluted and subjected to solid phase extraction to reduce contents of residual solvents. After washing with water the purified product was eluted with ethanol. Finally, the ethanolic product solution was formulated with saline and phosphate buffer and

sterile filtrated under aseptic conditions. Typically, 2-9 GBq of [$^{11}$C]DASB were prepared within 35±3min (n=60)
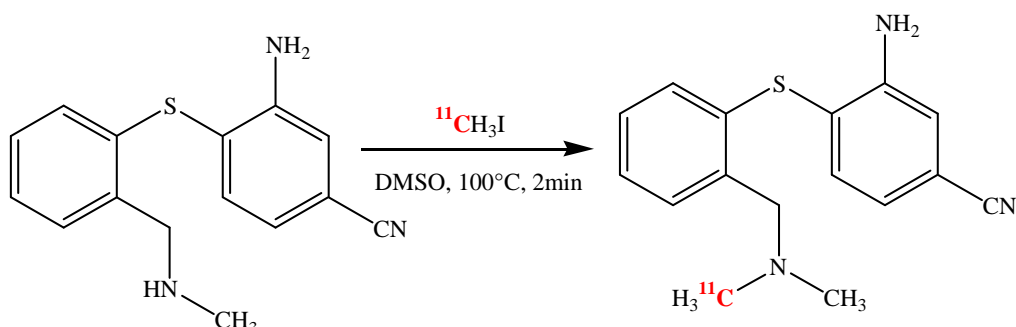


**Figure 31: Scheme of the synthesis of [$^{11}$C]DASB**

## AUTOMATISATION

Up-scaling and automatisation of radiosyntheses are useful tools, if the tracers shall or will be prepared on a routine basis for preclinical and/or clinical applications. Furthermore, the automatisation of a radiosynthetic procedure keeps the radiation burden for the operators to a minimum.

### A) [$^{18}$F]FE@SUPPY-Derivatives

The syntheses for the two A3R tracers were automated in a GE Tracerlab Fx synthesizer, remotely controlled by a standard laptop with dedicated processing software. Generally, the main steps of the automation process included: [$^{18}$F]fluoride fixation on an anion exchange column regenerating [$^{18}$O]water; azeotropically supported drying and activation of [$^{18}$F]fluoride; substitution of the precursor's leaving group by activated [$^{18}$F]fluoride ions; purification of the crude reaction mixture using semi-preparative reversed-phase HPLC and/or solid phase extraction (SPE) techniques; and formulation and sterile filtration of the purified product. Details about the automatisation of [$^{18}$F]FE@SUPPY and [$^{18}$F]FE@SUPPY:2 are given in paper 3 in the specific topic section.

### B) [$^{18}$F]FE@CIT

The automated preparation of [$^{18}$F]FE@CIT was not yet implemented.

### C) [$^{11}$C]DASB

As mentioned before, the automated procedure of the preparation of [11C]DASB is given in paper 1 in the scientific topic section.

## *Quality control*

Radiochemical purities always exceeded 95% for all four described PET-tracers ([11C]DASB, [18F]FE@SUPPY, [18F]FE@SUPPY:2 and [18F]FE@CIT), in accordance with the regulations of the European pharmacopoeia[144]. Radiochemical identity and purity were determined by analytical HPLC for all tracers and by TLC (except for [11C]DASB) by comparison of retention times (or retention factors, respectively) with an authentic sample of the investigated tracers. Sterility, presence of endotoxines, pH, osmolality and residual solvents were assessed by standard procedures routinely performed at the PET Centre of the Vienna General Hospital, all in accordance with the European Pharmacopoeia[144].

# 1.2.2. PRECLINICAL EVALUATION

In the process of PET-tracer development the first prerequisite is the successfull production of the radiopharmaceutical. The automatisation of the radiochemical preparation of the PET-tracer is a second very valuable prerequisite, especially, if further investigations with this tracer are planned. Then, as a next step, is the preclinical evaluation process, which is a crucial tool prior to the clinical application of the tracer. M. Bergström stated in 2003: "the process of development of new PET-tracers requires use of a range of preclinical methods. The purposes of these studies are to qualify a tentative labelled molecule for further testing in more labor intensive and more complex models, up to human validation studies. Because typically nine tentative tracers out of 10 would fail to show the desired property in vivo, it is essential to reject failures at an early stage, so as not to delay the utilization of PET in clinical trials. There is no single method today that can adequately predict the in-vivo behaviour of a tracer, and therefore, combinations of assays are needed to increase the propability of success"[145].

According to the stated need of combination of methods, the present thesis presents several evaluation methods: biodistribution testing, metabolic stability experiments and last but not least, autoradiography, to get a first estimate of the in-vitro and in-vivo behaviour of the dedicated tracers.

## BIODISTRIBUTION

Biodistribution testing is a very important tool in the preclinical evaluation process, since it gives a first estimate of the in-vivo distribution of the tracer in an animal model. One can divide organs with high, mediate and low uptake of the tracer, and see, for example, if there is uptake of the tracer in bones, which is important to know especially for [$^{18}$F]tracers. In case of high bone uptake of [$^{18}$F]tracers, one would have to consider a high degree of defluorination. Furthermore, the biodistribution model can give hints of the excretion pathways of the tracer, whether it is cleared hepatobilliary, or renally. Moreover, it is important to compare given mRNA data about the desired target with the data resulting from the biodistribution, and checking if there is analogy or not.

*A) [<sup>18</sup>F]FE@SUPPY-Derivatives*

*A) [$^{18}$F]FE@SUPPY-Derivatives*

Biodistribution experiments were conducted for [$^{18}$F]FE@SUPPY:2 and were planned in a similar manner as performed in various preceding tracer-evaluations at the Austrian Institute of Technology (AIT, Seibersdorf)[146, 54, 147].

Briefly, male wild-type rats were injected with 1-2.5 MBq of [$^{18}$F]FE@SUPPY:2 in ~200 µl physiological phosphate buffer through a tail vein. Subsequently, the rats were sacrificed by exsanguination from the abdominal aorta in ether anaesthesia after 5, 15, 30, 60 and 120 minutes. Organs were removed, weighed and counted with a Canberra Packard Cobra II auto-gamma counter. % Doses were calculated using two calibration curves (high and low activity) with known activities and decay corrected for the injection time. Preparation of the doses was done on a Capintec CRC15R dose calibrator and the rest body was counted on a planar NaI crystal assembled with Ortec Maestro 32MCA emulator data acquisition software.

Remaining activity in the rest body was calculated by correlation of the counts with a calibration curve acquired with known activities in the same geometry and decay corrected for the injection time. Radioactivity was expressed as percentage injected dose per gram tissue (% ID/g). All biodistribution studies performed at the AIT Austrian Institute of Technology GmbH, in Seibersdorf, followed a protocol of the NIH Animal Care and Use Committee and were in accordance with the national legislation on animal experiments ("Österreichisches Tierschutzgesetz").Results are given in the scientific topic section in paper 3.

*B) [$^{18}$F]FE@CIT & C) [$^{11}$C]DASB*

No biodistribution experiments were conducted for these two tracers.

## METABOLIC STABILITY

In the living organism, PET-tracers may undergo biotransformation reactions, including oxidation, hydrolysis or decarboxylation, as well as conjugation processes, as any other xenobiotics and drugs do. In consequence, the measured PET-signal in a PET-scan reflects the total of all radiolabelled compounds, including the parent tracer and possibly formed labelled metabolites[148]. Therefore, metabolic stability testing of new potential PET-tracers is

crucial regarding their possible future application in humans. Since, those tracers get applied intravenously, and enter the normal metabolisation process inside the body, it is important to know what happens to them. So, distinct information concerning the stability and degradation, as well as the amount of formation of radioactive metabolites, is needed. Radioactive metabolites – if present in the target tissue – could interfere with the signal of the intact molecule, which would lead to misinterpretation of the resulting PET-scans by the physicians. Addidionaly, tracer metabolism affects the arterial input function used for quantitative analysis of the resulting images. As a consequence, metabolite analysis in plasma is an essential prerequisite for determination of the exact arterial input functions[149]. Metabolic stability can be tested both, in-vitro and ex-vivo:

### In-vitro metabolite analysis

A first estimate of the metabolic characterisation of a PET-tracer can be gained by simulation of the typical reactions in-vitro. Carboxylesterases (CES) are considered to contribute significantly to cleavage and degradation of carboxylester- and thioester-functions. In-vitro assays of the biotransformations mediated by enzymes are performed to obtain detailed information of the substrate hydrolyis. Therefore, enzyme kinetic studies using CES were conducted to obtain information about ester cleavage of the unlabeled substrates of [$^{18}$F]FE@SUPPY, [$^{18}$F]FE@SUPPY:2 and [$^{18}$F]FE@CIT.

In general, kinetic studies were performed using carboxylesterase from a stock solution (500 µg/ml = 10 I.U.in distilled water). The determination of Michaelis-Menten kinetic parameters, $K_m$ and $V_{max}$, were performed with constant enzyme concentration (2.5 I.U) and various concentrations of unlabelled substrate under physiological conditions at given time points (1 minute to 6 hours). A linear regression analysis of the concentration versus time plot yielded a steady state velocity represented by the slope k. The same time points were used to determine steady-state kinetics for a range of increasing substrate concentrations. Substrate incubation took place at 37°C, in a final volume of 1 ml phosphate buffer. For quantification of the esterase experiments an HPLC (high performance liquid chromatography) system, containing of a diode array UV detector at 248nm and 250nm and a NaI Socket was used. Figure 32 shows a typical progression of enzymatic cleavage over a time period of 6 hours.
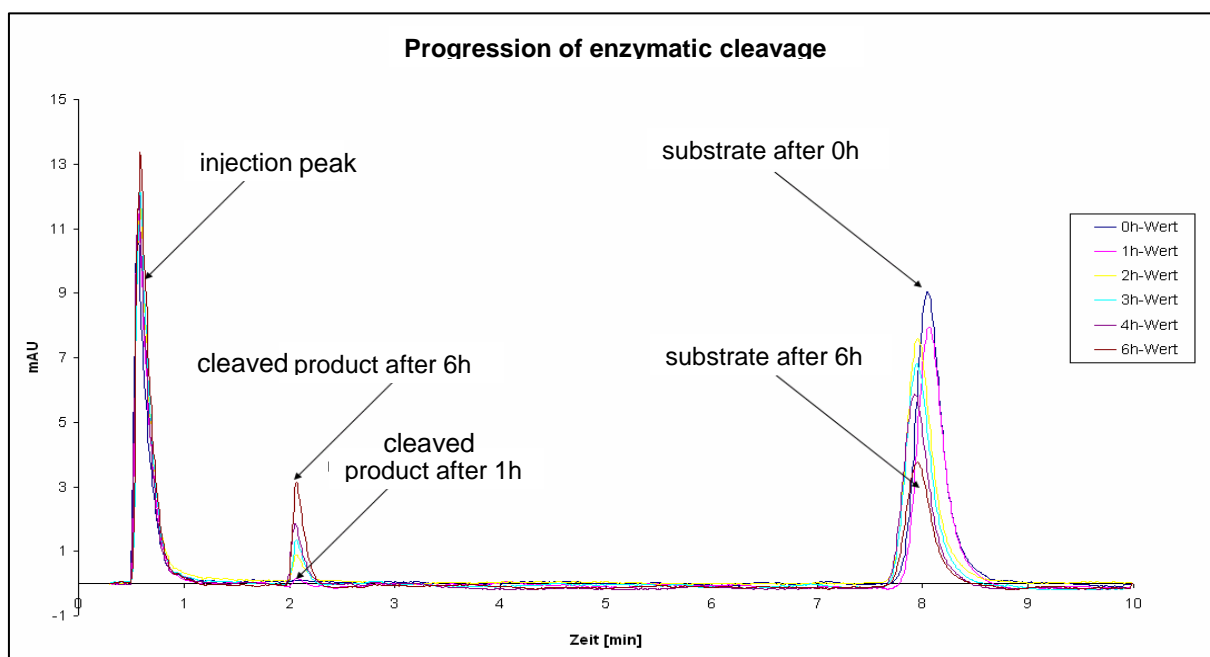
**Figure 32: Degradation of a dedicated substrate in dependence of CES**

A) [$^{18}$F]FE@SUPPY-Derivatives

Details and results of in-vitro behavior of FE@SUPPY and FE@SUPPY:2 concerning CES are given in the specific topics section, in Paper 4.

B) [$^{18}$F]FE@CIT

Details and results of in-vitro behavior of FE@CIT concerning CES are given in the specific topics section, in Paper 5.

C) [$^{11}$C]DASB

In-vitro experiments with CES have not been conducted with this tracer by our group.

**Ex-vivo metabolite analysis**

A next step towards a complete metabolic characterization, is the examination of potential metabolites of the dedicated tracer in an animal model. Hence, one has to establish an appropriate experimental setting, to allow simulation of the typical reactions in-vivo, and to detect the possible respective radiolabelled metabolites. Separation techniques for the detection of possible metabolites are e.g. radio-HPLC, radio-TLC (thin layer chromatograohy) or SPE (solid phase extraction). Therefore, samples have to be prepared immediately after explant of e.g. blood and brain from the animal.

53

In our case, we analyzed the tracers according to standart protocols via radio-HPLC. For quantification of the respective radioactive metabolites, the HPLC system was equipped with a lead-shielded high-sensitivity-radiodetector with a BGO crystal as detection device. Recovery was performed by comparing peak areas from spiked biological samples with those from samples of fluoroethyl-esters in aqueous solution. Aqueous and biological samples were processed under identical conditions.

*A) [$^{18}$F]FE@SUPPY-Derivatives*

Results of ex-vivo metabolite studies in rat plasma and rat brain of [$^{18}$F]FE@SUPPY and [$^{18}$F]FE@SUPPY:2 are given in the specific topics section, in Paper 4.

*B) [$^{18}$F]FE@CIT*

Ex-vivo experiments have not yet been conducted with this tracer.

*C) [$^{11}$C]DASB*

Ex-vivo experiments have not been conducted with this tracer by our group.

## AUTORADIOGRAPHY

Autoradiography is a method of self reproduction of radioactive sources by means of modified photographic techniques. The basis of autoradiography is the recording of radioactivity distribution in slices of various tissues. This can be performed with radioactivity added to premade tissue slices (in-vitro autoradiography), or administered to animals, which are thereafter sacrificed and sliced (ex-vivo autoradiography). Autoradiography experiments allow a range of frozen tissues to be sectioned and incubated with the dedicated PET-tracer, and additionally, with selective blocking agents. Hence, quantitative values can be obtained with respect to tracer binding and its regional distribution.

Nowadays, recording of radioactivity is typically made with an Instant Imager or with a Phosphor Imager, using imaging plates, being the most sensitive devices for the measurement of radioactivity from PET tracers[145]. Most frequently used nuclides for autoradiography are $^{3}$H, $^{14}$C and $^{125}$I. Differences in the resulting pictures derive from the emitted radioation sources, for example $^{3}$H emits ß-radiation with particle energy of

18.5KeV, whereas ^{125}I emits auger electrons with 35keV. Additionaly, also the half-life, as well as the ionisation degree of the nuclide show impact on the resulting images.

For autoradiographic experiments, different steps have to be processed one after the other, as explained and listed in the following. The exact preparation of the tissue sections (commonly rat tissues, if available also human brain or tumor tissues) is a prerequisite for autoradiographic studies:

### Step 1: Preparation of Tissue Sections for in-vitro autoradiography

In our autoradiographic experiments, the PET-tracers were examined in rat brain, so far. Hence, male wild-type rats, weighing 200 to 300g were deeply anesthetized by diethylether and rapidly decapitated. Since, freezing of the various tissues promotes blockage of all biological processes, including protein degradation and tissue hardening, rat brains were removed and subsequently quick-frozen in isopentane, which was cooled over dry ice to – 45°C.

Then, brains were stored at –80°C and transferred to –20°C the night before cutting in a cryostat. A cryostat is a microtome placed in a refrigerating compartment (see figure 33a). Frozen samples were left in the chamber of the cryostat to warm the slices to optimum temperature of -20°C before cutting (see figure 33b).
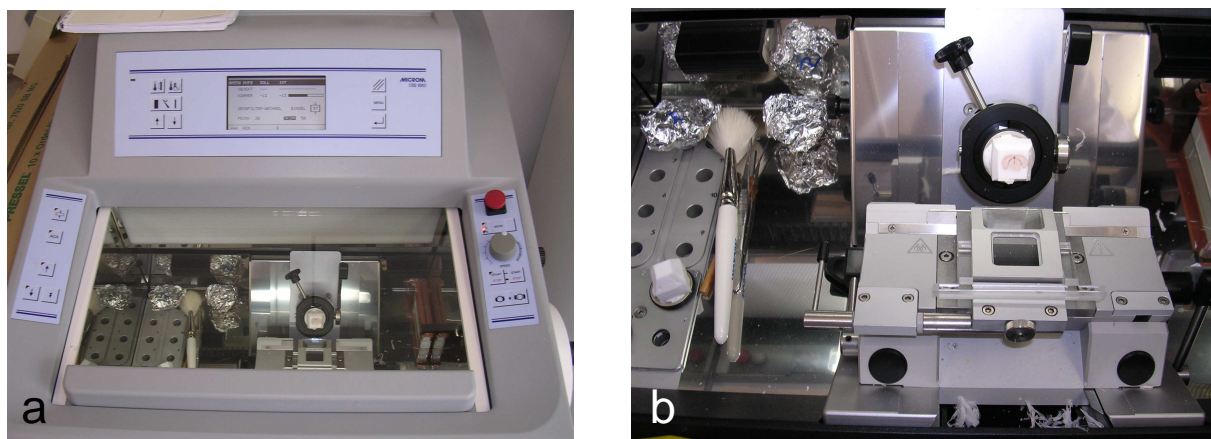


**Figure 33: (a) Cryo-microtome for sectioning frozen tissues**

**(b) inside view of the cutting chamber of the cryostat**

Then, frozen brains were fixed upon dedicated chucks (see figure 34) and immediately sectioned into 20µm thick coronal slices as schematically shown in figure 35. Sections were

thaw-mounted onto superfrost slides, and after drying at room temperature, the slides were stored at –40°C until processing.
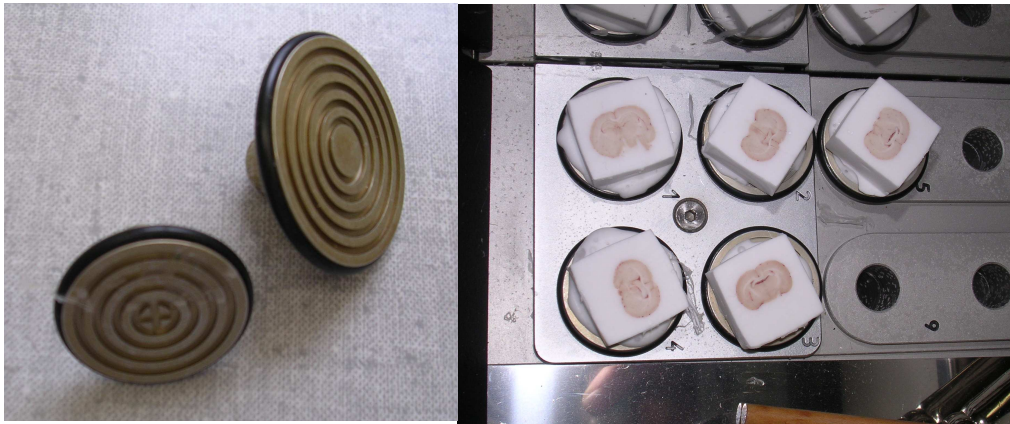


**Figure 34: Chucks for fixation of the rat brains**
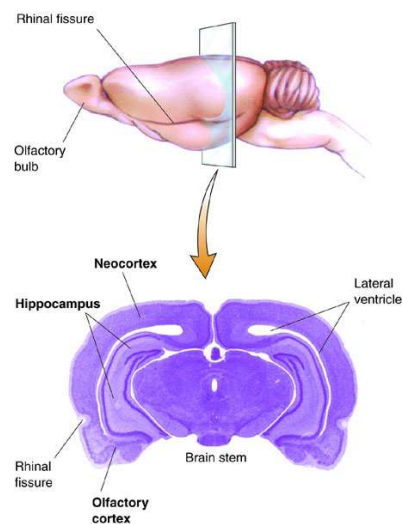


**Figure 35: Scheme of a coronal rat brain slice**

### Step 2: Autoradiographic set-up

Approximately 20 minutes before starting the experiment, the frozen tissue sections were preincubated for 2 minutes in a container with a TRIS-HCl buffer solution (pH 7.4) (see figure 36) to adjust the sections to the medium and to room temperature.
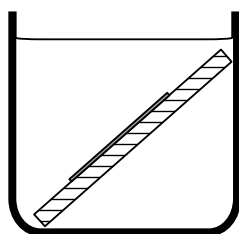
**Figure 36: Typical container filled with buffer solution for preincubation of frozen tissues**[150]

Subsequently, parallel slices were directly incubated with a solution containing the PET-tracer in a specific concentration expressed in nM of cold compound, and selective blocking agents for the various receptor subtypes, which might interfere with the signal of the tracer (scheme see in figure 37). Incubation time was chosen to fit optimal binding equilibrium with respect to the half-life of the tracer. After incubation, slides were washed in buffer twice, rinsed with ice-cold water, and dried.
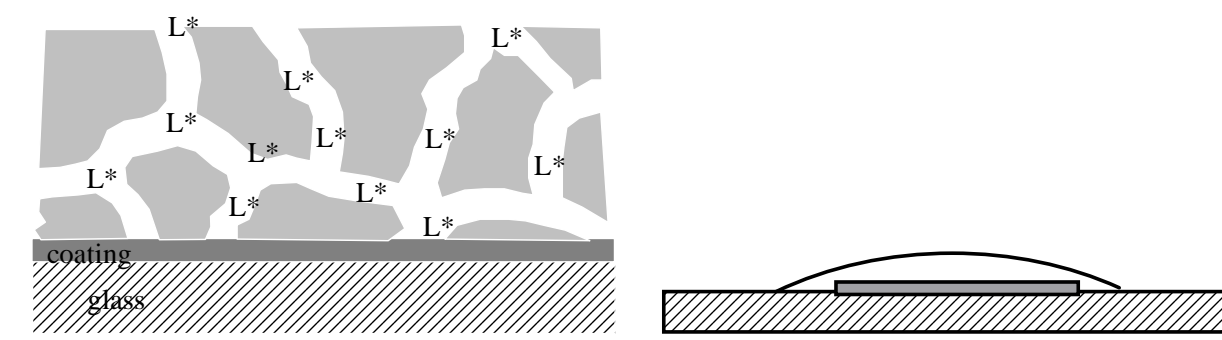


**Figure 37: Scheme of a tissue slide covered with the incubation mixture**[151]

Thereafter, samples were put in an Instant Imager, or placed on Phosphor Imager plates for exposure. According to the research question, it might be sufficient to observe the radioactivity distribution ([$^{18}$F]FE@SUPPY and [$^{18}$F]FE@SUPPY:2), while other studies might demand quantitative estimates ([$^{18}$F]FE@CIT).

# 1.3. AIM OF THE PRESENT THESIS

The technology of PET bases on radioactive molecules, the PET-tracers, which accumulate selectively at target binding sites, e.g. receptors, enzymes and transporters. Hence, these targets can be visualized and quantified non-invasively.

In case of the presented PhD-thesis, three different receptor and transporter targets are described: the dopamine and serotonin transporter -both well known targets since many decades, and, the recently identified adenosine $A_3$ receptor, as a completely new target. For the DAT and SERT, there exists already a wide range of excellent PET- tracers, which is not yet true for the A3R. But, since the A3R is involved in a variety of pathologies, especially neurological, psychiatric, cardiac and oncological diseases (such as solid tumors and metastases), the in-vivo visualisation and quantification of the A3R with PET would be of immense clinical and scientific interest.

In general, the successful and feasible preparation of radiopharmaceuticals, is the first prerequisite for their application in patients. Therefore, it is crucial to develop automated radiosynthetic procedures, to guarantee save and continuous availability of the tracers. Furthermore, in order to have the chance to realize application of newly developed radiopharmaceuticals in humans, a series of preclinical evaluations have to be performed. These evaluations should guarantee tracer safety, and give a first estimate of the in-vivo behaviour of these substances.

The publications, included in this thesis, aimed to contribute to these various aspects of the development and evaluation of the 4 different PET-tracers: The completely new compound [$^{18}$F]FE@SUPPY:2 was aimed to be introduced as a second potential A3R PET-tracer. Radiochemical procedures of [$^{11}$C]DASB, [$^{18}$F]FE@SUPPY and [$^{18}$F]FE@SUPPY:2 were aimed to be developed into fully-automated settings; and [$^{18}$F]FE@SUPPY, [$^{18}$F]FE@SUPPY:2 and [$^{18}$F]FE@CIT were aimed to be preclinically evaluated.

*The first major aim* was the optimization of the radiosynthesis of [$^{11}$C]DASB for routine application for psychiatric and scientifically demanding clinical trials. Thus, this radioligand has to be available on a routine basis in accordance to highest quality requirements.

Hence, we aimed to establish a fully-automated procedure for the synthesis and purification of [$^{11}$C]DASB with a high degree of reliability; to reduce overall synthesis time, while conserving high yields and purity; and to develop a suitable and fast quality control assay to assure safe application. Details and results about these improvements are given in the scientific section in paper 1.

*The second principal aim* was the development and evaluation of suitable PET-tracers for the visualisation and quantification of the adenosine A$_3$ receptor. In this context, it was first aimed, to radiochemically prepare [$^{18}$F]FE@SUPPY:2, the structural analogue of [$^{18}$F]FE@SUPPY, as a second potential A3R PET-tracer. Moreover, it was aimed to automate the radiosyntheses for both potential PET-tracers, and, in addition, as a consequential next step in the development procedure, to evaluate them preclinically. Comparisons of the resulting parameters of both tracers, and, in consequence, the decision upon their suitability as A3R PET-tracers, were the objective of these investigations.

*The third main focus* was the further preclinical evaluation of the fluoroethylated ß-CIT analogue, [$^{18}$F]FE@CIT, which was introduced by our group as a novel potential DAT PET-tracer in 2005. Since the preparation and first evaluation revealed promising results, this study aimed to further prove the suitability of the tracer (for future human application), regarding its in-vitro metabolic and autoradiographic characterisation.

Taken together, for researchers, working in the field of preclinical sciences, it is the major aim to bring new and improved molecules from bench to bedside.

# PART 2

# SPECIFIC TOPICS

# 2. SPECIFIC TOPICS

## 2.1. GENERAL

The thesis aimed in general for PET-tracer development and preclinical evaluation with special emphasis on novel [$^{18}$F]labelled ligands for the adenosine $A_3$ receptor. In the following chapters the results of the different investigations are presented in 5 manuscripts.

The first paper describes the optimization and automatisation of the radiochemical preparation of the well known and widely used SERT tracer [$^{11}$C]DASB. The radiosynthesis was modified into a rapid and simple set-up for an automated high-quality production for routine application of this tracer for various studies in cooperation with the department of psychiatry and psychotherapy.

The second paper deals with the radiochemical preparation of a completely new potential [$^{18}$F]labelled PET-tracer for the A3R, called [$^{18}$F]FE@SUPPY:2. This tracer was developed as a functional isomer of [$^{18}$F]FE@SUPPY, the first PET-tracer for the A3R.

The third paper shows the results of the automation of the radiosyntheses of the new potential A3R PET-tracers [$^{18}$F]FE@SUPPY and [$^{18}$F]FE@SUPPY:2. Furthermore, it also includes first preclinical evaluation parameters of [$^{18}$F]FE@SUPPY:2, and a comparison of the results with those of [$^{18}$F]FE@SUPPY.

The forth manuscript deals with the metabolic characterisation of the A3R PET-tracers [$^{18}$F]FE@SUPPY and [$^{18}$F]FE@SUPPY:2 in-vitro and in-vivo.

The fifth paper includes the metabolic and autoradiographic characterisation of the DAT PET-tracer [$^{18}$F]FE@CIT.

# 2.2. SCIENTIFIC PAPERS

## 2.2.1. AUTHOR´S CONTRIBUTION

I hereby declare to have significantly contributed to the realization of each of the five studies included in the present thesis.

In the first manuscript (*Simple and rapid preparation of [$^{11}$C]DASB with high quality and reliability for routine applications*), I participated in the study design and performed all the radiosyntheses. Additionally, I participated in the analysis and interpretation of the data, as well as in the conception and writing of the manuscript.

Regarding the second manuscript (*Radiosynthesis of a novel potential adenosine A$_3$ receptor ligand, 5-ethyl 2,4-diethyl-3-((2-[$^{18}$F]fluoroethyl)sulfanylcarbonyl)-6-phenylpyridine-5-carboxylate ([$^{18}$F]FE@SUPPY:2)*), I conceived of the study and was involved in the radiosyntheses. Moreover, I carried out the analysis and interpretation of the data, as well as the drafting of the manuscript.

Concerning the third study (*Automatisation and first evaluation of [$^{18}$F]FE@SUPPY:2, an alternative PET-Tracer for the Adenosine A$_3$ Receptor: A Comparison with [$^{18}$F]FE@SUPPY*), I participated in the study design and was involved in the radiosyntheses. Furthermore, I took part in the planning of the bioevaluation study and fully participated in the experiments at the AIT Seibersdorf. Additionally, I took a significant part in the writing of the manuscript.

In the fourth paper (*[$^{18}$F]FE@SUPPY and [$^{18}$F]FE@SUPPY:2 - Metabolic considerations*), I conceived of the study, contributed to the preparation of the radiotracers, and performed the ex-vivo metabolite experiments at the AIT. Moreover, I participated in the carboxylesterase experiments and carried out the data analysis and interpretation of the results, as well as the drafting of the manuscript.

Regarding the fifth study (*Metabolism and autoradiographic evaluation of [$^{18}$F]FE@CIT: a Comparison with [$^{123}$I]ß-CIT and [$^{123}$I]FP-CIT*), I participated in the study design and

performed the autoradiographic experiments. Additionally, I took part in the analysis and interpretation of the data, as well as in the drafting of the manuscript.


Mag. Daniela Häusler                                          Vienna, 03.03.2010

## 2.2.2. PAPER 1

# SIMPLE AND RAPID PREPARATION OF [$^{11}$C]DASB WITH HIGH QUALITY AND RELIABILITY FOR ROUTINE APPLICATIONS.

Authors: **Daniela Haeusler**[1,2], Leonhard Key. Mien[1,2], Lukas Nics[1,3], Johanna Ungersboeck[1,4], Cécile Philippe[1,2], Rupert R. Lanzenberger[5], Kurt Kletter[1], Robert Dudczak[1], Markus Mitterhauser[1,2,6], Wolfgang Wadsak[1,4,*].

[1] Dept of Nuclear Medicine, Medical University of Vienna, Austria

[2] Dept of Pharmaceutical Technology and Biopharmaceutics, University of Vienna, Austria

[3] Dept of Nutritional Sciences, University of Vienna, Austria

[4] Dept of Inorganic Chemistry, University of Vienna, Austria

[5] Dept of Psychiatry and Psychotherapy, Medical University of Vienna, Austria

[6] Hospital Pharmacy of the General Hospital of Vienna, Austria

**Abstract**

[$^{11}$C]DASB combines all major prerequisites for a successful SERT-ligand, providing excellent biological properties and in-vivo behaviour. Thus, we aimed to establish a fully-automated procedure for the synthesis and purification of [$^{11}$C]DASB with a high degree of reliability reducing the overall synthesis time while conserving high yields and purity. The optimized [$^{11}$C]DASB synthesis was applied in more than 60 applications with a very low failure rate (3.2%). We obtained yields up to 8.9GBq (average 5.3 ± 1.6GBq). Time consumption was kept to a minimum, resulting in 43 minutes from end of bombardment to release of the product after quality control.

Form our data, it is evident that the presented method can be implemented for routine preparations of [$^{11}$C]DASB with high reliability.

Key words: serotonin, SERT, PET, carbon-11, radiosynthesis, DASB

## 1. Introduction

The serotonin transporter (SERT) influences and controls extracellular serotonin levels in the synaptic cleft by decreasing the serotonin level through reuptake and is involved in the pathophysiology of psychiatric disorders, e.g. schizophrenia (Joyce et al., 1993), mood disorders (Ichimiya et al., 2002), depression (Meyer et al., 2001, Meyer et al., 2004a, OwensNemeroff, 1994, Parsey et al., 2006a, Reivich et al., 2004) and anxiety (Jarret et al., 2007). Hence, it is one of the main targets for antidepressant drugs, the so called SSRIs (selective serotonin reuptake inhibitors) (Meyer et al., 2001, Meyer et al., 2004b, Reivich et al., 2004, Spindelegger et al., 2008). Consequently, the imaging of the SERT before and after medication with SSRIs would be of great value for a deeper and further understanding of psychiatric disorders (Hesse et al., 2004, Meyer, 2008), the way of action of newly developed anti-psychotics, and could help to improve diagnosis and the planning of treatment.

Imaging with Positron Emission Tomography (PET) allows in vivo measurement of receptors and transporters in humans non-invasively. For the visualisation and quantification of the SERT, highly selective carbon-11 and fluorine-18 labelled PET-tracers have been developed and synthesised, such as [$^{11}$C]McN5256 (Suehiro et al., 1993), [$^{11}$C]DASB (Wilson et al., 2000b), [$^{11}$C]ADAM (Vercouillie et al., 2001) [$^{11}$C]MADAM (Tarkiainen et al., 2001), [$^{11}$C]DAPP (Wilson et al., 2000b), [$^{11}$C]DAPA (Huang et al., 2002), [$^{11}$C]AFM (Huang et al., 2004a), [$^{11}$C]AFA (Huang et al., 2004b), [$^{11}$C]AFE (Zhu et al., 2004), [$^{18}$F]ACF (Oya et al., 2002) and [$^{18}$F]F-ADAM (Shiue et al., 2003a, Shiue et al., 2003b), respectively. Structures are given in Figure1. So far, only, [$^{11}$C]McN5256 (Frankle et al., 2004, McCann et al., 2005, Parsey et al., 2000, Parsey et al., 2006a, Szabo et al., 1995), [$^{11}$C]DASB (Frankle et al., 2004, Houle et al., 2000, McCann et al., 2005, Meyer et al., 2001, Meyer et al., 2004b, Meyer, 2007, Parsey et al., 2006b, Praschak-Rieder et al., 2008), [$^{11}$C]DAPP (Houle et al., 2000) and [$^{11}$C]MADAM (Chalon et al., 2003, Jovanovic et al., 2008, Lundberg et al., 2005, Lundberg et al., 2006, Lundberg et al., 2007a, Lundberg et al., 2007b) have found their way into clinical measurements.

The best established and explored SERT ligand for PET-imaging is [$^{11}$C]DASB (3-amino-4-[N-methyl-N-[$^{11}$C]methyl-amino-methylphenylsulfanyl]-benzonitrile). It was firstly introduced and synthesised by Wilson et al. in 2000 (Wilson et al., 2000a, Wilson et al., 2000b) and

showed promising properties ($K_i$= 1.1nM, signal/noise ratio 7.9; cerebellar clearance 15.6min; $logP^{7.4}$ 2.7) (Wilson et al., 2000b).

DASB combines several advantages which makes it an excellent SERT-tracer for clinical use:

(1) high affinity (1.1nM);

(2) excellent selectivity (NET/SERT= 1230 and DAT/SERT= 1300);

(3) high specific binding;

(4) reversible, high brain uptake; and

(5) binding equilibrium within a reasonable timeframe.

Since, DASB provides all the prerequisites for a reliable quantification of the SERT binding potential in vivo, there is a great need for this specific SERT-tracer.

The radiosynthesis of [$^{11}$C]DASB was described already in 2000 (Wilson et al., 2000b) converting the secondary amine precursor (MASB) with freshly prepared [$^{11}$C]methyliodide into the derived dipenyl-sulfid-molecule. (Reaction scheme, see figure 2) A short time later, an evaluation of the reaction parameters was performed. (Solbach et al., 2004) Additionally, a synthetic procedure using [$^{11}$C]methyl triflate was described in 2004 (Belanger et al., 2004).

Nevertheless, for routine application, the production has to fulfil even more requirements than just high yields and purity. Full-automation to reduce the radiation burden for the operator, a low probability of failed syntheses and a short overall production time are also of great importance.

Thus, we aimed

(1) to establish a fully-automated procedure for the synthesis and purification of [$^{11}$C]DASB with a high degree of reliability;

(2) to reduce overall synthesis time while conserving high yields and purity; and

(3) to develop a suitable and fast quality control assay to assure safe application in a routine setting.

Hence, our investigation should provide a simple method for the quick preparation of [$^{11}$C]DASB with high quality and reliability.

## 2. Experimental

### 2.1. Materials

All chemicals and solvents were obtained from commercial sources with analytical grade and used without further purification.

Iodine (sublimated grade for analysis; ACS, Pharm.Eur.) was purchased from Merck (Darmstadt, Germany; product number: 1.04761). MASB precursor (N-Methyl-2-(2-amino-4-cyanophenylthio)-benzylamine) and DASB reference compound (3-amino-4-(2-dimethyl-amino-methylphenylsulfanylbenzonitrile) were obtained from ABX (ABX- Advanced Biochemical Compounds Radeberg, Germany). Dimethylsulfoxide (DMSO, >99.9%, anhydrous) was obtained from Sigma Aldrich (Vienna, Austria). Acetonitrile, ammonium formate, ammonium acetate and ethanol (absolute) were purchased from Merck (Darmstadt, Germany). C18plus SepPak® cartridges were purchased from Waters (Waters® Associates Milford, MA, USA). Low-protein binding Millex GS® 0.22 μm sterile filters were pruchased from Millipore® (Bedford, MA, USA). Semipreparative HPLC (High performance liquid chromatography) column (Supelcosil™ LC-ABZ⁺; 5μm, 250mm x 10mm; Nr. 59179) was purchased from Supelco (*Bellfonte, PA, USA)*. Analytical HPLC-column (Prodigy 5μ Phenyl-3 (PH-3); 250 x 4.6mm) was obtained from Phenomenex (Aschaffenburg, Germany). GC capillary column (HP-Innowax 30m x 0.32mm x 0.25μm; Nr. 19091N-113) was from Agilent (Santa Clara, CA, USA).

### 2.2. Instruments

For the fully automated preparation of [$^{11}$C]DASB, a C11-methylation PET-synthesizer (*formerly:* Nuclear Interface®, *now:* General Electric Medical Systems, Uppsala, Sweden) was used and remotely controlled via GINAstar software (Raytest Isotopenmessgeräte GmbH, Straubenhardt, Germany) installed on a standard PC.

Semipreparative HPLC was performed using the original Nuclear Interface® PET synthesizer chromatographic equipment. Analytical HPLC was performed with a Merck-Hitachi LaChrom

system consisting of a L-7100 pump, a Merck-Hitachi LaChrom L-7400 UV detector (operated at 254nm) and a lead shielded NaI-radiodetector (Berthold technologies, Bad Wildbach, Germany) for radiation detection. Gas chromatography was performed using an HP 6890 series system (Agilent, Santa Clara, CA, USA) with flame ionisation detector (FID).

## 2.3. Fully automated radiosynthesis

A scheme of the synthesis module is presented in Figure 3. All details given in the following section refer to this figure.

### 2.3.1. Preparation of the synthesis module

All parts prior to HPLC-purification (reactor, HPLC injector, tubing) were rinsed with DMSO or acetone and then dried with a stream of helium. Parts after HPLC (SPE, product collection vial, product outlet tubing) were cleaned using ethanol and physiological saline.

Vessels were filled as followed:

Vial 2: 1mL of HPLC solvent for quenching of the reaction;

Flask 3: 100mL of sterile water for dilution of the lipophilic HPLC fraction;

Vial 4: 5mL of saline solution 0.9% for final rinsing of the SPE cartridge and dilution of the eluate;

Vial 5: 1.5mL ethanol for elution of the SPE cartridge;

Vial 6: 10mL sterile water for washing the SPE cartridge.

A C18plus SepPak® cartridge was preconditioned using ethanol and sterile water, dried and connected to its designated position. The product collection vial was filled with 4mL 0.9% saline, 1mL 3% saline and 1mL phosphate buffer (125mM). The reactor was filled with 1mg MASB dissolved in 0.5mL DMSO and subsequently placed into the heating block.

### 2.3.2. Production of [$^{11}$C]CH$_3$I

[$^{11}$C]CO$_2$ was produced at the GE PETtrace cyclotron (General Electric Medical Systems, Uppsala, Sweden) by irradiation of a gas target containing N$_2$ and 0.5% O$_2$ using the $^{14}$N(p,$\alpha$)$^{11}$C nuclear reaction with 16.5MeV protons. Typical beam currents were 50-60 µA

and irradiation was stopped as soon as the desired activity level was reached (e.g. 70-90 GBq). [$^{11}$C]CH$_3$I was produced using the gas phase conversion described by Larsen et al. in 1997 in an automated synthesis module (MeI-Microlab, General Electric Medical Systems). (Larsen et al., 1997) Briefly, [$^{11}$C]CO$_2$ was trapped on molecular sieve (4Å) and converted to [$^{11}$C]CH$_4$ within 120 seconds in presence of Ni catalyst (Shimalilte Ni reduced, Shimadzu) and hydrogen at 360°C. Subsequently, [$^{11}$C]CH$_4$ was reacted with elemental iodine at 720°C to [$^{11}$C]CH$_3$I and recirculated for 300 seconds. [$^{11}$C]CH$_3$I was trapped online on Porapak N in a small glass column and finally released by heating to 190°C in a stream of helium (45 mL/min) within 160 seconds.

### 2.3.3. Preparation of [$^{11}$C]DASB

Gaseous [$^{11}$C]methyl iodide produced by the MeI-Microlab module was delivered through V10 into the reactor of the previously prepared synthesizer system and trapped on-line in the reaction mixture containing 1mg MASB in 500µL of DMSO at 22°C. The reactor was heated to 100°C and kept at this temperature for 2min to achieve conversion of MASB to [$^{11}$C]DASB. After cooling down to room temperature, the reaction mixture was quenched by addition of 1mL HPLC-eluent (through V2) and subsequently transferred to the 5mL injection loop of the HPLC-system through V11 passing the fluid detector.

### 2.3.4. Product purification

Injection of the crude reaction mixture to the semi-preparative RP-HPLC column was controlled by an automated fluid detector. Semi-preparative HPLC was performed with acetonitrile and 0.1M ammonium acetate (40/60; v/v) as mobile phase with a flow of 8mL/min. Chromatograms were registered using an UV-detector (254nm) and a NaI radioactivity detector in series. An example is given in Figure 4.

The [$^{11}$C]DASB fraction was cut into flask (3) through V7 and diluted with 100mL water. The resulting solution was then pushed over a C18plus SepPak®. After washing with 10mL water (Vial 6) the pure product was completely eluted with 1.5mL ethanol (Vial 5) and 5mL 0.9% saline (Vial 4). Formulation was done with a further 4mL saline solution 0.9%, 1mL saline solution 3% and 1mL physiological phosphate buffer (125mM) in the product collection vial.

This final solution was transferred to a shielded laminar-air-flow hot cell and, there, sterile-filtered (0.22μm) into a sterile 25mL vial containing another 5 mL of saline solution 0.9%.

## 2.4. Quality control

Chemical and radiochemical impurities were detected using radio-HPLC according to the monograph in the European Pharmacopoeia (2005b).

Quality was assessed with analytical RP-HPLC; acetonitrile and 0.1M ammonium formate (55/45; v/v) were used as the mobile phase with a flow rate of 2mL/min. The whole quality control was completed within 8 minutes, the retention time of the precursor (MASB) was 4.4-4.8min (k´=2.2-2.7) and the product [11C]DASB was eluted with a retention time of 6.7-7.2min (k´=3.8-4.6). The chemical identity of [11C]DASB was determined by co-injection of the unlabeled reference compound, [12C]DASB. To check for contaminations with higher retention factors, we investigated the RP-HPLC chromatograms for 20 min but did not find any substance eluting from the HPLC after 8 min.

Residual solvents were analyzed by gas chromatography (GC) (carrier gas: He, flow 2.7mL/min, 45°C (2.5min); 20°C/min to 110°C; 30°C/min to 200; 200°C (10min); FID: 270°C). Osmolality and pH were determined to assure safe administration using standard methods.

Radionuclidic purity was assessed by recording of the corresponding gamma spectrum (annihilation radiation at 511keV and sum peak at 1022keV) and additional measurement of the physical half-life (20.2 ± 1.5min).

Testing of sterility and concentration of bacterial endotoxines was performed using standard protocols at the Department of Microbiology (General Hospital of Vienna).

## 3. Results

So far, we performed 60 successful radiosyntheses of [11C]DASB using the optimum reaction conditions. We obtained high average yields of 5.3 ± 1.6 GBq (arithmetic mean ± SD; range: 2.6 - 8.9GBq). Radiochemical yields based on [11C]CH$_3$I, (corrected for decay) were 66.3 ± 6.9% with a specific radioactivity (A$_s$) of 86.8 ± 24.3 GBq/μmol (both at the end of synthesis, EOS). Overall, the whole synthetic procedure – including [11C]methyl iodide production,

radiosynthesis, HPLC and SPE purification, formulation and sterile filtration - took 35 ± 3 min. Semi-preparative HPLC revealed excellent separation of MASB and DASB: retention times were 2.9–3.4min (k`= 0.9–1.3) for MASB and 6.4–7.1min (k`= 3.3–3.7) for DASB, respectively (Figure 4). SPE purification resulted in a recovery of >98% using 1.5 mL of ethanol followed by 5 mL of saline solution. Typical loss during sterile filtration was 200-350 MBq (4-8% of the product activity). From a total of 62 preparations for patient routine, we observed two failures, both due to problems with the HPLC injection valve.

The product was obtained as a sterile solution (total volume: 17.5mL) ready for application. Radiochemical purity always exceeded 98% as determined by radio-HPLC. Residual solvents as determined by GC were found to be 4ppm DMSO and 20ppm acetonitrile. Typical HPLC and GC chromatograms are given in Figure 5. MASB content was 0.06 ± 0.04µg/mL; pH was 7.54 ± 0.16 and osmolality was 286 ± 20mosmol/kg. Endotoxines were found to be below 0.5EU/ml and all samples passed the test for sterility.


## 4. Discussion

Given, that a successful PET tracer requires more than high affinity to the binding site, also high selectivity, high specific to non-specific binding ratio, suitable pharmacokinetics and, moreover, a good synthetic availability are essential for application in a routine setting. [11C]DASB combines excellent biological properties (high affinity and selectivity to the SERT) with distinguished in-vivo behaviour (low non-specific binding, suitable pharmacokinetical profile). Since it is used in PET-centres all over the world for routine applications, e.g. for PET imaging of psychiatric disorders, it is crucial to have a reliable, simple and quick radiosynthesis at hand, providing high yields with high purity.

Set-up of the preparation was straight forward and needed only 10 runs prior to productions for human use. Since the short half-life of carbon-11 (20.4min) requires a rapid preparation and purification in the radiochemical process, we were interested in a significant reduction of the overall synthesis time. We were able to reduce it from 45min to 35min. Furthermore, we were able to further optimize the amount of precursor used in the synthesis as compared to the literature (Solbach et al., 2004). A 50% reduction, from 4mg/mL to 2mg/mL, was applied without loss of reactivity. Radiochemical yields in our presented work were 66.3 ± 6.9%, overall, using a fully automated set-up. This is a significant improvement as compared

to previously published data (Solbach et al., 2004) where 43 ± 3%, overall yield, was reported in the case of automation. Absolute yields were also improved by 30%.

As shown in Figure 4, the separation of precursor and product was excellent. In the final product solution, we observed only 0.06µg/mL MASB. Furthermore, separation of residual solvents (e.g. acetonitrile, DMSO) was satisfying, resulting in contaminations far below the limits set by the European Pharmacopoiea (2005a). Consequently, all of our product solutions could be used in human PET applications. Set-up of the quality control (QC) was simple, using only standard methods and equipment. The whole QC procedure was performed within 8 minutes.

The fully-automated synthesis and purification of [$^{11}$C]DASB was performed with extremely high reliability. The failure rate was only 3.2% (2 out of 62). These two failed syntheses were both due to technical problems with the injection valve of the semi-preparative HPLC (attenuator did not switch from load to inject). No failure was observed due to lack in chemical reactivity or operator mishandling.

Overall, we were able

(1) to establish a fully-automated procedure for the synthesis and purification of [$^{11}$C]DASB with a high degree of reliability;

(2) to reduce overall synthesis time while conserving high yields and purity; and

(3) to develop a suitable and fast quality control assay to assure safe application in a routine setting.

Hence, our investigations provide the basis for a simple and quick preparation of [$^{11}$C]DASB with high reliability for routine PET applications.

**5. Conclusion**

We established the rapid preparation and purification of [$^{11}$C]DASB on a commercial synthesizer module. The presented method was applied in more than 60 applications with a very low failure rate (3.2%). Time consumption was kept to a minimum, resulting in 43 minutes from EOB to release of the product after QC. Thus, the presented work should provide the basis for routine preparations of [$^{11}$C]DASB with high reliability.

## 6. Acknowledgements

## 7. References

[1]   Residual   Solvents   (Lösungsmittel-Rückstände;   5.0/5.04.00.00).   In:   European Pharmacopoeia (Europäisches Arzneibuch). 5th edition (5. Ausgabe Grundwerk), official Austrian version. Vienna:Verlag Österreich GmbH; 2005a, p. 729-734.

[2]   Radiopharmaceutical   Preparations   (Radiopharmaceutica,   5.0/0125).   In:   European Pharmacopoeia (Europäisches Arzneibuch). 5th edition (5. Ausgabe Grundwerk), official Austrian version. Vienna:Verlag Österreich GmbH; 2005b, p. 823-831.

[3]  M.J. Belanger, N.R. Simpson, T. Wang, R.L. Van Heertum, J.J. Mann, R.V. Parsey, Biodistribution and radiation dosimetry of [11C]DASB in baboons, Nucl Med Biol. 31 (2004) 1097-1102.

[4] S. Chalon, J. Tarkiainen, L. Garreau, H. Hall, P. Emond, J. Vercouillie, L. Farde, P. Dasse, K. Varnas, J.C. Besnard, C. Halldin, D. Guilloteau, Pharmacological characterization of N,N-dimethyl-2-(2-amino-4-methylphenyl thio)benzylamine as a ligand of the serotonin transporter with high affinity and selectivity, J Pharmacol Exp Ther. 304 (2003) 81-87.

[5] W.G. Frankle, Y. Huang, D.R. Hwang, P.S. Talbot, M. Slifstein, R. Van Heertum, A. Abi-Dargham, M. Laruelle, Comparative evaluation of serotonin transporter radioligands 11C-DASB and 11C-McN 5652 in healthy humans, J Nucl Med. 45 (2004) 682-694.

[6] S. Hesse, H. Barthel, J. Schwarz, O. Sabri, U. Muller, Advances in in vivo imaging of serotonergic neurons in neuropsychiatric disorders, Neurosci Biobehav Rev. 28 (2004) 547-563.

[7] S. Houle, N. Ginovart, D. Hussey, J.H. Meyer, A.A. Wilson, Imaging the serotonin transporter with positron emission tomography: initial human studies with [11C]DAPP and [11C]DASB, Eur J Nucl Med. 27 (2000) 1719-1722.

[8] Y. Huang, D.R. Hwang, Z. Zhu, S.A. Bae, N. Guo, Y. Sudo, L.S. Kegeles, M. Laruelle, Synthesis and pharmacological characterization of a new PET ligand for the serotonin transporter:  [11C]5-bromo-2-[2-(dimethylaminomethylphenylsulfanyl)]phenylamine ([11C]DAPA), Nucl Med Biol. 29 (2002) 741-751.

[9] Y. Huang, D.R. Hwang, S.A. Bae, Y. Sudo, N. Guo, Z. Zhu, R. Narendran, M. Laruelle, A new positron emission tomography imaging agent for the serotonin transporter: synthesis, pharmacological characterization, and kinetic analysis of [11C]2-[2-(dimethylaminomethyl)phenylthio]-5-fluoromethylphenylamine ([11C]AFM), Nucl Med Biol. 31 (2004a) 543-556.

[10] Y. Huang, R. Narendran, S.A. Bae, D. Erritzoe, N. Guo, Z. Zhu, D.R. Hwang, M. Laruelle, A PET imaging agent with fast kinetics: synthesis and in vivo evaluation of the serotonin transporter ligand [11C]2-[2-dimethylaminomethylphenylthio)]-5-fluorophenylamine ([11C]AFA), Nucl Med Biol. 31 (2004b) 727-738.

[11] T. Ichimiya, T. Suhara, Y. Sudo, Y. Okubo, K. Nakayama, M. Nankai, M. Inoue, F. Yasuno, A. Takano, J. Maeda, H. Shibuya, Serotonin transporter binding in patients with mood disorders: a PET study with [11C](+)McN5652, Biol Psychiatry. 51 (2002) 715-722.

[12] M.E. Jarret, R. Kohen, K.C. Cain, R.L. Burr, A. Poppe, G.P. Navaja, M.M. Heitkemper, Relationship of SERT polymorphisms to depressive and anxiety symtoms in irritable bowel syndrome, Biol Res Nurs. 9 (2007) 161-169.

[13] H. Jovanovic, J. Lundberg, P. Karlsson, A. Cerin, T. Saijo, A. Varrone, C. Halldin, A.L. Nordstrom, Sex differences in the serotonin 1A receptor and serotonin transporter binding in the human brain measured by PET, Neuroimage. 39 (2008) 1408-1419.

[14] J.N. Joyce, A. Shane, N. Lexow, A. Winokur, M.F. Casanova, J.E. Kleinman, Serotonin uptake sites and serotonin receptors are altered in the limbic system of schizophrenics, Neuropsychopharmacology. 8 (1993) 315-336.

[15] P. Larsen, J. Ulin, K. Dahlstrom, M. Jensen, Synthesis of [11C]Iodomethane by Iodination of [11C]Methane, Appl Radiat Iost. 48 (1997) 153-157.

[16] J. Lundberg, I. Odano, H. Olsson, C. Halldin, L. Farde, Quantification of 11C-MADAM binding to the serotonin transporter in the human brain, J Nucl Med. 46 (2005) 1505-1515.

[17] J. Lundberg, C. Halldin, L. Farde, Measurement of serotonin transporter binding with PET and [11C]MADAM: a test-retest reproducibility study, Synapse. 60 (2006) 256-263.

[18] J. Lundberg, J. Borg, C. Halldin, L. Farde, A PET study on regional coexpression of 5-HT1A receptors and 5-HTT in the human brain, Psychopharmacology 195 (2007a) 425-433.

[19] J. Lundberg, J.S. Christophersen, K.B. Petersen, H. Loft, C. Halldin, L. Farde, PET measurement of serotonin transporter occupancy: a comparison of escitalopram and citalopram, Int J Neuropsychopharmacol. 10 (2007b) 777-785.

[20] U.D. McCann, Z. Szabo, E. Seckin, P. Rosenblatt, W.B. Mathews, H.T. Ravert, R.F. Dannals, G.A. Ricaurte, Quantitative PET studies of the serotonin transporter in MDMA users and controls using [11C]McN5652 and [11C]DASB, Neuropsychopharmacology. 30 (2005) 1741-1750.

[21] J.H. Meyer, A.A. Wilson, N. Ginovart, V. Goulding, D. Hussey, K. Hood, S. Houle, Occupancy of serotonin transporters by paroxetine and citalopram during treatment of depression: a [(11)C]DASB PET imaging study, Am J Psychiatry. 158 (2001) 1843-1849.

[22] J.H. Meyer, S. Houle, S. Sagrati, A. Carella, D.F. Hussey, N. Ginovart, V. Goulding, J. Kennedy, A.A. Wilson, Brain serotonin transporter binding potential measured with carbon 11-labeled DASB positron emission tomography: effects of major depressive episodes and severity of dysfunctional attitudes, Arch Gen Psychiatry. 61 (2004a) 1271-1279.

[23] J.H. Meyer, A.A. Wilson, S. Sagrati, D. Hussey, A. Carella, W.Z. Potter, N. Ginovart, E.P. Spencer, A. Cheok, S. Houle, Serotonin transporter occupancy of five selective serotonin reuptake inhibitors at different doses: an [11C]DASB positron emission tomography study, Am J Psychiatry. 161 (2004b) 826-835.

[24] J.H. Meyer, Imaging the serotonin transporter during major depressive disorder and antidepressant treatment, J Psychiatry Neurosci. 32 (2007) 86-102.

[25] J.H. Meyer, Applying neuroimaging ligands to study major depressive disorder, Semin Nucl Med. 38 (2008) 287-304.

[26] M.J. Owens, C.B. Nemeroff, Role of serotonin in the pathophysiology of depression: focus on the serotonin transporter, Clin Chem. 40 (1994) 288-295.

[27] S. Oya, S.R. Choi, H. Coenen, H.F. Kung, New PET imaging agent for the serotonin transporter: [(18)F]ACF (2-[(2-amino-4-chloro-5-fluorophenyl)thio]-N,N-dimethyl-benzenmethanamine), J Med Chem. 45 (2002) 4716-4723.

[28] R.V. Parsey, L.S. Kegeles, D.R. Hwang, N. Simpson, A. Abi-Dargham, O. Mawlawi, M. Slifstein, R.L. Van Heertum, J.J. Mann, M. Laruelle, In vivo quantification of brain serotonin transporters in humans using [11C]McN 5652, J Nucl Med. 41 (2000) 1465-1477.

[29] R.V. Parsey, R.S. Hastings, M.A. Oquendo, Y.Y. Huang, N. Simpson, J. Arcement, Y. Huang, R.T. Ogden, R.L. Van Heertum, V. Arango, J.J. Mann, Lower serotonin transporter binding potential in the human brain during major depressive episodes, Am J Psychiatry. 163 (2006a) 52-58.

[30] R.V. Parsey, A. Ojha, R.T. Ogden, K. Erlandsson, D. Kumar, M. Landgrebe, R. Van Heertum, J.J. Mann, Metabolite considerations in the in vivo quantification of serotonin transporters using 11C-DASB and PET in humans, J Nucl Med. 47 (2006b) 1796-1802.

[31] N. Praschak-Rieder, M. Willeit, A.A. Wilson, S. Houle, J.H. Meyer, Seasonal variation in human brain serotonin transporter binding, Arch Gen Psychiatry. 65 (2008) 1072-1078.

[32] M. Reivich, J.D. Amsterdam, D.J. Brunswick, C.Y. Shiue, PET brain imaging with [11C](+)McN5652 shows increased serotonin transporter availability in major depression, J Affect Disord. 82 (2004) 321-327.

[33] G.G. Shiue, S.R. Choi, P. Fang, C. Hou, P.D. Acton, C. Cardi, J.R. Saffer, J.H. Greenberg, J.S. Karp, H.F. Kung, C.Y. Shiue, N,N-dimethyl-2-(2-amino-4-(18)F-fluorophenylthio)-benzylamine (4-(18)F-ADAM): an improved PET radioligand for serotonin transporters, J Nucl Med. 44 (2003a) 1890-1897.

[34] G.G. Shiue, P. Fang, C.Y. Shiue, Synthesis of N,N-dimethyl-2-(2-amino-4-[18F]fluorophenylthio)benzylamine as a serotonin transporter imaging agent, Appl Radiat Isot. 58 (2003b) 183-191.

[35] C. Solbach, G. Reischl, H.J. Machulla, Determination of reaction parameters for the synthesis of the serotonin transporter ligand [11C]DASB: Application to a remotely controlled high yield synthesis, Radiochimica Acta. 92 (2004) 341-344.

[36] C. Spindelegger, R. Lanzenberger, W. Wadsak, L.K. Mien, P. Stein, M. Mitterhauser, U. Moser, A. Holik, L. Pezawas, K. Kletter, S. Kasper, Influence of escitalopram treatment on 5-HT(1A) receptor binding in limbic regions in patients with anxiety disorders, Mol Psychiatry. (2008) 1-11.

[37] M. Suehiro, U. Scheffel, R.F. Dannals, H.T. Ravert, G.A. Ricaurte, H.N. Wagner, Jr., A PET radiotracer for studying serotonin uptake sites: carbon-11-McN-5652Z, J Nucl Med. 34 (1993) 120-127.

[38] Z. Szabo, P.F. Kao, U. Scheffel, M. Suehiro, W.B. Mathews, H.T. Ravert, J.L. Musachio, S.E. Kim, G.A. Ricaurte, Positron emission tomography imaging of serotonin transporters in the human brain using [11C](+)McN5652, Synapse. 20 (1995) 37-43.

[39] J. Tarkiainen, J. Vercouillie, P. Emond, J. Sandell, J. Hiltunen, Y. Frangin, D. Guilloteau, C. Halldin, Carbon-11 labelling of MADAM in two different positions: a highly selective PET radioligand for the serotonin transporter, J Labelled Cpd Radiopharm. 44 (2001) 1013-1023.

[40] J. Vercouillie, J. Tarkiainen, C. Halldin, P. Emond, S. Chalon, J. Sandell, O. Langer, D. Guilloteau, Precursor synthesis and radiolabelling of [11C]ADAM: A potential radioligand for the serotonin transporter exploration by PET, J Labelled Cpd Radiopharm. 44 (2001) 113-120.

d[41] A.A. Wilson, A. Garcia, L. Jin, S. Houle, Radiotracer synthesis from [((11)C)-iodomethane: a remarkably simple captive solvent method, Nucl Med Biol. 27 (2000a) 529-532.

[42] A.A. Wilson, N. Ginovart, M. Schmidt, J.H. Meyer, P.G. Threlkeld, S. Houle, Novel radiotracers for imaging the serotonin transporter by positron emission tomography: synthesis, radiosynthesis, and in vitro and ex vivo evaluation of (11)C-labeled 2-(phenylthio)araalkylamines, J Med Chem. 43 (2000b) 3103-3110.

[43] Z. Zhu, N. Guo, R. Narendran, D. Erritzoe, J. Ekelund, D.R. Hwang, S.A. Bae, M. Laruelle, Y. Huang, The new PET imaging agent [11C]AFE is a selective serotonin transporter ligand with fast brain uptake kinetics, Nucl Med Biol. 31 (2004) 983-994.

## 8. Figure Captions

**Figure 1:** Chemical structures of various important SERT-tracers.

**Figure 2:** Reaction scheme of the radiosynthesis of [$^{11}$C]DASB.

**Figure 3:** Illustration of the automated procedure for the radiosynthesis and purification of [$^{11}$C]DASB with a commercial C11-synthesizer. For details in set-up and processing refer to section 2.3.

**Figure 4:** Typical chromatograms of the product purification via semi-preparative RP-HPLC: (a) Radioactivity detector and (b) UV detector @ 254nm.

**Figure 5:** Typical chromatograms of the quality control (QC) of [$^{11}$C]DASB:

(a) reference compounds: MASB (1µg/ml) and DASB (1µg/ml) in acetonitrile – HPLC (UV detector, 254nm):

(b) final product solution: HPLC (Radioactivity detector) showing radiochemical purity (>98%)

(c) final product solution: HPLC (UV detector, 254nm) showing chemical purity and content of unlabelled DASB

(d) final product solution: GC (FID detector) showing residual solvents. Acetone peak results from the initial washing procedure of the synthesizer parts.
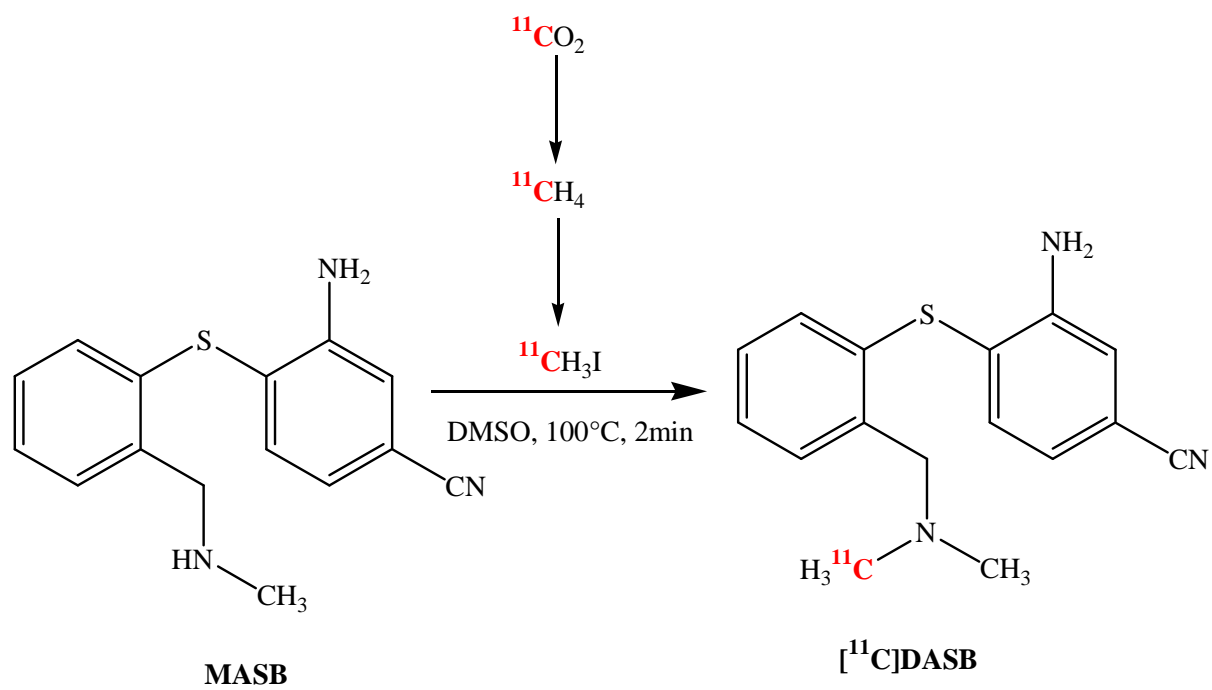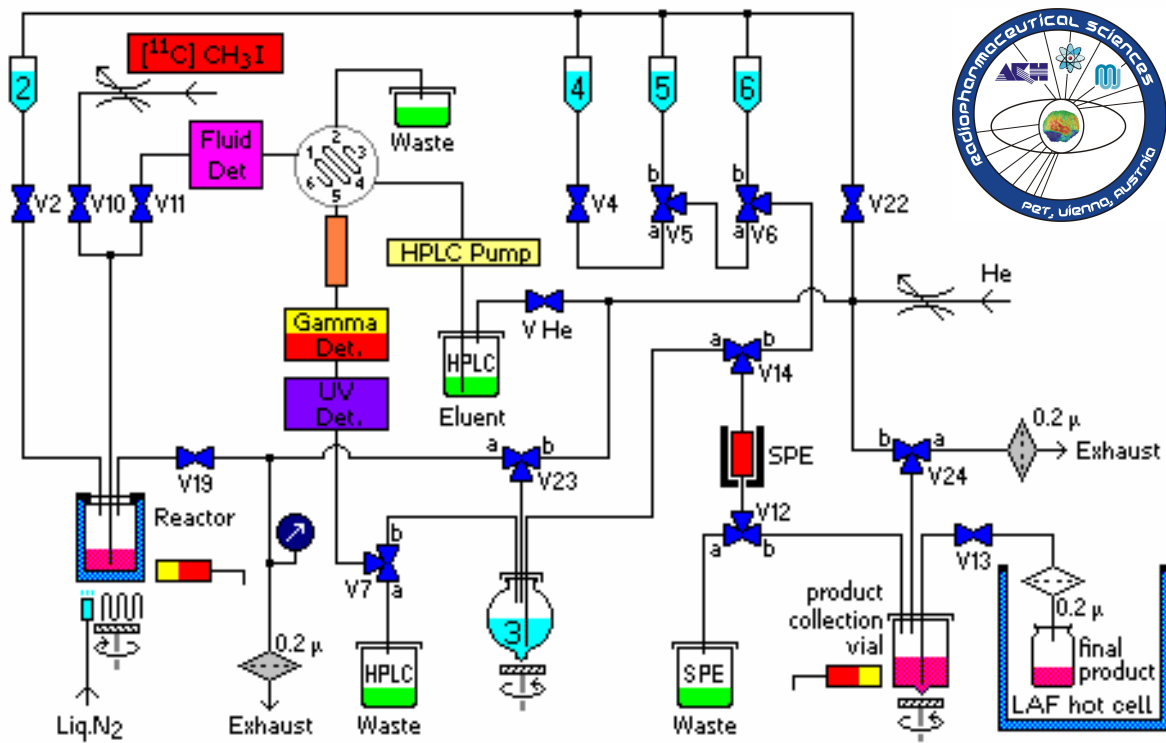
**[¹¹C]McN(+)5652**

**[¹¹C]DASB**

**[¹¹C]MADAM**

**[¹¹C]ADAM**

**4-[¹⁸F]ADAM**

**[¹¹C]DAPA**

**[¹¹C]AFM**

**[¹¹C]AFA**

**[¹¹C]DAPP**

**[¹¹C]AFE**

**[¹⁸F]ACF**

**Figure 1**

**Figure 2**

**Figure 3**
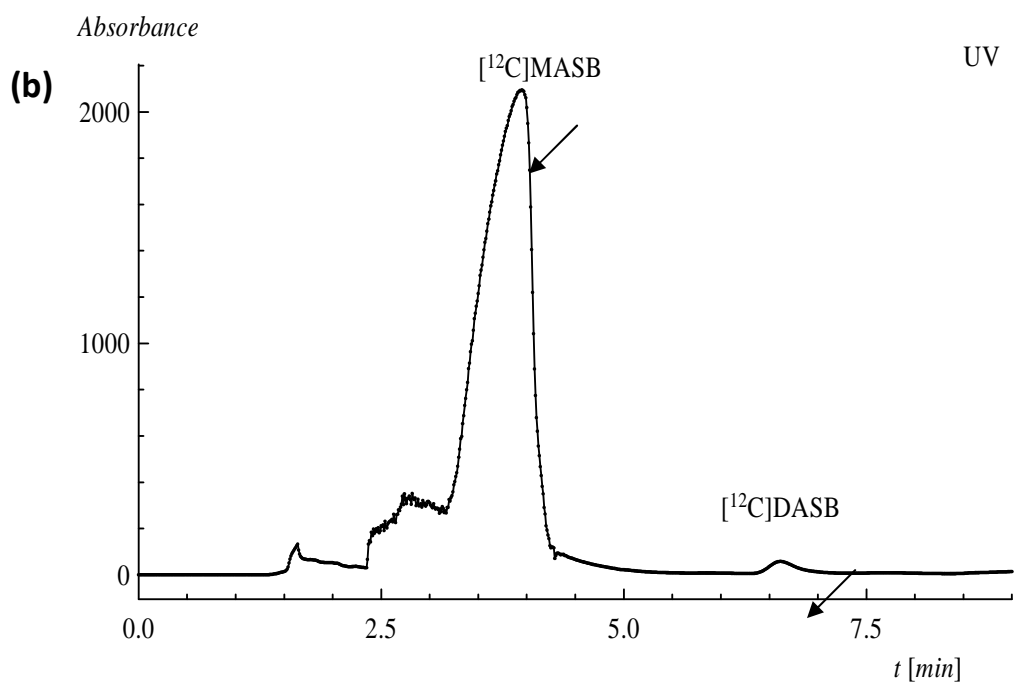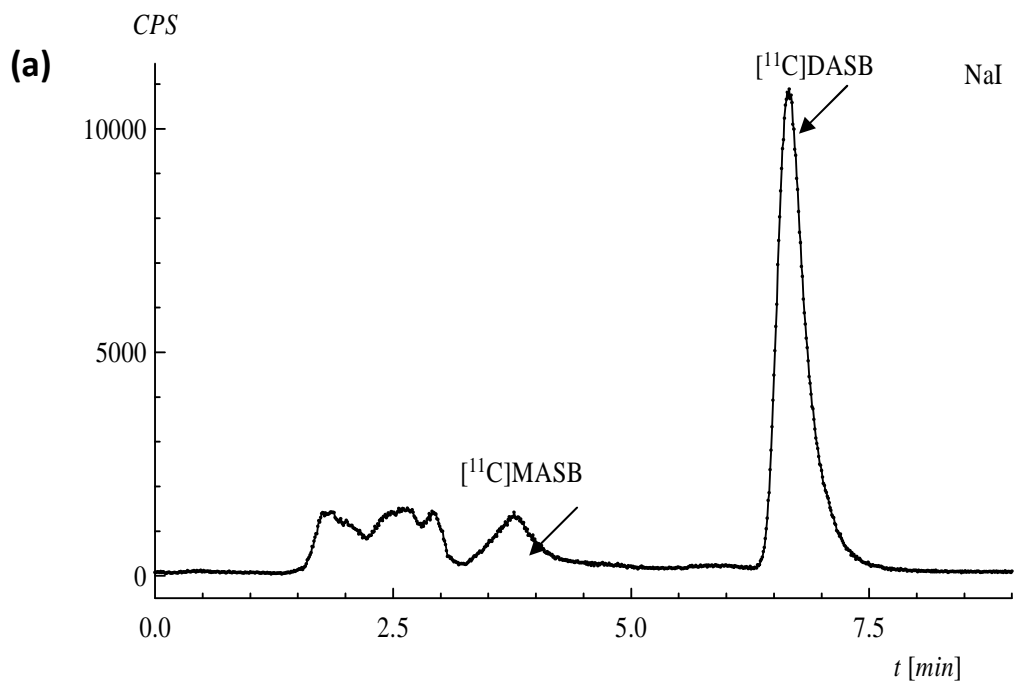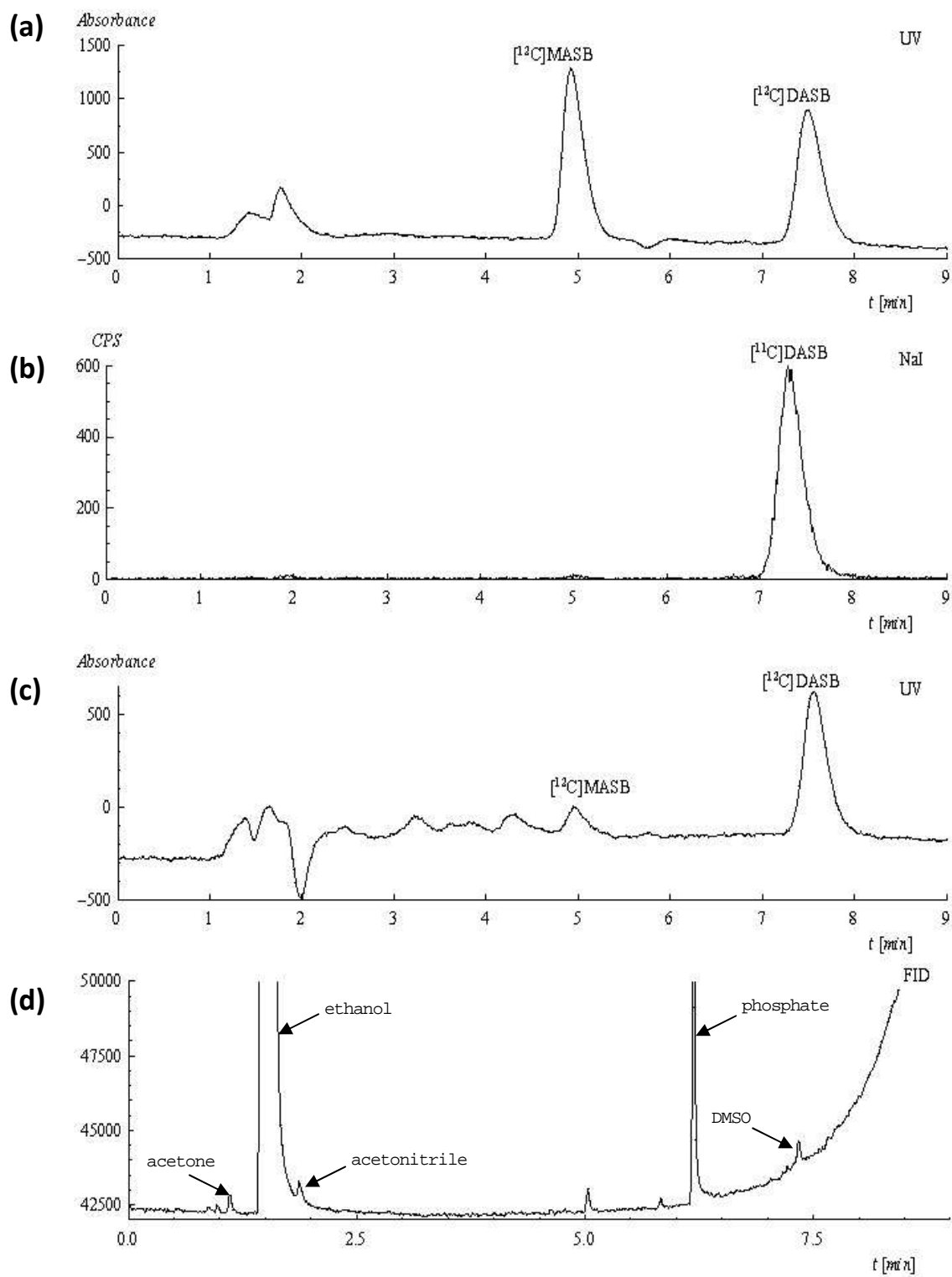
**(a)**

CPS

[¹¹C]DASB — NaI

[¹¹C]MASB

**(b)**

Absorbance

[¹²C]MASB — UV

[¹²C]DASB

**Figure 4**

**Figure 5**

# RADIOSYNTHESIS OF A NOVEL POTENTIAL ADENOSINE A$_3$ RECEPTOR LIGAND, 5-ETHYL 2,4-DIETHYL-3-((2-[$^{18}$F]FLUOROETHYL) SULFANYLCARBONYL)-6-PHENYL PYRIDINE-5-CARBOXYLATE ([$^{18}$F]FE@SUPPY:2).

Authors: **Daniela Haeusler**[1,2], Markus Mitterhauser[1,2,3], Leonhard-Key Mien[1,2,4], Karem Shanab[5], Rupert R Lanzenberger[4], Eva Schirmer[1,5], Johanna Ungersboeck[1,6], Lukas Nics[1,7], He lmut Spreitzer[5], Helmut Viernstein[2], Robert Dudczak[1], Kurt Kletter[1], Wolfgang Wadsak[1,6,*].

[1] Dept of Nuclear Medicine, Medical University of Vienna, Austria

[2] Dept of Pharmaceutical Technology and Biopharmaceutics, University of Vienna, Austria

[3] Hospital Pharmacy of the General Hospital of Vienna, Austria

[4] Dept of Psychiatry and Psychotherapy, Medical University of Vienna, Austria

[5] Dept of Drug and Natural Product Synthesis, University of Vienna, Austria

[6] Dept of Inorganic Chemistry, University of Vienna, Austria

[7] Dept of Nutritional Sciences, University of Vienna, Austria

**Summary**

Since, to date very limited information on the distribution and function of the adenosine $A_3$ receptor is available, the development of suitable radioligands is needed. Recently, we introduced [$^{18}$F]FE@SUPPY (5-(2-[$^{18}$F]fluoroethyl) 2,4-diethyl-3-(ethylsulfanylcarbonyl)-6-phenylpyridine-5-carboxylate) as the first PET-ligand for the A3R. Regarding the metabolic profile – this class of dialkylpyridines comprises two ester functions within one molecule, one carboxylic and one thiocarboxylic – one could expect carboxylesterases significantly contributing to cleavage and degradation. Therefore, our aim was the development of [$^{18}$F]FE@SUPPY:2 (5-ethyl 2,4-diethyl-3-((2-[$^{18}$F]fluoroethyl)sulfanylcarbonyl)-6-phenylpyridine-5-carboxylate), the functional isomer containing the label at the thiocarboxylic moiety.

For satisfactory yields in high scale radiosyntheses, a reaction temperature of 75°C has to be applied for at least 20 minutes using 20 mg/mL of precursor. So far, 6 complete high-scale radiosyntheses were performed. Starting from an average of 51.2 ± 21.8GBq (mean ± SD) [$^{18}$F]fluoride, 5.8 ± 4.1GBq of formulated [$^{18}$F]FE@SUPPY:2 (12.0 ± 5.4%, based on [$^{18}$F]fluoride, not corrected for decay) were prepared in 75 ± 8 minutes.

Key words: Adenosine / PET / Receptor / Fluorine-18 / Radioligand

## Introduction

Adenosine is one of the key modulators in humans and exhibits its mechanism of action through four different receptor subtypes, namely the $A_1$, $A_{2A}$, $A_{2B}$, and $A_3$ receptors, respectively (A1R, A2AR, A2BR, and A3R). The most recently identified receptor subtype was the A3R, and, so far, there is little known regarding its distribution and density in vivo. PET (positron emission tomography) is a suitable technique to collect these lacking data. As a prerequisite for successful molecular imaging with PET, there is demand for suitable radioligands. Such a suitable receptor-radioligand is characterized by high affinity, high selectivity, low nonspecific binding and the absence of interfering radioactive metabolites in the target tissue. Beside these prerequisites, the most important premise for a successful PET-tracer is its broad availability and reliable preparation.

Recently, we introduced [$^{18}$F]FE@SUPPY (5-(2-[$^{18}$F]fluoroethyl) 2,4-diethyl-3-(ethylsulfanylcarbonyl)-6-phenylpyridine-5-carboxylate) as the first PET-ligand for the A3R. [1, 2] The preparation followed a simple one-pot one-step reaction with good and reliable radiolabelling yields. So far, [$^{18}$F]FE@SUPPY is the most suitable radioligand for the A3R amongst the well characterized family of 3,5-diacyl-2,4-dialkylpyridines with all derivatives showing considerable affinity for the adenosine receptor system. [3] FE@SUPPY was shown to display a $K_i$ of 4.2nM to human A3R and a selectivity of 2700 (ratio A1R/A3R). [3] Regarding the metabolic profile – these dialkylpyridines all comprise two ester functions within one molecule, one carboxylic and one thiocarboxylic – one could expect carboxylesterases significantly contributing to cleavage and degradation. Carboxylesterases are known to attack mainly carboxylic and thiocarboxylic functions. [4, 5] To the best of our knowledge, there is no conclusive data regarding the stability differences of carboxylic and thiocarboxylic esters within one molecule. Since Azema et al. [6] in a comparative study even presented evidence for increased stability of the thioester function compared to carboxylic esters, we translated the fluoroethyl ester [$^{18}$F]FE@SUPPY into the fluoroethyl - thioester [$^{18}$F]FE@SUPPY:2 (5-ethyl 2,4-diethyl-3-((2-[$^{18}$F]fluoroethyl)sulfanylcarbonyl)-6-phenylpyridine-5-carboxylate; see figure 1). Therefore, we expect a better metabolic profile of [$^{18}$F]FE@SUPPY:2 as compared to [$^{18}$F]FE@SUPPY. Preliminary binding studies and blocking experiments demonstrated high affinity for the A3R (even higher than for [$^{18}$F]FE@SUPPY and for the standard A3-selective compound MRS1523) and excellent selectivity against the other adenosine receptor subtypes.

Aims of the present study were (1) the preparation of the suitable labelling precursor and reference standard for [18F]FE@SUPPY:2, (2) the establishment of a radiosynthetic procedure for the preparation of the fluorine-18 labelled analogue, [18F]FE@SUPPY:2, (3) the evaluation and optimization of the reaction conditions to allow the large scale production of [18F]FE@SUPPY:2 and (4) the comparison of the results with those obtained with [18F]FE@SUPPY.

Both, [18F]FE@SUPPY and [18F]FE@SUPPY:2, will finally serve as radioligands for the determination of $K_d$ and $B_{max}$ on human A3R.

## Materials and Methods

### General

^{1}H- and ^{13}C-NMR spectra were recorded on a Bruker Avance DPX-200 spectrometer at 27 °C (200.13MHz for ^{1}H, 50.32MHz for ^{13}C). Mass spectra were obtained on a Shimadzu QP 1000 instrument (EI, 70eV). IR spectra were recorded on a Perkin-Elmer FTIR spectrum 1000 spectrometer. Melting points were determined on a Reichert-Kofler hot-stage microscope. Elemental analyses were performed at the Microanalytical Laboratory, University of Vienna (Austria). Analysis of radio-TLC plates was performed using a digital autoradiograph (Instant Imager, Canberra-Packard, Rüsselsheim, Germany). Analytical high-performance liquid chromatography (HPLC) was performed using a Merck-Hitachi LaChrom system equipped with an L-7100 pump, an L-7400 UV detector (operated at 248 nm) and a lead-shielded NaI-radiodetector (Berthold Technologies, Bad Wildbach, Germany). The semi-preparative HPLC system consisted of a Sykam S1021 pump, and an UV detector (254 nm) and a radioactivity detector in series.

Solid phase extraction (SPE) cartridges (SepPak® C18plus) were purchased from Waters Associates (Milford, MA). [18F]Fluoride was produced via the $^{18}O(p,n)^{18}F$ reaction in a GE PETtrace cyclotron (16.5MeV protons; GE medical systems, Uppsala, Sweden). $H_2^{18}O$ (>98%) was purchased from Rotem Europe (Leipzig, Germany). Anion exchange cartridges (PS-HCO3) for [18F]fluoride separation were obtained from Macherey-Nagel (Dueringen, Germany).

If not stated otherwise, all starting materials for precursor and reference standard syntheses as well as for radiosyntheses were obtained from Merck (Darmstadt, Germany), Fluka or Sigma-Aldrich (Vienna, Austria). All reagents were at least of analytical grade and used without further purification.

5-ethyl 2,4-diethyl-3-((2-hydroxyethyl)sulfanylcarbonyl)-6-phenylpyridine-5-carboxylate (OH@SUPPY:2; **1**) was prepared as described previously in detail. [7] (*see* Figure 2)

*Precursor chemistry – 5-ethyl 2,4-diethyl-3-((2-tosyloxyethyl)sulfanylcarbonyl)-6-phenylpyridine-5-carboxylate (Tos@SUPPY:2; **2**)*

A reaction scheme is presented in Figure 3. A solution of toluene-4-sulfonyl chloride (1.64g, 8.59mmol) in THF (15mL) was added drop wise to a stirred mixture of OH@SUPPY:2 (**1**; 1.69g, 4.36mmol) and triethylamine (1.18g, 1.6ml, 11.67mmol) in THF (40mL) at 0°C. Then the reaction mixture was refluxed for 62h and the solvent was evaporated *in vacuo.* Finally, the residue was purified via column chromatography (length: 55.5cm; diameter: 2.5cm): combined straight phase silica gel (KG60 Merck; 70-230 mesh ASTM) with ligroin/ethyl acetate 3/1 as mobile phase and RP-18 (Merck LiChroprep RP-18; 40-63 µm) with acetonitrile/water as mobile phase were used.

*Reference standard – 5-ethyl 2,4-diethyl-3-((2-fluoroethyl)sulfanylcarbonyl)-6-phenyl-pyridine-5-carboxylate (FE@SUPPY:2; **3**)*

OH@SUPPY:2 (**1**; 1.00g, 2.58mmol) was dissolved in water-free dichloromethane (30mL) at -78°C under inert gas. Diethylaminosulfur trifluoride (DAST; 0.69g, 5.17mmol) was slowly added dropwise to obtain crude FE@SUPPY:2. The reaction was kept at -78°C for half an hour and then slowly heated to room temperature. After completion of the reaction, the mixture was cooled to 0°C and hydrolysis was performed by addition of 10mL of water. The organic phase was separated and the aqueous phase was extracted 3-times with diethylether. The combined organic phases were dried over magnesium sulphate and the solvent was evaporated under reduced pressure. Subsequent purification was performed using again combined straight phase and reversed-phase column chromatography (for details see previous section).

*Radiosynthesis – 5-ethyl 2,4-diethyl-3-((2-[$^{18}$F]fluoroethyl) sulfanylcarbonyl)-6-phenyl-pyridine-5-carboxylate ([$^{18}$F]FE@SUPPY:2; **3a**)*

No-carrier-added (n.c.a.) aqueous [$^{18}$F]fluoride was fixed on an anion exchange cartridge (carbonate form) on-line and separated from excess water. Subsequently, [$^{18}$F]fluoride was eluted with a solution containing the aminopolyether Kryptofix 2.2.2. (4,7,13,16,21,24-hexaoxo-1,10-diaza-bicyclo[8.8.8]hexacosane; 20mg, 53.2µmol; *for synthesis*; Merck) and potassium carbonate (4.5mg, 32.6µmol; 99.9%+, Sigma-Aldrich) in acetonitrile/water (70/30 vol/vol; V=1.0mL). This solution was heated to 100°C and azeotropic drying was performed by subsequent addition of at least four 250µL portions of acetonitrile (DNA grade, <10ppm water, Merck).

To the dried [$^{18}$F]fluoride-aminopolyether complex, 0.1-4.0mg of Tos@SUPPY:2 (0.2-7.4µmol) in 500µL of acetonitrile was added, the vial was sealed and heated up to 120°C for 1-60min. The mixture was cooled to room temperature and the radiochemical yield was determined using analytical radio-HPLC (column: Merck Chromolith® Performance RP18e 100 x 4.6mm; mobile phase: acetonitrile/water/acetic acid (60/38.8/1.2 v/v/v; 2.5g/L ammonium acetate; pH 3.2); flow 2mL/min) and radio-TLC (plate: Merck TLC aluminium sheets RP-18 F$_{254s}$; mobile phase: acetonitrile/water 95/5 (v/v)).

*Purification of [$^{18}$F]FE@SUPPY:2*

After cooling to ambient temperature, the crude reaction mixture was subjected to semi-preparative reversed-phase HPLC (HPLC: column: Merck Chromolith® SemiPrep RP-18e, 100x10mm; mobile phase: acetonitrile/water/acetic acid (60/38.8/1.2 v/v/v; 2.5g/L ammonium acetate; pH 3.2); flow: 10mL/min). Product peak of [$^{18}$F]FE@SUPPY:2 eluted after 4.0-4.9min, all other radioactive impurities were observed to elute clearly separated and accounted only for minor amounts of radioactivity. Tos@SUPPY:2 showed a retention time (t$_R$) of 6.2-8.5min and was also completely removed from the product fraction.

The [$^{18}$F]FE@SUPPY:2 fraction was cut and diluted with 80mL water (*Aqua ad injectabilia*; Meditrade, Kufstein, Austria) to reduce lipophilicity of the solvent and subjected to SPE. This additional purification was performed in order to avoid potential contamination of the formulated product solution with toxic solvents. It is noteworthy that inadequate dilution resulted in partial breakthrough of [$^{18}$F]FE@SUPPY:2. The resulting solution was then fixed

on a C18plus SepPak®. Solid phase extraction was shown to have significant advantages in the preparation of radiopharmaceuticals compared to evaporation using a rotary evaporator [8]. Time needed is decreased, technical requirements are kept to a minimum and potential radiolytic processes are diminished. After washing with 10mL water (*Aqua ad injectabilia*; Meditrade, Kufstein, Austria), the pure product was eluted with 2.0mL ethanol (100%, *Pharm.Eur.* grade, Merck), sterile filtered (0.22μm Millipore GS®) and formulated with 0.9% sodium chloride solution (15mL; *for injection*; Fresenius-Kabi, Graz, Austria).

*Quality control of [$^{18}$F]FE@SUPPY:2*

Chemical and radiochemical impurities were detected using radio-HPLC and radio-TLC (for conditions see Radiochemistry section). Quality control systems revealed excellent separation and quantification properties: HPLC retention times were 8.9 ± 0.3min (range: 8.5-9.2min) for [$^{18}$F]FE@SUPPY:2 and 15.0 ± 0.5min (range: 14.4-15.6min) for Tos@SUPPY:2, respectively; Radio-TLC $R_f$-values were 0.0-0.1 for [$^{18}$F]fluoride and 0.63 ± 0.03 (range: 0.58-0.68) for [$^{18}$F]FE@SUPPY:2. All values were verified by the corresponding inactive reference substances.

Residual solvents were analyzed by GC (carrier gas: He; flow: 2.7mL/min; 45°C (2.5min) – 20°C/min to 110°C – 30°C/min to 200°C – 200°C (10 min); FID: 270°C). Residuals of Kryptofix 2.2.2 were analyzed using a dedicated test kit obtained through Rotem GmbH (Leipzig, Germany); semi-quantitative analysis was performed in accordance with the regulations laid down in the FDG monograph within the European Pharmacopoeia [9]. pH and osmolality were checked with dedicated equipment. Specific radioactivity was determined by dividing the activity of the final product (GBq) by the amount of "cold" FE@SUPPY:2 (μmoles) within this final product solution. A calibration curve was determined using different amounts of FE@SUPPY:2 standards in the previously given HPLC assay.

**Results and Discussion**

*General*

Herewith, we present the successful preparation of [$^{18}$F]FE@SUPPY:2 as a consequential close analogue of [$^{18}$F]FE@SUPPY, which was presented recently. [2, 1] The two tracers were

selected according to Li et al. [3] who evaluated a series of adenosine A3 receptor antagonists. Amongst these antagonists, FE@SUPPY displayed favourable properties making it a promising candidate compound for a PET tracer. As evident from figure 1, [18F]FE@SUPPY and [18F]FE@SUPPY:2 are isomers with exchanged carboxylic and thiocarboxylic substituents. Having these two ester-moieties within one molecule, ester-cleavage is expected as one of the primary metabolic routes. There is evidence in literature, that – as a general trend – thioesters are seemingly hydrolytically more stable than their corresponding oxy analogues [10]. However, for the hydrolysis of two different ester functions within one single molecule, to the best of our knowledge, there is no stability data available. In first preliminary kinetic experiments with carboxylesterases we observed the trend towards a higher stability of FE@SUPPY:2 as compared to FE@SUPPY (data not shown).

On the other hand, beside these exciting metabolic features, knowing, that the A3R is according to Gessi et al. such an "enigmatic player in cell biology", and there is still strong need for suitable antagonists or agonists for this receptor subtype [11], we could provide a second antagonist for the imaging of the A3R.

So far, for autoradiography and binding studies, the well known and commercially available [125I]AB-MECA is the most used radioligand for the A3R. However, it is undisputed, that [125I]AB-MECA also displays considerable affinity for the A1R and A2AR. [12] Since the A3R is known to be the adenosine receptor subtype with the lowest density in most tissues, significance of the quantification of the A3R beside the other subtypes with [125I]AB-MECA is limited.

Hence, additionally to the application as in-vivo radiotracers for PET, [18F]FE@SUPPY and [18F]FE@SUPPY:2 could serve as selective and high affinity radiotracers for quantitative autoradiography and binding studies.

*Precursor chemistry*

2.10 g purified Tos@SUPPY:2 was obtained (89%) as yellowish oil. For NMR-analysis, the solvent signal was used as an internal standard which was related to TMS with $\delta$ = 7.26ppm ($^1$H in CDCl$_3$) and $\delta$ = 77.0ppm ($^{13}$C in CDCl$_3$), respectively.

$^1$H-NMR (200 MHz, CDCl$_3$): δ (ppm) 7.82 (m, 2H), 7.58 (m, 2H), 7.38 (m, 4H), 4.26 (t, 2H, $J$ = 6.30 Hz), 4.09 (q, 2H, $J$ = 7.18 Hz), 3.39 (t, 2H, $J$ = 6.20 Hz), 2.77 (q, 2H, $J$ = 7.44 Hz), 2.64 (q, 2H, $J$ = 7.82 Hz), 2.44 (s, 3H), 1.28 (t, 3H, $J$ = 7.56 Hz), 1.17 (t, 3H, $J$ = 6.94 Hz), 0.98 (t, 3H, $J$ = 7.06 Hz).

$^{13}$C-NMR (50 MHz, CDCl$_3$): δ (ppm) 194.2, 168.2, 159.2, 157.3, 148.0, 145.1, 139.6, 132.6, 132.3, 129.9, 128.9, 128.3, 127.9, 126.6, 67.7, 61.5, 29.1, 28.8, 24.1, 21.6, 15.6, 14.0, 13.5.

IR (KBr): ν (cm$^{-1}$) 2978, 2938, 2878, 1724, 1678, 1598, 1556, 1495, 1463, 1447, 1403, 1362, 1278, 1250.

MS: m/z (%) 543 (M$^+$ + 2, 1), 542 (1), 311 (24), 310 (100), 282 (17), 264 (4), 236 (3), 155 (3), 91 (9).

Elemental analysis: calculated for C$_{28}$H$_{31}$NO$_6$S$_2$: C, 62.08; H, 5.77; N, 2.59. found: C, 61.92; H, 5.77; N, 2.57.

The preparation and purification of the precursor molecule were accomplished straight forward without any significant problems. Surprisingly, the tosylation reaction was unexpectedly sluggish (62 hours under refluxing in THF).

*Reference standard*

0.37 g FE@SUPPY:2 was obtained after purification (37%) as yellowish oil.

$^1$H-NMR (200 MHz, CDCl$_3$): δ (ppm) 7.60 (m, 2H), 7.42 (m, 3H), 4.76 (t, 1H, $J$ = 5.92 Hz), 4.53 (t, 1H, $J$ = 5.94 Hz), 4.10 (q, 2H, $J$ = 7.06 Hz), 3.50 (t, 1H, $J$ = 5.94 Hz), 3.39 (t, 1H, $J$ = 5.92 Hz), 2.86 (q, 2H, $J$ = 7.44 Hz), 2.72 (q, 2H, $J$ = 7.58 Hz), 1.34 (t, 3H, $J$ = 7.46 Hz), 1.23 (t, 3H, $J$ = 7.44 Hz), 0.98 (t, 3H, $J$ = 7.06 Hz).

$^{13}$C-NMR (50 MHz, CDCl$_3$): δ (ppm) 194.4, 168.2, 159.2, 157.2, 148.0, 139.6, 132.6, 126.6, 81.3 (d, $J$ = 170.5 Hz), 61.5, 30.0 (d, $J$ = 21.8 Hz), 29.1, 24.1, 15.6, 14.0, 13.5.

IR (KBr): ν (cm$^{-1}$) 3061, 2978, 2939, 2902, 2879, 1726, 1678, 1557, 1465, 1448, 1405, 1380, 1279, 1251, 1175, 1144, 1091, 1076, 1014, 973.

MS: m/z (%) 389 (M$^+$, 3), 343 (4), 311 (20), 310 (100), 282 (14), 236 (7),105 (20), 77 (12).

High-resolution mass spectroscopy (HRMS): m/z calculated for $C_{21}H_{24}NO_3SF$: 389.1461; found: 389.1473.

*Radiosynthesis*

The general reaction scheme of the radiochemical preparation of [$^{18}$F]FE@SUPPY:2 is given in Figure 3. Distinct temperature dependence was observed. Maximum yields were obtained at 100°C with no conversion at 120°C (Figure 4a). However, at temperatures above 75°C, we observed disproportional thermal load for the septa of the reaction vials. With focus for future automation we decided to keep this mechanical risk for the synthesizer module at a minimum and decided to perform the radiosynthesis at 75°C, below the boiling point of acetonitrile (~82°C). Additionally, possible leakage in the stressed septa could result in evaporation of solvent. Regarding the reaction kinetics, our data indicate that a minimum reaction time of 20 minutes is required to achieve satisfactory conversion results (Figure 4b). The slightly higher yields after 60 minutes are clearly outweighed by the decay of fluorine-18. As evident from the present data, a continuous increase in the radiochemical yields is observed using increasing amounts of Tos@SUPPY:2 (Figure 4c). Interestingly, we observed the demand of drastically elevated amounts of precursor for the preparation of [$^{18}$F]FE@SUPPY:2 as compared to [$^{18}$F]FE@SUPPY (Figure 4c). Obviously, the SUPPY:2 derivative is more sluggish than the SUPPY molecule. Scaling up the radiosynthesis, we found that a larger amount of precursor was needed for satisfactory conversion (20mg/mL) using starting activities up to 85.5GBq. Hence, optimum reaction conditions for large scale preparation of [$^{18}$F]FE@SUPPY:2 were found to be 75°C with 20mg/mL of precursor for at least 20 minutes.

So far, 6 complete high-scale radiosyntheses were performed. Starting from an average of 51.2 ± 21.8GBq (mean ± SD; range: 10.8-85.5 GBq) [$^{18}$F]fluoride, 5.8 ± 4.1GBq (range: 1.7-14GBq) of formulated [$^{18}$F]FE@SUPPY:2 (12.0 ± 5.4%, based on [$^{18}$F]fluoride, not corrected for decay) was prepared in 75 ± 8 minutes (range: 61–84 min). Total recovery of radioactivity from SPE was higher than 97%.

In comparison, we found for [$^{18}$F]FE@SUPPY 32.3 ± 12.4% radiochemical yield, which is almost a threefold higher than for [$^{18}$F]FE@SUPPY:2. [1] Once again, the sluggishness of the

reaction in the preparation of [18F]FE@SUPPY:2 due to the different position of the fluoroethyl-ester in the molecule seems to be the reason for this drastic change.

*Quality control of [18F]FE@SUPPY:2*

Radiochemical purity as determined via the given radio-TLC and radio-HPLC methods always exceeded 98%. Specific radioactivity was determined via HPLC and found to be 344 ± 133 GBq/μmol; range: 187-575 GBq/μmol (9300 ± 3600 Ci/mmol; range: 5050-15500 Ci/mmol) at the end of synthesis (EOS). [18F]FE@SUPPY:2 was found to be stable for at least 10 hours (checked by chromatography).

In comparison, we found for [18F]FE@SUPPY a specific radioactivity of 70.4 ± 26.1 GBq/μmol at EOS which is approximately a fifth of the value of [18F]FE@SUPPY:2. [1] For this fact, we are left without an explanation.

**Conclusion**

[18F]FE@SUPPY:2, a potential PET-ligand for the adenosine $A_3$ receptor, was successfully prepared in a feasible and reliable manner. Purification using RP-HPLC and subsequent SPE methodology lead to high radiochemical purities and specific radioactivities. Compared with [18F]FE@SUPPY, the preparation of [18F]FE@SUPPY:2 demanded higher amounts of precursor and overall radiochemical yields were lower.

The preparation of [18F]FE@SUPPY:2 will enable a direct comparison with [18F]FE@SUPPY in preclinical tests to select the optimum molecule for further applications.

**Acknowledgements**

**References**

[1] Wadsak, W., Mien, L. K., Shanab, K., Weber, K., Schmidt, B., Sindelar, K. M., Ettlinger, D. E., Haeusler, D., Spreitzer, H., Keppler, B. K., Viernstein, H., Dudczak, R., Kletter, K., Mitterhauser, M.: Radiosynthesis of the adenosine $A_3$ receptor ligand 5-(2-[$^{18}$F]fluoroethyl)2,4-diethyl-3-(ehtylsulfanylcarbonyl)-6-phenylpyridine-5-carboxylate ([$^{18}$F]FE@SUPPY), Radiochim. Acta. **96**, 119 (2008).

[2] Wadsak, W., Mien, L. K., Shanab, K., Ettlinger, D. E., Haeusler, D., Sindelar, K., Lanzenberger, R. R., Spreitzer, H., Viernstein, H., Keppler, B. K., Dudczak, R., Kletter, K., Mitterhauser, M.: Preparation and first evaluation of [$^{18}$F]FE@SUPPY: a new PET tracer for the adenosine $A_3$ receptor, Nucl Med Biol. **35**, 61 (2008).

[3] Li, A. H., Moro, S., Forsyth, N., Melman, N., Ji, X. D., Jacobson, K. A.: Synthesis, CoMFA analysis, and receptor docking of 3,5-diacyl-2, 4-dialkylpyridine derivatives as selective A3 adenosine receptor antagonists, J Med Chem. **42**, 706 (1999).

[4] Liederer, B. M., Borchardt, R. T.: Enzymes involved in the bioconversion of ester-based prodrugs, J Pharm Sci. **95**, 1177 (2006).

[5] Rooseboom, M., Commandeur, J. N., Vermeulen, N. P.: Enzyme-catalyzed activation of anticancer prodrugs, Pharmacol Rev. **56**, 53 (2004).

[6] Azéma, L., Lherbet, C., Baudoin, C., Blonski, C.: Cell permeation of a Trypanosoma brucei aldolase inhibitor: Evaluation of different enzyme-labile phosphate protecting groups, Bioorg Med Chem Lett. **16**, 3440 (2006).

[7] Shanab, K.: Synthese von Precursoren von $A_3$ Adenosin Rezeptor PET Tracern und möglichen Metaboliten, PhD-thesis/Dissertation; University of Vienna.  (10.12.2007).

[8] Lemaire, C., Plenevaux, A., Aerts, J., Del Fiore, G., Brihaye, C., Le Bars, D., Comar, D., Luxen, A.: Solid phase extraction - an alternative to the use of rotary evaporators for solvent removal in the rapid formulation of PET radiopharmaceuticals, J. of Label. Compd. Radiopharm. **42**, 63 (1999).

[9] Radiopharmaceutical Preparations (Radiopharmaceutica; 5.0/1325). In: *European Pharmacopoeia (Europäisches Arzneibuch). 5th edition (5. Ausgabe Grundwerk), official Austrian version*. Vienna:Verlag Österreich GmbH, 2005, p.  1167.

[10] Venuti, M. C., Young, J. M., Maloney, P. J., Johnson, D., McGreevy, K.: Synthesis and biological evaluation of omega-(N,N,N-trialkylammonium)alkyl esters and thioesters of carboxylic acid nonsteroidal antiinflammatory agents, Pharm Res. **6**, 867 (1989).

[11] Gessi, S., Merighi, S., Varani, K., Leung, E., Mac Lennan, S., Borea, P. A.: The A3 adenosine receptor: an enigmatic player in cell biology, Pharmacol Ther. **117**, 123 (2008).

[12] Shearman, L. P., Weaver, D. R.: [125I]4-aminobenzyl-5'-N-methylcarboxamidoadenosine ([125I]AB-MECA) labels multiple adenosine receptor subtypes in rat brain, Brain Res. **745**, 10 (1997).

**Captions**


Figure 1 – Structural differences in fluoroethylated SUPPY and SUPPY:2 compounds and their precursor molecules.


Figure 2 – Reaction scheme for the preparation of OH@SUPPY:2 (**1**, according to [7]).


Figure 3 – Reaction scheme for the preparation of Tos@SUPPY:2, FE@SUPPY:2 and [$^{18}$F]FE@SUPPY:2 starting from OH@SUPPY:2.


Figure 4 – The dependence of the radiochemical yield of [$^{18}$F]FE@SUPPY:2 on

  (a) reaction temperature (6 mg/mL precursor conc., 20 min);

  (b) reaction time (6 mg/mL precursor conc., 75°C); and

  (c) amount of precursor (75°C, 20 min) including data for [$^{18}$F]FE@SUPPY.

Bold data points represent arithmetic means ± SD for n≥4. Additionally, all single values are presented as light coloured crosses.

Figure 1
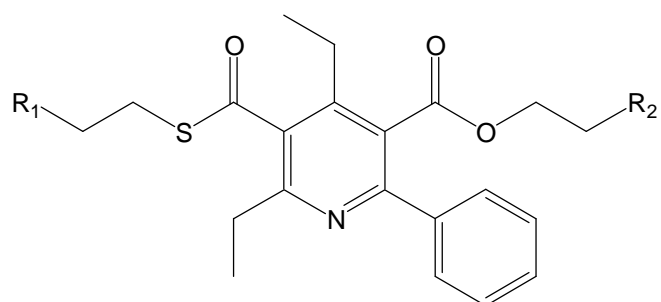


| compound | R$_1$ | R$_2$ |
|---|---|---|
| [$^{18}$F]FE@SUPPY | -H | -$^{18}$F |
| [$^{18}$F]FE@SUPPY:2 | -$^{18}$F | -H |
| Tos@SUPPY | -H | -OTos |
| Tos@SUPPY:2 | -OTos | -H |

Figure 2



100

Figure 3



**1; OH@SUPPY:2**

tosyl chloride,THF
triethylamine
r.t.; 62 h

DAST
dichloromethane
-78°C --> r.t.

**2; Tos@SUPPY:2**

**3; FE@SUPPY:2**

[$^{18}$F]fluoride
acetonitrile
75°C; 20min

**3a; [$^{18}$F]FE@SUPPY:2**

Figure 4

**(c)**
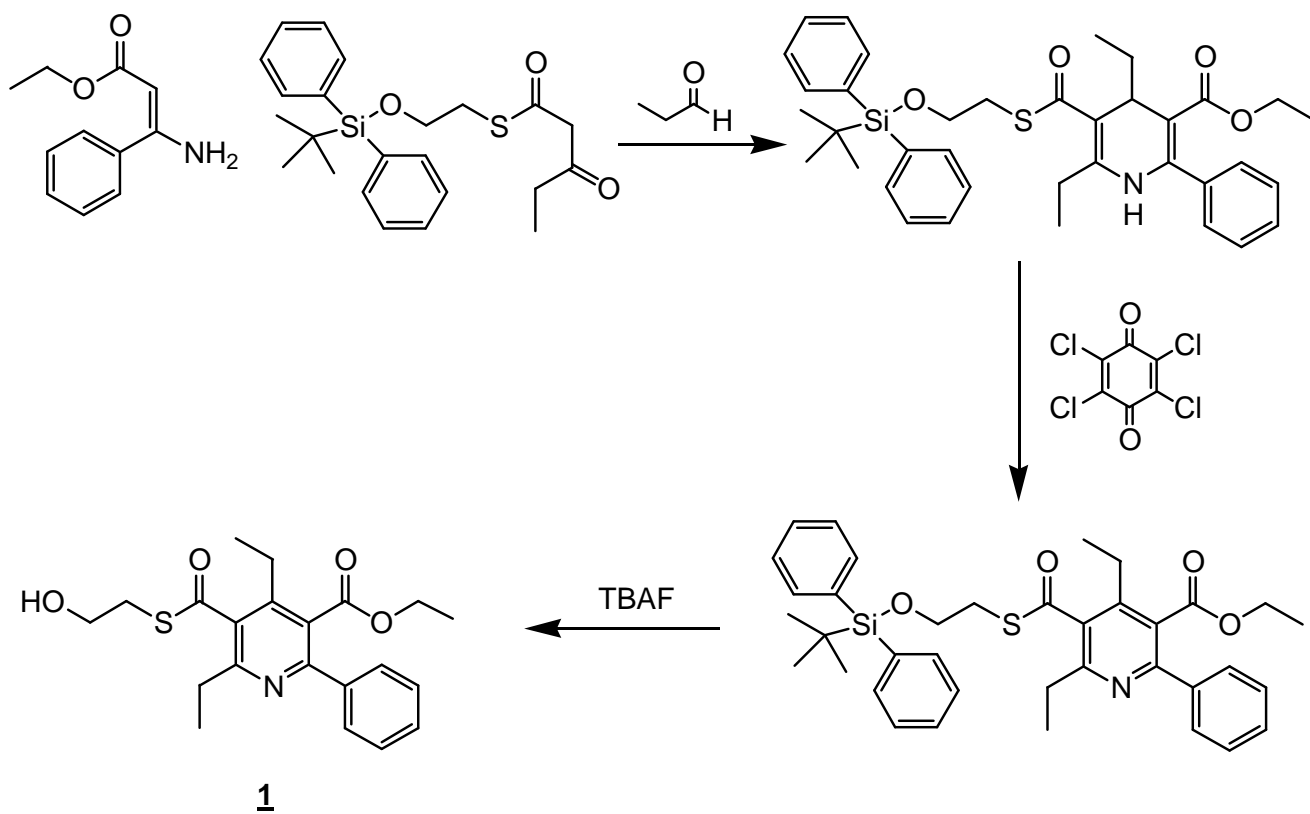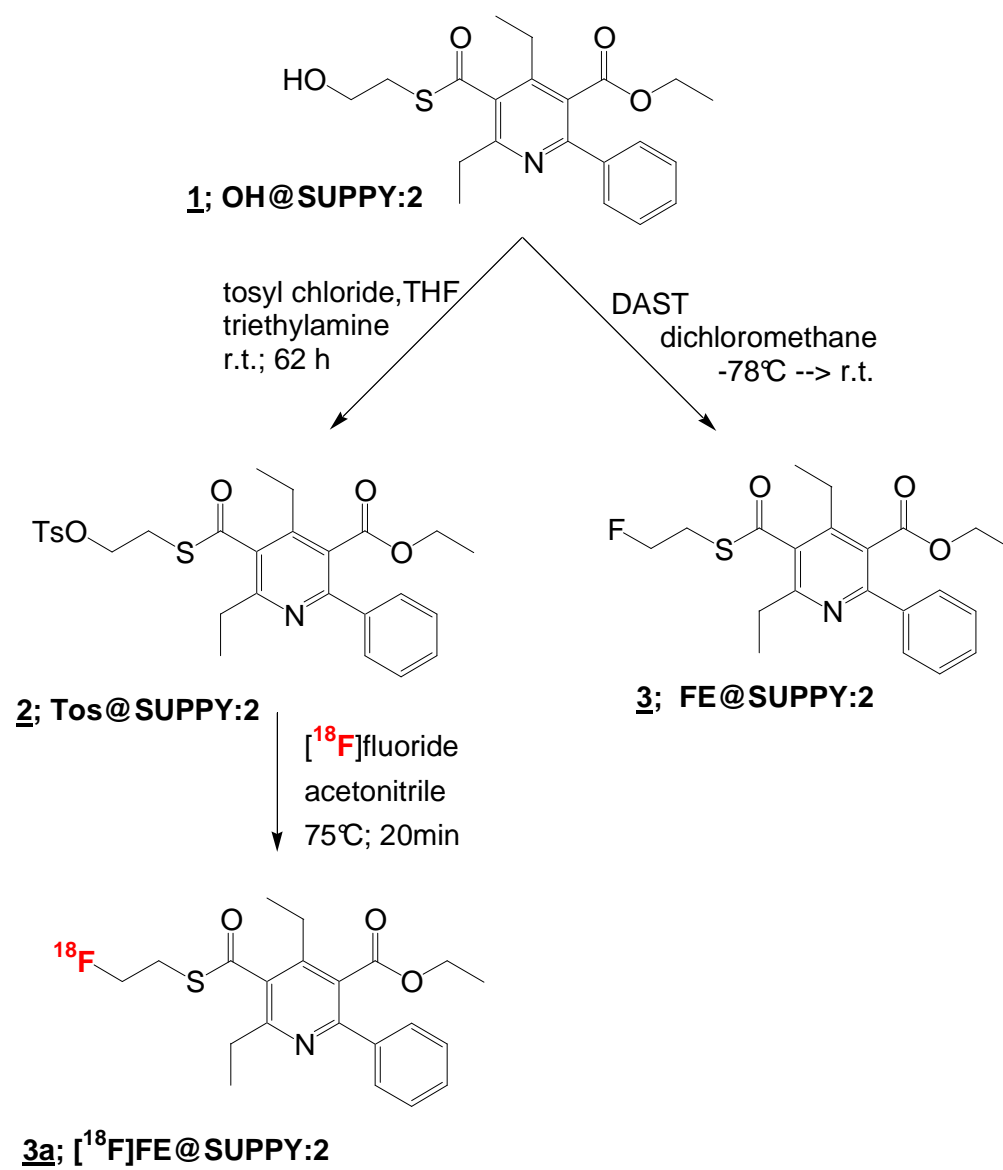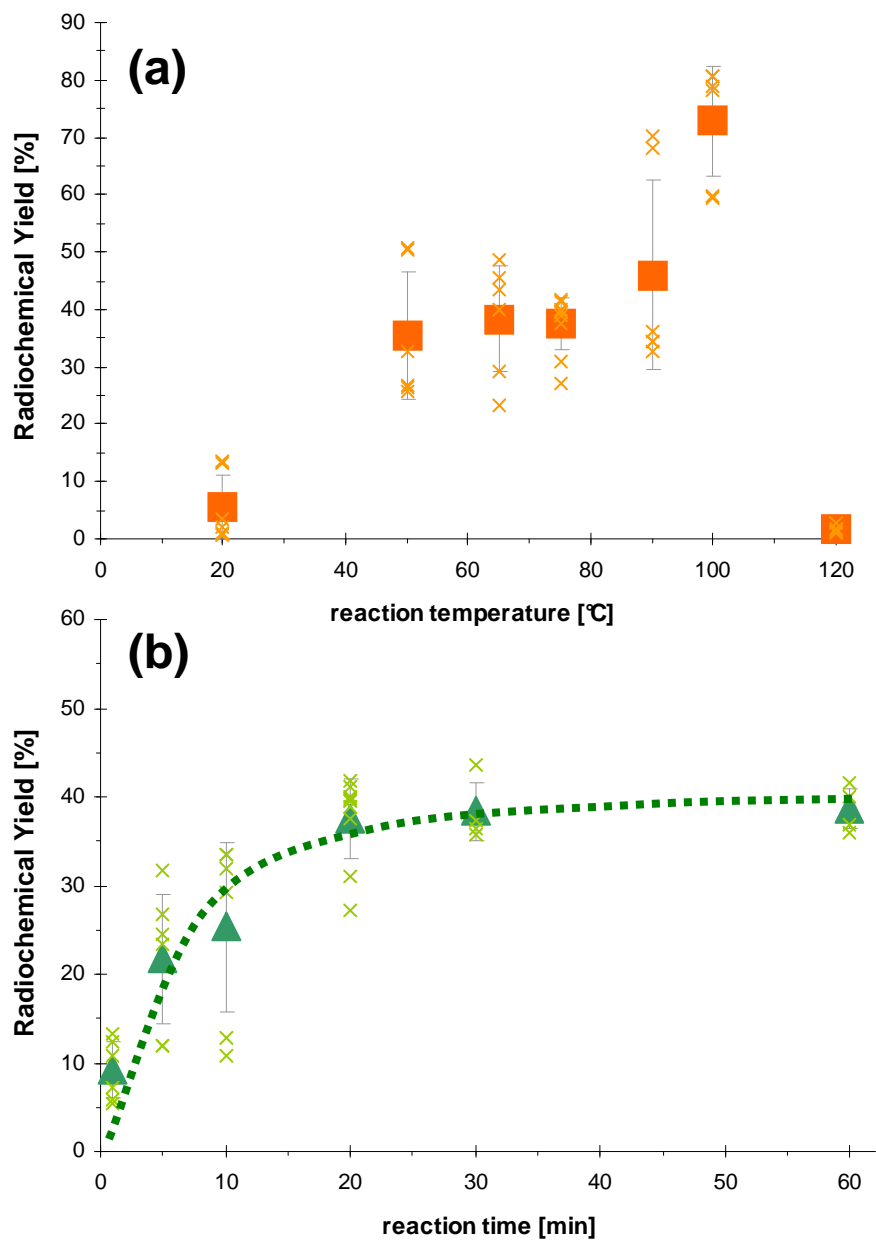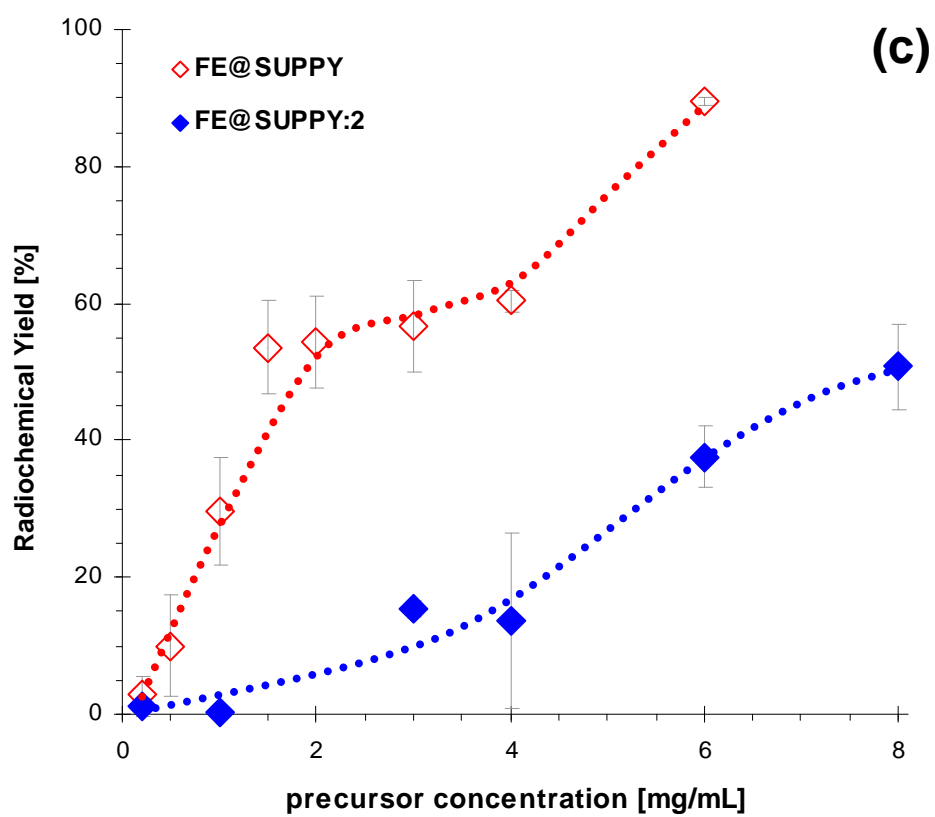
# 2.2.4. PAPER 3

# AUTOMATISATION AND FIRST EVALUATION OF [$^{18}$F]FE@SUPPY:2, AN ALTERNATIVE PET-TRACER FOR THE ADENOSINE A$_3$ RECEPTOR: A COMPARISON WITH [$^{18}$F]FE@SUPPY.

Authors: Markus Mitterhauser[1,2,3,*], **Daniela Haeusler[1,3]**, Leonhard-Key Mien[1,3,4], Johanna Ungersboeck[1,5], Lukas Nics[1,6], Rupert R Lanzenberger[4], Karoline Sindelar[1], Helmut Viernstein[3], Robert Dudczak[1], Kurt Kletter[1], Helmut Spreitzer[7], Wolfgang Wadsak[1,5]

[1] Dept of Nuclear Medicine, Medical University of Vienna, Austria

[2] Hospital Pharmacy of the General Hospital of Vienna, Austria

[3] Dept of Pharmaceutical Technology and Biopharmaceutics, University of Vienna, Austria

[4] Dept of Psychiatry and Psychotherapy, Medical University of Vienna, Austria

[5] Dept of Inorganic Chemistry, University of Vienna, Austria

[6] Dept of Nutritional Sciences, University of Vienna, Austria

[7] Dept of Drug and Natural Product Synthesis, University of Vienna, Austria

## Abstract

**Introduction** Since the Adenosine-$A_3$-receptor was identified in the late 1990´s, there is little data available describing its distribution in vivo. Recently, we introduced [$^{18}$F]FE@SUPPY as the first PET-tracer for this receptor. In the present investigation we translated this fluoroethyl-ester into the fluoroethyl-**thioester** [$^{18}$F]FE@SUPPY:2 (5-ethyl 2,4-diethyl-3-((2-[$^{18}$F]fluoroethyl) sulfanylcarbonyl)-6-phenylpyridine-5-carboxylate). Aims of the present study were the evaluation of (1) the automatized preparation of both [$^{18}$F]FE@SUPPY-derivatives, (2) the biodistribution of [$^{18}$F]FE@SUPPY:2, (3) the lipophilicity and (4) the comparison of the findings of [$^{18}$F]FE@SUPPY and [$^{18}$F]FE@SUPPY:2. **Methods** The automated preparations of both [$^{18}$F]FE@SUPPY-analogues were performed on a GE *TRACERlab Fx$_{FN}$* synthesizer using suitable precursors. Biodistribution experiments were performed using Sprague-Dawley rats/Him:OFA. Lipophilicity of the compounds was determined using an HPLC assay. **Results** 22 automated radiosyntheses were performed for both radiotracers. Specific radioactivity was 70±26GBq/µmol for [$^{18}$F]FE@SUPPY and 340±140GBq/µmol for [$^{18}$F]FE@SUPPY:2. Biodistribution experiments evinced bowels and liver as organs with highest uptake and intermediate uptake in kidney, lung and heart. LogP values of both molecules ranged from 3.99 to 4.12 at different pH. **Conclusion** From a radiopharmaceutical perspective, drastically better specific radioactivities would militate in favour of [$^{18}$F]FE@SUPPY:2; preclinical evaluations, so far, do not permit the decision upon the selection of the optimum [$^{18}$F]FE@SUPPY-derivative. With [$^{18}$F]FE@SUPPY:2, we are able to provide a second potential tracer that could help to further characterize the still quite unexplored Adenosine-$A_3$-receptor.

**Key words:** Adenosine, PET, Adenosine A3 Receptor, Fluorine-18, Radioligand, SUPPY

**Introduction**

Adenosine is one of the key modulators of the human body and acts through four different receptor subtypes: the $A_1$, $A_{2A}$, $A_{2B}$, and $A_3$ receptors, respectively (A1AR, A2AAR, A2BAR, and A3AR). The A3AR was identified in the late 1990´s, and, so far, there is little data available describing its distribution and density in vivo. The most suitable technique to collect these lacking data in the living organism would be PET (positron emission tomography). As a premise for molecular PET imaging with high quality, there is need for suitable radioligands displaying high affinity, high selectivity and low unspecific binding. Also, the absence of interfering radioactive metabolites in the target tissue is of importance. Beside these prerequisites, the most important premise for a successful PET-tracer is its widespread availability and reliable preparation. Additionally, to keep radiation burden for the operators as low as possible, a fully automated preparation would be beneficial.

Recently, we introduced [$^{18}$F]FE@SUPPY (5-(2-[$^{18}$F]fluoroethyl) 2,4-diethyl-3-(ethylsulfanylcarbonyl)-6-phenylpyridine-5-carboxylate) as the first PET-tracer for the A3AR. [1, 2] The radiosynthesis was performed in a simple one-pot one-step reaction with good and reliable radiolabelling yields and good specific radioactivities. [$^{18}$F]FE@SUPPY was selected due to its favourable binding characteristics for the A3AR out of the well characterized chemical family of 3,5-diacyl-2,4-dialkylpyridines – with all derivatives showing considerable affinity for the adenosine receptor system [3]. Regarding the metabolic profile – these diacyl-derivatives all carry two ester moieties within one molecule, one carboxylic and one thiocarboxylic – enzymes derived from the family of carboxylesterases would be expected to significantly contribute to cleavage and degradation [4, 5]. To the best of our knowledge, there is no conclusive data regarding differences in stability of carboxylic and thiocarboxylic esters within one molecule. In a comparative study, Azema et al. [6] even

presented evidence for increased stability of the thioester function compared to carboxylic esters. Hence, we translated the fluoroethyl ester [$^{18}$F]FE@SUPPY into the fluoroethyl-**thioester** [$^{18}$F]FE@SUPPY:2 (5-ethyl 2,4-diethyl-3-((2-[$^{18}$F]fluoroethyl) sulfanylcarbonyl)-6-phenylpyridine-5-carboxylate; see figure 1). Being close structural analogues, even lipophilicity of both molecules could be expected to be comparable.

Thus, aims of the present study were

(1) the fully automated preparation of both [$^{18}$F]FE@SUPPY:2 and [$^{18}$F]FE@SUPPY,

(2) the evaluation of the biodistribution of [$^{18}$F]FE@SUPPY:2 in rats,

(3) the characterisation of the lipophilicity using standardized methods and

(4) the comparison of the findings of [$^{18}$F]FE@SUPPY and [$^{18}$F]FE@SUPPY:2.

**Materials and Methods**

*General*

Mass spectra were obtained on a Shimadzu QP 1000 instrument (EI, 70 eV; Shimadzu, Kyoto, Japan). IR spectra were recorded on a Perkin-Elmer FTIR spectrum 1000 spectrometer (Perkin Elmer, Watford, UK). Elemental analyses were performed at the Microanalytical Laboratory at the University of Vienna, Austria (http://www.univie.ac.at/Mikrolabor/ind_eng.htm). $^{1}$H- and $^{13}$C-NMR spectra were recorded on a Bruker Avance DPX-200 spectrometer at 27°C (200.13 MHz for $^{1}$H, 50.32 MHz for $^{13}$C; Bruker AXS GmbH, Karlsruhe, Germany). High resolution mass spectroscopy was performed on a Finnigan MAT 8230 (EI; 70eV; Thermo Finnigan Waltham, MA, USA). Radio-analytical

thin-layer chromatography (radio-TLC) was performed using silicagel 60F$_{254}$ plates from Merck (Darmstadt, Germany). Analysis of radio-TLC plates and autoradiography were performed using a Canberra-Packard Instant Imager (Perkin Elmer, Watford, UK). Analytical high-performance liquid chromatography (HPLC) was performed using a Merck-Hitachi LaChrom system with a NaI-radiodetector from Berthold Technologies (Bad Wildbach, Germany). The semi-preparative HPLC system (as part of the GE *TRACERlab Fx $_{FN}$* synthesizer) consisted of a Sykam S1021 pump (Sykam GmbH, Eresing, Germany) and a UV detector (254 nm) and a radioactivity detector in series.

Solid phase extraction (SPE) cartridges (SepPak$^{®}$ C18plus) were purchased from Waters Associates (Milford, USA). All starting materials for precursor and reference standard syntheses were commercially available and used without further purification. [$^{18}$F]Fluoride was produced via the $^{18}$O(p,n)$^{18}$F reaction in a GE PETtrace cyclotron (16.5MeV protons; GE Medical systems, Uppsala, Sweden). H$_2$$^{18}$O (>98%) was purchased from Rotem Europe (Leipzig, Germany). Anion exchange cartridges (PS-HCO$_3$) for [$^{18}$F]fluoride fixation were obtained from Macherey-Nagel (Dueringen, Germany).

*Precursor chemistry — 5-(2-tosyloxyethyl) 2,4-diethyl-3-(ethylsulfanylcarbonyl)-6-phenylpyridine-5-carboxylate (Tos@SUPPY)*

This precursor was prepared as described previously [1, 2, 7]. Briefly, OH@SUPPY, prepared according to [8] was reacted with toluene-4-sulfonyl chloride in THF and purified by recrystallization.

*5-ethyl 2,4-diethyl-3-((2-tosyloxyethyl)sulfanylcarbonyl)-6-phenylpyridine-5-carboxylate (Tos@SUPPY:2)*

A solution of toluene-4-sulfonyl chloride (1.64g, 8.59mmol) in THF (15mL) was added to OH@SUPPY:2 [8] (1.69g, 4.36mmol) and triethylamine (1.18g, 1.6ml, 11.67mmol) in THF (40mL) at 0°C. Then the reaction mixture was refluxed and the solvent was evaporated in vacuo. The residue was purified via column chromatography.

*Reference standard – 5-(2-fluoroethyl) 2,4-diethyl-3-(ethylsulfanylcarbonyl)-6-phenyl-pyridine-5-carboxylate (FE@SUPPY)*

The reference compound was obtained according to [1, 2, 7]. Briefly, OH@SUPPY [8] was treated with diethylaminosulfur trifluoride (DAST) at -78°C. Purification was performed using column chromatography.

*5-ethyl 2,4-diethyl-3-((2-fluoroethyl)sulfanylcarbonyl)-6-phenyl-pyridine-5-carboxylate*

*(FE@SUPPY:2)* OH@SUPPY:2 (1.00g, 2.58mmol, [8]) was reacted with DAST (0.69g, 5.17mmol) in water-free dichloromethane at -78°C. After hydrolysis, purification was performed using column chromatography.

*Automated radiosynthesis – [$^{18}$F]FE@SUPPY and [$^{18}$F]FE@SUPPY:2*

The automated preparation of both fluorinated FE@SUPPY analogues was preformed on a GE *TRACERlab Fx$_{FN}$* synthesizer. A comprehensive overview of all components of the system is given in figure 2. The following preparation steps were performed prior to synthesis start: a C18plus SPE cartridge (360mg, SepPak® Waters) and a PS-HCO3 SPE cartridge (45mg, Macherey-Nagel) were placed on their designated spots and connected to the corresponding tubing. The vials were filled with the following solutions: vial 1 – Kryptofix K2.2.2 (4,7,13,16,21,24-hexaoxo-1,10-diaza-bicyclo[8.8.8]hexacosane; 20mg, 53.2µmol) and potassium carbonate (4.5mg, 32.6µmol) in a mixture of 700µL acetonitrile and 300µL water; vial 2 – 1mL acetonitrile; vial 3 – 0.5mL acetonitrile; vial 4 – 1mL of precursor solution (e.g.

10mg Tos@SUPPY (18.5μmol) in acetonitrile for [$^{18}$F]FE@SUPPY and 15mg Tos@SUPPY:2 (27.8 μmol) in acetonitrile for [$^{18}$F]FE@SUPPY:2, respectively); vial 5 – 0.5mL water; vial 7 – 15mL physiological saline; vial 8 – 2mL ethanol and vial 9 – 10mL water. The round bottom flask was filled with 80mL water and the reactor was filled with 1mL acetonitrile.

No-carrier-added aqueous [$^{18}$F]fluoride was produced via the $^{18}$O(p,n)$^{18}$F reaction in a GE Gen2-silver target filled with 2.4mL [$^{18}$O]water (>98%) and delivered to a 5mL v-vial. This vial was placed on the designated spot of the synthesizer (left hand side, see figure 2) and connected. Then, vacuum was applied and [$^{18}$F]fluoride was sucked over the anion exchange cartridge on-line (via V10 and V11) and separated from excess water. [$^{18}$F]fluoride was eluted with a solution containing Kryptofix 2.2.2. and potassium carbonate in acetonitrile/water into the reactor (V1, V10, V11, V13). The resulting solution was heated for 2 minutes at 60°C and acetonitrile was added (V2). Heating was continued for another 3min at 60°C and then for 5min at 120°C in a stream of helium (V20) while adding the final portion of acetonitrile (V3) to complete azeotropic drying. The dried [$^{18}$F]fluoride-aminopolyether complex was cooled to 65°C, precursor was added (V4) and the mixture was heated to 75°C for 18min. After cooling to 35°C, the crude reaction mixture was quenched with water (V5) and transferred (V14) to the injector of the semi-preparative reversed-phase HPLC system (column: Merck Chromolith® SemiPrep RP-18e, 100x10mm, mobile phase: acetonitrile/water/acetic acid (60/38.8/1.2 v/v/v; 2.5 g/L ammonium acetate; pH 3.2); flow: 10 mL/min). Triggered by the fluid detector, the injector automatically changed from the "load" to the "inject" position and the chromatographic plotting started. Using the pre-settings from our evaluation runs, the desired peak was cut automatically and collected in the round bottom flask (V18). The diluted solution was transferred over a C18plus SepPak® in a stream of helium (V17, V21). After washing with water (V9), the purified product was

eluted with ethanol (V8) directly into a sterile vial within a laminar air-flow hot-cell (V15) and on-line sterile filtered (0.22μm). The product was diluted and formulated using physiological saline (V7).

*Biodistribution experiments*

The experiments were approved by the Austrian law on animal experiments and the procedure followed the protocol established in various previous studies of our group. Male Sprague-Dawley rats/Him:OFA (n=20, 271-346 g) were injected with 2.17–7.52 MBq (180-225μL) through a tail vein. Subsequently, individuals were sacrificed by exsanguination from the abdominal aorta in ether anaesthesia after 5, 15, 30, 60 and 120 minutes (n=4 each). Organs were removed, dry weighed and counted. Results are expressed as percent injected dose per gram tissue (%I.D./g).

*Lipophilicity*

The lipophilicity of the title compounds was determined using an HPLC assay based on Donovan and Pescatore [9]. Briefly, a short octadecyl-poly(vinyl alcohol) HPLC column (Supelco ODP-50; 4.6 x 20mm) was eluted with a flow rate of 2mL/min. A linear gradient from 10 to 100% methanol (organic phase) within 7 min was applied and buffers for pH 2, 7.4 and 10 (aqueous phase) were prepared; UV-detection was done at 270 nm. Toluene and triphenylene (dissolved in methanol) were used as internal standards and the injection volume was 20μL. Between consecutive HPLC runs, 5min for re-equilibration of the HPLC column were allowed. The $_{HPLC}$logP of a compound was then determined using the following equation:

$$_{HPLC}\log P_x = \frac{\left(\log P_{tol} - \log P_{tri}\right) \cdot t_{R,x} + t_{R,tol} \log P_{tri} - t_{R,tri} \log P_{tol}}{t_{R,tol} - t_{R,tri}}$$

where $logP_{tol}$ and $logP_{tri}$ are the logP values for toluene and triphenylene, respectively, from the literature [10] and $t_{R,tol}$ and $t_{R,tri}$ are the retention times for toluene and triphenylene, respectively, determined in the HPLC run. $t_{R,x}$ is the retention time of the compound.

$_{c}$logP-values were calculated based on the structural formulas of the compounds using the logP add-on within the ACD/chemsketch software (ACD labs; version 11.01; October 2007).

**Results**

*Precursor chemistry*

1.7g Tos@SUPPY was obtained as white crystalline powder and fully characterized as presented recently [1, 2].

2.10g purified Tos@SUPPY:2 was obtained (89%) as yellowish oil. For NMR-analysis, the solvent signal was used as an internal standard which was related to TMS with δ = 7.26ppm ($^1$H in CDCl$_3$) and δ = 77.0ppm ($^{13}$C in CDCl$_3$), respectively.

$^1$H-NMR (200 MHz, CDCl$_3$): δ (ppm) 7.82 (m, 2H), 7.58 (m, 2H), 7.38 (m, 4H), 4.26 (t, 2H, *J* = 6.30 Hz), 4.09 (q, 2H, *J* = 7.18 Hz), 3.39 (t, 2H, *J* = 6.20 Hz), 2.77 (q, 2H, *J* = 7.44 Hz), 2.64 (q, 2H, *J* = 7.82 Hz), 2.44 (s, 3H), 1.28 (t, 3H, *J* = 7.56 Hz), 1.17 (t, 3H, *J* = 6.94 Hz), 0.98 (t, 3H, *J* = 7.06 Hz).

$^{13}$C-NMR (50 MHz, CDCl$_3$): δ (ppm) 194.2, 168.2, 159.2, 157.3, 148.0, 145.1, 139.6, 132.6, 132.3, 129.9, 128.9, 128.3, 127.9, 126.6, 67.7, 61.5, 29.1, 28.8, 24.1, 21.6, 15.6, 14.0, 13.5.

IR (KBr): ν (cm$^{-1}$) 2978, 2938, 2878, 1724, 1678, 1598, 1556, 1495, 1463, 1447, 1403, 1362, 1278, 1250.

MS: m/z (%) 543 ($M^+$ + 2, 1), 542 (1), 311 (24), 310 (100), 282 (17), 264 (4), 236 (3), 155 (3), 91 (9).

Elemental analysis: calculated for $C_{28}H_{31}NO_6S_2$: C, 62.08; H, 5.77; N, 2.59. found: C, 61.92; H, 5.77; N, 2.57.

*Reference standards*

136.8mg FE@SUPPY was obtained as yellowish oil and fully characterized as presented recently [1, 2].

0.37g FE@SUPPY:2 was obtained after purification as yellowish oil.

$^1$H-NMR (200 MHz, CDCl$_3$): δ (ppm) 7.60 (m, 2H), 7.42 (m, 3H), 4.76 (t, 1H, *J* = 5.92 Hz), 4.53 (t, 1H, *J* = 5.94 Hz), 4.10 (q, 2H, *J* = 7.06 Hz), 3.50 (t, 1H, *J* = 5.94 Hz), 3.39 (t, 1H, *J* = 5.92 Hz), 2.86 (q, 2H, *J* = 7.44 Hz), 2.72 (q, 2H, *J* = 7.58 Hz), 1.34 (t, 3H, *J* = 7.46 Hz), 1.23 (t, 3H, *J* = 7.44 Hz), 0.98 (t, 3H, *J* = 7.06 Hz).

$^{13}$C-NMR (50 MHz, CDCl$_3$): δ (ppm) 194.4, 168.2, 159.2, 157.2, 148.0, 139.6, 132.6, 126.6, 81.3 (d, *J* = 170.5 Hz), 61.5, 30.0 (d, *J* = 21.8 Hz), 29.1, 24.1, 15.6, 14.0, 13.5.

IR (KBr): ν (cm$^{-1}$) 3061, 2978, 2939, 2902, 2879, 1726, 1678, 1557, 1465, 1448, 1405, 1380, 1279, 1251, 1175, 1144, 1091, 1076, 1014, 973.

MS: m/z (%) 389 ($M^+$, 3), 343 (4), 311 (20), 310 (100), 282 (14), 236 (7),105 (20), 77 (12).

High-resolution mass spectroscopy (HRMS): m/z calculated for $C_{21}H_{24}NO_3SF$: 389.1461; found: 389.1473.

*Automated radiosynthesis – [$^{18}$F]FE@SUPPY and [$^{18}$F]FE@SUPPY:2*

The described automated preparation of both fluorinated FE@SUPPY analogues was set up using standard PET radiochemistry equipment. The whole preparation including radiosynthesis, purification, sterile filtration and formulation was completed within 70-80min. Semi-preparative HPLC revealed consistent retention patterns for [$^{18}$F]FE@SUPPY and [$^{18}$F]FE@SUPPY:2 (retention times: 4.2-4.9min; k': 2.8-3.5). SPE purification led to a recovery of more than 90% using 2.0mL of ethanol.

So far, 15 complete high-scale radiosyntheses were performed for [$^{18}$F]FE@SUPPY and 7 preparations were conducted for [$^{18}$F]FE@SUPPY:2. Starting from 51 ± 25 GBq of [$^{18}$F]fluoride, 9.4 ± 3.6 GBq of formulated [$^{18}$F]FE@SUPPY and 5.1 ± 4.2 GBq of formulated [$^{18}$F]FE@SUPPY:2 were achieved.

Radiochemical purity as determined using radio-TLC and radio-HPLC always exceeded 97%. The only radioactive contaminant was found to be [$^{18}$F]fluoride. Specific radioactivity was determined via HPLC and found to be 70 ± 26 GBq/μmol for [$^{18}$F]FE@SUPPY and 340 ± 140 GBq/μmol for [$^{18}$F]FE@SUPPY:2, respectively, at the end of synthesis (EOS).

*Biodistribution experiments*

All values are shown in Table 1. The organ with the lowest uptake was fat showing 0.05±0.02%I.D./g after 5 minutes, followed by lung (0.07±0.05%I.D./g), spleen (0.07±0.03%I.D./g) and brain (0.07±0.01%I.D./g, all values after 120 minutes). Organs with highest uptake were bowels with 1.45±0.97%I.D./g after 15 minutes followed by the liver showing 1.08±0.39%I.D/g after 5 minutes. Other organs with pronounced uptake were kidney and heart. Blood activity was 0.12-0.18%I.D./g throughout the whole experiment. Remaining activity in the carcass was 0.15-0.39%I.D./g.

*Lipophilicity*

We found retention times of 4.95-5.15min for toluene and 8.05-8.15min for triphenylene. Both [$^{18}$F]FE@SUPPY and [$^{18}$F]FE@SUPPY:2 eluted at 6.48-6.67min. Using 2.74 as *logP*$_{tol}$ and 5.49 as *logP*$_{tri}$ [10], the $_{HPLC}$logP values of [$^{18}$F]FE@SUPPY and [$^{18}$F]FE@SUPPY:2 were calculated according to the equation given in the methods section. These $_{HPLC}$logP values at three different pH values and the calculated $_c$logP of [$^{18}$F]FE@SUPPY and [$^{18}$F]FE@SUPPY:2 are presented in table 2. All HPLC-experiments were repeated at least 4-times; given values are arithmetic means.

**Discussion**

*General*

Collectively, adenosine receptors are widespread on virtually every organ and tissue and represent promising drug targets for pharmacological intervention in many pathophysiological conditions such as asthma, neurodegenerative disorders, chronic inflammatory diseases, and cancer. The A3AR is the most recently identified adenosine receptor and its involvement in tumors has recently been shown: the A3ARs are highly expressed on the cell surface of tumor cells [11-16] and in human enteric neurons [17] but not in the majority of normal tissues [15]. In a very comprehensive study, A3AR mRNA expression in various tumor tissues was tested using reverse transcription-PCR analysis and A3AR protein expression was studied in fresh tumors and was correlated with that of the adjacent normal tissue. The authors conclude that primary and metastatic tumor tissues highly express A3AR indicating that high receptor expression is a characteristic of solid tumors. These findings suggest the A3AR as a potential target for tumor growth intervention

or imaging [18]. The A3ARs are also known to be involved in many other diseases, such as cardiac [19] and cerebral ischemia [20], glaucoma [21], stroke [22] and epilepsy [23].

Li et al [3] published a series of chemical structures, with most of them displaying reasonable affinities for the A3AR. Amongst all the investigated structures, FE@SUPPY (see figure 1) was the most affine compound for the A3AR ($K_i$ 4.22 nM) and thus was selected and developed as [18F]FE@SUPPY, the first PET-tracer [1,2]. Hence, having developed a series of fluoroethyl-esters over the last five years [24-29], it was obvious for us to develop [18F]FE@SUPPY:2.

*Precursor and reference standard*

Organic chemistry of precursor and reference molecules were accomplished in straightforward procedures. Preparations and purifications were performed with good yields; unexpectedly the tosylation reactions for both precursors were time-consuming.

*Automated radiosynthesis – [18F]FE@SUPPY and [18F]FE@SUPPY:2*

Automation of the radiosyntheses of [18F]FE@SUPPY and [18F]FE@SUPPY:2 was straight forward using the GE *TRACERlab Fx$_{FN}$* synthesizer with minor modifications (shortcuts). No problems were encountered when implementing the "manual" radiosynthesis [1, 2] on this synthesizer platform and, so far, not a single failed preparation was observed.

For the satisfying synthesis of [18F]FE@SUPPY:2, a higher amount of precursor was needed (+50%) in comparison to [18F]FE@SUPPY. Nevertheless, radiochemical yields were drastically lower for [18F]FE@SUPPY:2 – 16.4 ± 9.7 % compared to 32.3 ± 12.4 % for [18F]FE@SUPPY (values based on [18F]fluoride, corrected for decay). Nucleophilic substitution of the tosyl-leaving group on a thiocarboxylic ester moiety therefore seems to be slower than on a

carboxylic ester. Interestingly, the found specific radioactivities were dramatically higher for [$^{18}$F]FE@SUPPY:2.

*Biodistribution experiments*

As presented in Table 1, organs displaying highest uptake were the bowels, followed by liver. Initially, uptake in the kidneys was high, too, yet decreasing significantly after 15 minutes. Since our group has demonstrated recently that [$^{18}$F]fluoroethyl esters are primarily metabolized by carboxylic esterases, high kidney uptake could be explained by the renal excretion route of the major expected metabolite, [$^{18}$F]fluoroethanol [30, 31]. High liver uptake could be explained by metabolism taking place in the cytochrome P-450-rich hepatosomes.

Comparing maximum uptake values over time of [$^{18}$F]FE@SUPPY and [$^{18}$F]FE@SUPPY:2, we found good correlations in brain, muscle and testes; all other organs showed pronounced uptake variations. Comparing mean uptake values over time, only muscle and testes showed some degree of correlation. Figure 3 shows a comparison of the six most expedient organs and tissues: liver, fat, colon, ileum/jejunum, femur and brain. Interestingly - in contrast to [$^{18}$F]FE@SUPPY - uptake of [$^{18}$F]FE@SUPPY:2 increased over time in fat and femur. Increasing uptake in fat could be explained by the relatively pronounced lipophilicity of [$^{18}$F]FE@SUPPY:2 (see table 2), whereas usually bone uptake is attributed to defluorination. Initially high uptake in ileum/jejunum associated with increasing uptake in colon over time could be due to potential hepatobiliary clearance of [$^{18}$F]FE@SUPPY:2. This fact could not be observed for [$^{18}$F]FE@SUPPY. Calculating brain to blood ratios, we observed a dramatic increase of the ratio for [$^{18}$F]FE@SUPPY (2.73-18.33; see figure 4), whereas [$^{18}$F]FE@SUPPY:2

remained constant over time. So far, we are left without an explanation for this phenomenon.

*Lipophilicity*

As a prerequisite for its successful application as a radiopharmaceutical, a molecule has to exhibit several properties: it should be widely available, it should accumulate in the target tissue in stable condition and within a reasonable time flow and it should bind to the desired structures (receptor sites, enzymes, transporters, proteins…) with high affinity, selectivity and specificity. Since logP is known to influence many of these pharmacokinetic and pharmacodynamic parameters, especially unspecific binding of radiopharmaceuticals and blood brain barrier permeability [32], we tried to pay specific deference to this measure although we are well aware of the fact, that logP is of limited value as a predictor for lipophilicity. Nevertheless, it is the most commonly used and prominent measure.

LogP (or more precisely $_{OW}$logP where OW stands for octanol/water) is defined as the decadal logarithm of the partition coefficient between equal volumes of 1-octanol and water. Normally, an aliquot of the solid compound is dissolved directly in a mixture of 1-octanol and water, the phases are separated and then the content is determined using e.g. chromatographic or spectroscopic methods. But in the case of radiopharmaceutical preparations, on the one hand, one has the advantage of using the radioactivity for very accurate measurement of the product concentration but, on the other hand, one rarely has access to solid compounds. Furthermore, the final preparation is always contaminated by small amounts of other radioactive species (e.g. by-products, educts…). Even these small amounts (1-3%) would significantly bias the outcome of the measurement of the $_{OW}$logP: if, for instance, the final product solution of a typical lipophilic compound displayed a

radiochemical purity of 99% and the remaining 1% could be attributed to a contamination with hydrophilic [18F]fluoride, the partition coefficient would never be higher than 99 to 1 and therefore the $_{OW}$logP measurement would always give a result lower than 2! Thus, optimized methods have been proposed to overcome this problem [33]. In our mind, the most elegant solution to get an accurate and simple measure of the lipophilicity is using the $_{HPLC}$logP instead of $_{OW}$logP. Since contaminations are separated within the HPLC run they do not interfere with the retention of the main compound. Additionally, the used HPLC method is very simple and inexpensive, it may be used both with radioactive and non-radioactive compounds and the pH of the aqueous phase may be adjusted easily to whatever value is desired.

As shown in table 2, logP values for both [18F]FE@SUPPY-derivatives are comparatively high. It is known, that high lipophilicity significantly contributes to the amount of unspecific binding. However, $_{HPLC}$logP values measured for well established PET-tracers such as [11C]DASB ($_{HPLC}$logP: 3.81), [11C]carfentanil ($_{HPLC}$logP: 3.37) or [11C]verapamil ($_{HPLC}$logP: 3.35) are also high and found their way into scientific routine. Hence, although being in the upper range, logP values should not be an obstacle for further expedient application of [18F]FE@SUPPY-derivatives.

**Conclusion**

Aims of the present study were (1) the automatized preparation of both [18F]FE@SUPPY-derivatives, (2) the biodistribution of [18F]FE@SUPPY:2 in rats, (3) the characterisation of the lipophilicity and (4) the comparison of the findings of [18F]FE@SUPPY and [18F]FE@SUPPY:2.

Results show that

(1) [$^{18}$F]FE@SUPPY:2, an alternative to [$^{18}$F]FE@SUPPY, the first PET-ligand for the adenosine A$_3$ receptor, was prepared in a reliable and feasible manner. Automation yields for both molecules were sufficient for further preclinical and clinical applications.

(2) Biodistribution experiments evinced bowels and liver as organs with highest uptake, suggesting metabolic activity and hepatobiliary excretion. Intermediate uptake was found in kidney, lung and heart, all organs known to express A3AR.

(3) LogP values are in the upper range but should not pose any hindrance for successful application of [$^{18}$F]FE@SUPPY and [$^{18}$F]FE@SUPPY:2 in future.

(4) The uptake pattern of [$^{18}$F]FE@SUPPY:2 differed from [$^{18}$F]FE@SUPPY, especially brain to blood ratios are considerably higher for [$^{18}$F]FE@SUPPY.

Hence, from a radiopharmaceutical perspective, drastically better specific radioactivities would militate in favour of [$^{18}$F]FE@SUPPY:2; preclinical evaluations, so far, seem to point in favour of [$^{18}$F]FE@SUPPY. Taken together, our preliminary data do not yet permit the decision upon the selection of the optimum [$^{18}$F]FE@SUPPY-derivative. With [$^{18}$F]FE@SUPPY:2, we are able to provide a second potential tracer that could help to further characterize the still quite unexplored A3AR.

# References

[1] Wadsak W, Mien LK, Shanab K, Weber K, Schmidt B, Sindelar KM, Ettlinger DE, Haeusler D, Spreitzer H, Keppler BK, Viernstein H, Dudczak R, Kletter K, Mitterhauser M. Radiosynthesis of the adenosine $A_3$ receptor ligand 5-(2-[$^{18}$F]fluoroethyl)2,4-diethyl-3-(ehtylsulfanylcarbonyl)-6-phenylpyridine-5-carboxylate ([$^{18}$F]FE@SUPPY). Radiochim. Acta 2008; 96:119-24.

[2] Wadsak W, Mien LK, Shanab K, Ettlinger DE, Haeusler D, Sindelar K, Lanzenberger RR, Spreitzer H, Viernstein H, Keppler BK, Dudczak R, Kletter K, Mitterhauser M. Preparation and first evaluation of [$^{18}$F]FE@SUPPY: a new PET tracer for the adenosine $A_3$ receptor. Nucl Med Biol 2008; 35:61-6.

[3] Li AH, Moro S, Forsyth N, Melman N, Ji XD, Jacobson KA. Synthesis, CoMFA analysis, and receptor docking of 3,5-diacyl-2, 4-dialkylpyridine derivatives as selective A3 adenosine receptor antagonists. J Med Chem 1999; 42:706-21.

[4] Liederer BM, Borchardt RT. Enzymes involved in the bioconversion of ester-based prodrugs. J Pharm Sci 2006; 95:1177-95.

[5] Rooseboom M, Commandeur JN, Vermeulen NP. Enzyme-catalyzed activation of anticancer prodrugs. Pharmacol Rev 2004; 56:53-102.

[6] Azéma L, Lherbet C, Baudoin C, Blonski C. Cell permeation of a Trypanosoma brucei aldolase inhibitor: Evaluation of different enzyme-labile phosphate protecting groups. Bioorg Med Chem Lett 2006; 16:3440-3.

[7] Shanab K, Wadsak, W., Mien, L-K., Mitterhauser, M., Holzer, W., Polster, V., Viernstein, H., Spreitzer, H. Synthesis of in vivo metabolites of the new Adenosine $A_3$ Receptor PET-Radiotracer [$^{18}$F]FE@SUPPY. Heterocycles 2008; 75:339-56.

[8] Shanab K. Synthese von Precursoren von A3-Adenosin-Rezeptor PET-Tracern: Im Dienste der Nuklearmedizin. Wien: Vdm Verlag; 2008.

[9] Donovan SF, Pescatore MC. Method for measuring the logarithm of the octanol-water partition coefficient by using short octadecyl-poly(vinyl alcohol) high-performance liquid chromatography columns. J Chromatogr A 2002; 952:47-61.

[10] Tomlin C. The pesticide manual-a world compendium. 12th edition. Bath: British Corp Protection Council/Royal Society of Chemistry; 2000.

[11] Gessi S, Varani K, Merighi S, Morelli A, Ferrari D, Leung E, Baraldi PG, Spalluto G, Borea PA. Pharmacological and biochemical characterization of A3 adenosine receptors in Jurkat T cells. Br J Pharmacol 2001; 134:116-26.

[12] Merighi S, Varani K, Gessi S, Cattabriga E, Iannotta V, Ulouglu C, Leung E, Borea PA. Pharmacological and biochemical characterization of adenosine receptors in the human malignant melanoma A375 cell line. Br J Pharmacol 2001; 134:1215-26.

[13] Suh BC, Kim TD, Lee JU, Seong JK, Kim KT. Pharmacological characterization of adenosine receptors in PGT-beta mouse pineal gland tumour cells. Br J Pharmacol 2001; 134:132-42.

[14] Gessi S, Varani K, Merighi S, Cattabriga E, Iannotta V, Leung E, Baraldi PG, Borea PA. A3 adenosine receptors in human neutrophils and promyelocytic HL60 cells: a pharmacological and biochemical study. Mol Pharmacol 2002; 61:415-24.

[15] Fishman P, Bar-Yehuda S, Madi L, Cohn I. A3 adenosine receptor as a target for cancer therapy. Anticancer Drugs 2002; 13:437-43.

[16] Fishman P, Bar-Yehuda S, Ardon E, Rath-Wolfson L, Barrer F, Ochaion A, Madi L. Targeting the A3 adenosine receptor for cancer therapy: inhibition of prostate carcinoma cell growth by A3AR agonist. Anticancer Res 2003; 23:2077-83.

[17] Christofi FL, Zhang H, Yu JG, Guzman J, Xue J, Kim M, Wang YZ, Cooke HJ. Differential gene expression of adenosine $A_1$, $A_{2A}$, $A_{2B}$, and $A_3$ receptors in the human enteric nervous system. J Comp Neurol 2001; 439:46-64.

[18] Madi L, Ochaion A, Rath-Wolfson L, Bar-Yehuda S, Erlanger A, Ohana G, Harish A, Merimski O, Barer F, Fishman P. The A3 adenosine receptor is highly expressed in tumor versus normal cells: potential target for tumor growth inhibition. Clin Cancer Res 2004; 10:4472-9.

[19] Liang BT, Jacobson KA. A physiological role of the adenosine A3 receptor: sustained cardioprotection. Proc Natl Acad Sci U S A 1998; 95:6995-9.

[20] von Lubitz DK, Ye W, McClellan J, Lin RC. Stimulation of adenosine A3 receptors in cerebral ischemia. Neuronal death, recovery, or both? Ann N Y Acad Sci 1999; 890:93-106.

[21] Avila MY, Stone RA, Civan MM. Knockout of A3 adenosine receptors reduces mouse intraocular pressure. Invest Ophthalmol Vis Sci 2002; 43:3021-6.

[22] Von Lubitz DK, Simpson KL, Lin RC. Right thing at a wrong time? Adenosine A3 receptors and cerebroprotection in stroke. Ann N Y Acad Sci 2001; 939:85-96.

[23] Laudadio MA, Psarropoulou C. The A3 adenosine receptor agonist 2-Cl-IB-MECA facilitates epileptiform discharges in the CA3 area of immature rat hippocampal slices. Epilepsy Res 2004; 59:83-94.

[24] Mitterhauser M, Wadsak W, Wabnegger L, Sieghart W, Viernstein H, Kletter K, Dudczak R. In vivo and in vitro evaluation of [$^{18}$F]FETO with respect to the adrenocortical and GABAergic system in rats. Eur J Nucl Med Mol Imaging 2003; 30:1398-401.

[25] Mitterhauser M, Wadsak W, Wabnegger L, Mien LK, Togel S, Langer O, Sieghart W, Viernstein H, Kletter K, Dudczak R. Biological evaluation of 2'-[$^{18}$F]fluoroflumazenil ([$^{18}$F]FFMZ), a potential GABA receptor ligand for PET. Nucl Med Biol 2004; 31:291-5.

[26] Mitterhauser M, Wadsak W, Mien LK, Hoepping A, Viernstein H, Dudczak R, Kletter K. Synthesis and biodistribution of [$^{18}$F]FE@CIT, a new potential tracer for the dopamine transporter. Synapse 2005; 55:73-9.

[27] Wadsak W, Mien LK, Ettlinger DE, Eidherr H, Haeusler D, Sindelar KM, Keppler BK, Dudczak R, Kletter K, Mitterhauser M. [$^{18}$F]fluoroethylations: different strategies for the rapid translation of 11C-methylated radiotracers. Nucl Med Biol 2007; 34:1019-28.

[28] Wadsak W, Mien L-K, Ettlinger D, Feitscher S, Toegl S, Lanzenberger R, Marton J, Dudczak R, Kletter K, Mitterhauser M. Preparation and Biodistribution [$^{18}$F]FE@CFN (2-[$^{18}$F]fluoroethyl-4-[N-(1-oxopropyl)-N-phenylamino]-1-(2-phenylethyl)-4-piperidine-carboxylate) a Potential μ-Opioid Receptor Imaging Agent. Radiochim. Acta 2007; 95:33-8.

[29] Wadsak W, Mitterhauser M. Synthesis of [$^{18}$F]FETO, a novel potential 11-ß hydroxylase inhibitor. J Label Compd Radiopharm 2003; 46:379-88.

[30] Ettlinger DE, Wadsak W, Mien LK, Machek M, Wabnegger L, Rendl G, Karanikas G, Viernstein H, Kletter K, Dudczak R, Mitterhauser M. [$^{18}$F]FETO: metabolic considerations. Eur J Nucl Med Mol Imaging 2006; 33:928-31.

[31] Ettlinger DE, Haeusler D, Wadsak W, Girschele F, Sindelar KM, Mien LK, Ungersboeck J, Viernstein H, Kletter K, Dudczak R, Mitterhauser M. Metabolism and autoradiographic evaluation of [$^{18}$F]FE@CIT: a Comparison with [$^{123}$I]beta-CIT and [$^{123}$I]FP-CIT. Nucl Med Biol 2008; 35:475-9.

[32] Lipinski CA, Lombardo F, Dominy BW, Feeney PJ. Experimental and computational approaches to estimate solubility and permeability in drug discovery and development settings. Adv Drug Del Rev 1997; 23:3-25.

[33] Wilson AA, Jin L, Garcia A, DaSilva JN, Houle S. An admonition when measuring the lipophilicity of radiotracers using counting techniques. Appl Radiat Isot 2001; 54:203-8.

**Captions**

Figure 1 – Structural differences in fluoroethylated SUPPY and SUPPY:2 compounds and their precursor molecules.

Figure 2 – Graphical illustration of the automated set-up of the commercially available TRACERlab Fx $_{FN}$ module for [$^{18}$F]FE@SUPPY and [$^{18}$F]FE@SUPPY:2 synthesis.

Figure 3 – A comparison of the uptake of [$^{18}$F]FE@SUPPY and [$^{18}$F]FE@SUPPY:2 in several organs. Values represent %I.D./g, n=4, error bars represent standard deviation.

Figure 4 – Brain to blood ratios of [$^{18}$F]FE@SUPPY and [$^{18}$F]FE@SUPPY:2 after various time points. Values represent arithmetic means of individually calculated ratios, n=4, error bars represent standard deviation.

Table 1 – Biodistribution values of [$^{18}$F]FE@SUPPY:2 in rats at different time points.

Table 2 – Experimentally determined $_{HPLC}$logP and calculated $_c$logP values of [$^{18}$F]FE@SUPPY and [$^{18}$F]FE@SUPPY:2.

Figure 1 – Structural differences in fluoroethylated SUPPY and SUPPY:2 compounds and their precursor molecules.



| compound | $R_1$ | $R_2$ |
|---|---|---|
| [$^{18}$F]FE@SUPPY | -H | -$^{18}$F |
| [$^{18}$F]FE@SUPPY:2 | -$^{18}$F | -H |
| Tos@SUPPY | -H | -OTos |
| OH@SUPPY | -H | -OH |
| Tos@SUPPY:2 | -OTos | -H |
| OH@SUPPY:2 | -OH | -H |

Figure 2 – Graphical illustration of the automated set-up of the commercially available

TRACERlab Fx $_{FN}$ module for [18F]FE@SUPPY and [18F]FE@SUPPY:2 synthesis.

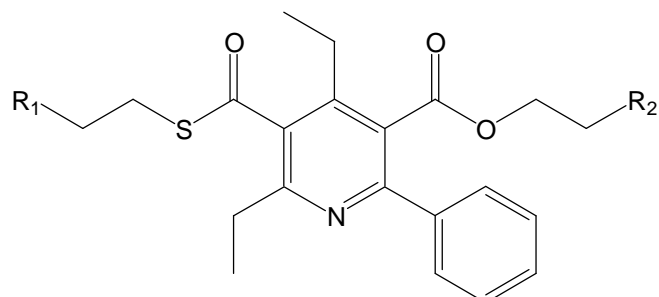Figure 3 – A comparison of the uptake of [$^{18}$F]FE@SUPPY and [$^{18}$F]FE@SUPPY:2 in several organs. Values represent %I.D./g, n=4, error bars represent standard deviation.
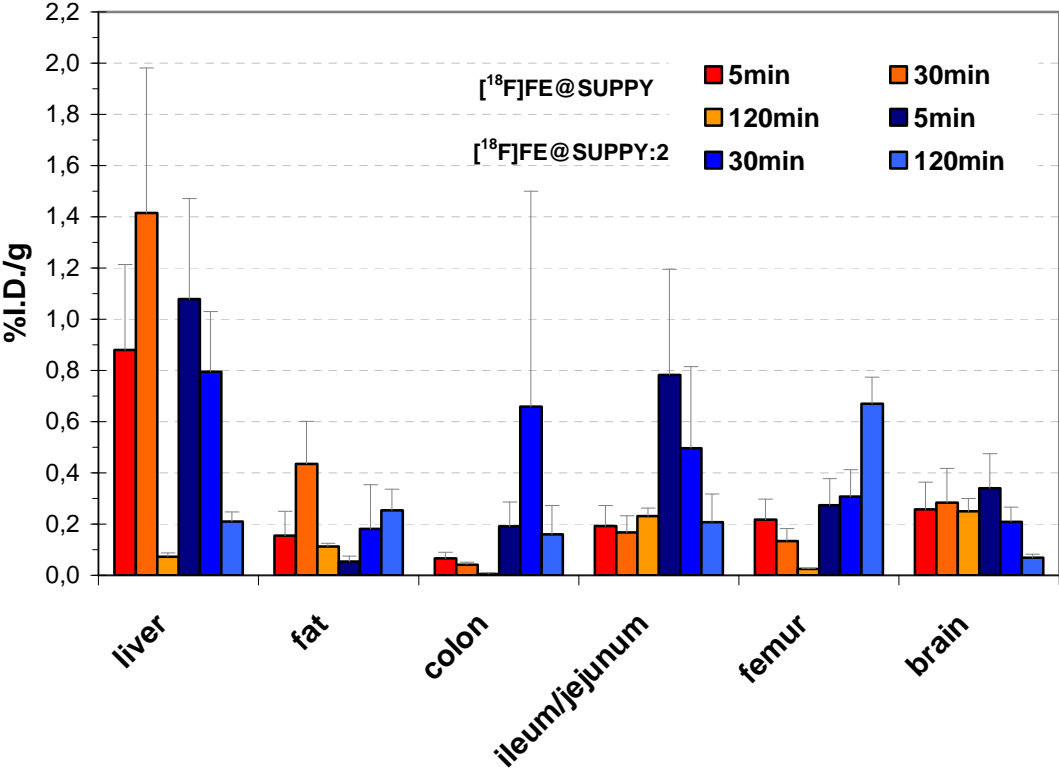
Figure 4 – Brain to blood ratios of [$^{18}$F]FE@SUPPY and [$^{18}$F]FE@SUPPY:2 after various time points. Values represent arithmetic means of individually calculated ratios, n=4, error bars represent standard deviation.
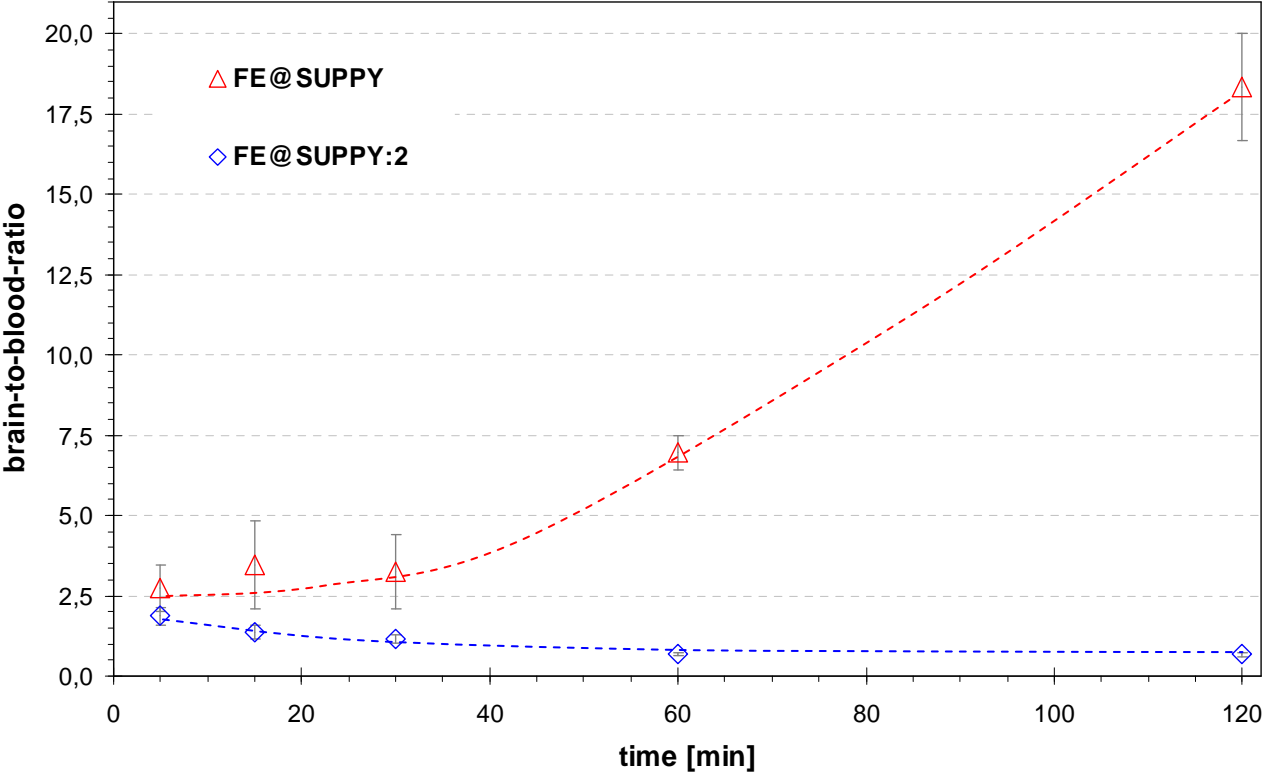
Table 1 – Biodistribution values of [$^{18}$F]FE@SUPPY:2 in rats at different time points.

| Tissue | 5min | 15min | 30min | 60min | 120min |
|---|---|---|---|---|---|
| blood | 0,18 ± 0,05 | 0,15 ± 0,05 | 0,18 ± 0,05 | 0,14 ± 0,02 | 0,12 ± 0,03 |
| liver | 1,08 ± 0,39 | 0,76 ± 0,34 | 0,79 ± 0,24 | 0,40 ± 0,06 | 0,21 ± 0,04 |
| femur | 0,27 ± 0,10 | 0,20 ± 0,10 | 0,31 ± 0,10 | 0,48 ± 0,08 | 0,67 ± 0,10 |
| lung | 0,48 ± 0,14 | 0,31 ± 0,11 | 0,25 ± 0,06 | 0,12 ± 0,04 | 0,07 ± 0,05 |
| heart | 0,85 ± 0,24 | 0,40 ± 0,07 | 0,31 ± 0,08 | 0,15 ± 0,03 | 0,10 ± 0,03 |
| thyroid | 0,41 ± 0,13 | 0,24 ± 0,09 | 0,30 ± 0,13 | 0,21 ± 0,03 | 0,14 ± 0,09 |
| kidney | 1,06 ± 0,37 | 0,56 ± 0,16 | 0,61 ± 0,13 | 0,43 ± 0,11 | 0,26 ± 0,05 |
| testes | 0,10 ± 0,04 | 0,08 ± 0,04 | 0,13 ± 0,05 | 0,11 ± 0,02 | 0,09 ± 0,03 |
| fat | 0,05 ± 0,02 | 0,08 ± 0,04 | 0,18 ± 0,17 | 0,19 ± 0,03 | 0,25 ± 0,08 |
| muscle | 0,26 ± 0,10 | 0,15 ± 0,09 | 0,18 ± 0,08 | 0,12 ± 0,04 | 0,08 ± 0,04 |
| colon | 0,19 ± 0,09 | 0,21 ± 0,15 | 0,66 ± 0,84 | 0,69 ± 1,00 | 0,16 ± 0,11 |
| ileum/jejunum | 0,78 ± 0,41 | 1,45 ± 0,97 | 0,50 ± 0,32 | 0,45 ± 0,28 | 0,21 ± 0,11 |
| spleen | 0,33 ± 0,13 | 0,18 ± 0,05 | 0,17 ± 0,05 | 0,09 ± 0,02 | 0,07 ± 0,03 |
| brain | 0,34 ± 0,13 | 0,18 ± 0,02 | 0,21 ± 0,06 | 0,09 ± 0,02 | 0,07 ± 0,01 |
| carcass | 0,31 ± 0,09 | 0,39 ± 0,13 | 0,33 ± 0,13 | 0,26 ± 0,05 | 0,15 ± 0,05 |

Values represent percentage of injected dose per gram of tissue (% I.D./g; arithmetic means ± standard deviation)

Table 2 – Experimentally determined $_{HPLC}$logP and calculated $_c$logP values of [$^{18}$F]FE@SUPPY and [$^{18}$F]FE@SUPPY:2.

| | $_{HPLC}$logP | | | $_c$logP |
|---|---|---|---|---|
| | pH 2 | pH 7.4 | pH 10 | |
| [$^{18}$F]FE@SUPPY | 3.99 | 4.04 | 4.06 | 5.81 |
| [$^{18}$F]FE@SUPPY:2 | 4.12 | 4.05 | 4.10 | 5.81 |

# [18F]FE@SUPPY AND [18F]FE@SUPPY:2 - METABOLIC CONSIDERATIONS

Authors: **Daniela Haeusler**[1,2#], Lukas Nics[1,3#], Leonhard-Key Mien[1,2], Johanna Ungersboeck[1,4], Rupert R. Lanzenberger[5], Karem Shanab[6], Karoline M. Sindelar[1], Helmut Viernstein[2], Karl-Heinz Wagner[3], Robert Dudczak[1], Kurt Kletter[1], Wolfgang Wadsak[1,4] Markus Mitterhauser[1,2,7*]

[1]Dept of Nuclear Medicine, Medical University of Vienna, Austria

[2]Dept of Pharmaceutical Technology and Biopharmaceutics, University of Vienna, Austria

[3]Dept of Nutritional Sciences, University of Vienna, Austria

[4]Dept of Inorganic Chemistry, University of Vienna, Austria

[5]Dept of Psychiatry and Psychotherapy, Medical University of Vienna, Austria

[6]Dept of Drug and Natural Product Synthesis, University of Vienna, Austria

[7]Hospital Pharmacy of the General Hospital of Vienna, Austria

#... the authors contributed equally

**Abstract**

**Introduction:** Recently, [$^{18}$F]FE@SUPPY and [$^{18}$F]FE@SUPPY:2 were introduced as the first PET-tracers for the adenosine A$_3$ receptor. Thus, aim of the present study was the metabolic characterisation of the two adenosine A$_3$ receptor PET tracers. **Methods:** *In-vitro* carboxylesterase experiments were conducted using incubation mixtures containing of different concentrations of the two substrates, porcine carboxylesterase and phosphate buffered saline. Enzymatic reactions were stopped by adding acetonitrile/methanol (10:1) after various timepoints, and analyzed by a HPLC standard protocol. *In-vivo* experiments were conducted in male wild type rats; tracers were injected through a tail vein. Rats were sacrificed after various timepoints (n=3) and blood and brain samples were collected. Sample clean-up was performed by a HPLC standard protocol. **Results:** The rate of enzymatic hydrolysis by carboxylesterase demonstrated Michaelis-Menten constants in a µM range (FE@SUPPY: 20.15µM and FE@SUPPY:2: 13.11µM) and limiting velocities of 0.035µM/min and 0.015µM/min for FE@SUPPY and FE@SUPPY:2, respectively. Degree of metabolism in blood showed: 15min p.i. 47.7% of [$^{18}$F]FE@SUPPY were intact compared to 33.1% of [$^{18}$F]FE@SUPPY:2; 30min p.i. 30.3% intact [$^{18}$F]FE@SUPPY were found compared to 15.6% [$^{18}$F]FE@SUPPY:2. In brain [$^{18}$F]FE@SUPPY:2 formed an early hydrophilic metabolite, whereas metabolism of [$^{18}$F]FE@SUPPY was not observed before 30 minutes p.i. **Conclusion:** Knowing, that metabolism in rats is several times faster than in human, we conclude that [$^{18}$F]FE@SUPPY should be stable for the typical time span of a clinical investigation. As a consequence, from a metabolic point of view, one would tend to decide in favour of [$^{18}$F]FE@SUPPY.

**Keywords:** PET, Adenosine A$_3$ Receptor, Fluorine-18, SUPPY, Metabolism, Carboxylesterase

**Introduction**

Adenosine is an important regulatory molecule which activates four receptors named $A_1$, $A_{2A}$, $A_{2B}$, and $A_3$ (A1R, A2AR, A2BR, A3R), respectively, which all belong to the G-protein–coupled superfamily of receptors. There exists a lot of information about the $A_1$ and $A_{2A}$ receptors, because good pharmacological tools - including radioligands - are available. In the case of the $A_3$ receptors, these tools have been presented lately, but there is still little information in literature regarding the distribution and density of these receptors in humans.

Yet, A3R agonists and antagonists are discussed for the treatment of pathophysiological conditions, such as asthma, neurodegenerative disorders and inflammatory diseases [1]. Moreover, it was repeatedly shown that A3Rs are highly expressed on the cell surface of various tumor cell lines [2, 3]. Hence, the A3R may also serve as a potential target for tumor growth inhibition and tumor imaging. The most suitable and accurate technique to gain information about receptors in the living organism is PET (positron emission tomography). As a prerequisite for molecular PET imaging, there is need for suitable radioligands displaying high affinity, high selectivity and low nonspecific binding.

The fluoroethylester FE@SUPPY (5-(2-fluoroethyl) 2,4-diethyl-3-(ethylsulfanyl-carbonyl)-6-phenylpyridine-5-carboxylate), which was evaluated by Li et al., displays high affinity ($K_i$=4.22nM) as well as excellent selectivity for the A3R (ratio $A_1/A_3$=2700) [4]. Recently, we introduced [$^{18}$F]FE@SUPPY as the first PET-tracer for the A3R [5, 6]. Meanwhile, a second potential PET-radiotracer has been presented, radiolabelled with the radionuclide bromine-76 [7].

Regarding possible metabolic pathways for [$^{18}$F]FE@SUPPY, it has to be pointed out that this diacyl-derivative carries two ester moieties, one carboxylic and one thiocarboxylic ester.

134

Enzymes derived from the family of porcine carboxylesterases EC 3.1.1.1 (CES) would be expected to significantly contribute to cleavage of the ester function and thus to the degradation of this molecule [8]. [18F]FE@SUPPY carries the [18F]fluoroethyl-substituent on the carboxylic function, whereas the thiocarboxylic moiety carries an ethyl-ester group. It appeared promising to exchange these fluoroethyl and ethyl substituents within the molecule to generate a structural analogue which could be evaluated as a second potential PET-tracer.

Hence, we translated the fluoroethyl-ester [18F]FE@SUPPY into the fluoroethyl-thioester [18F]FE@SUPPY:2 (5-ethyl 2,4-diethyl-3-((2-[18F]fluoroethyl) sulfanylcarbonyl)-6-phenylpyridine-5-carboxylate) [9, 10]. As far as assessable from literature, there is no conclusive data regarding differences in stability of carboxylic and thiocarboxylic ester moieties within one molecule. Interestingly, Azema et al. presented evidence for increased stability of a thioester function compared to a carboxylic ester group [11].

The radiosyntheses of both molecules were performed in simple one-pot, one-step reactions with good and reliable radiolabelling yields and good specific radioactivities [5, 9]. Biodistribution experiments revealed that the uptake pattern of the two tracers mainly followed the distribution pattern of the A3R mRNA [6, 10].

As a next step in the preclinical evaluation of these two radioligands, their metabolic profiles had to be examined to gain further information regarding their stability and degradation *in-vitro* and *ex-vivo*. Since radioactive metabolites – if present in the target tissue – could interfere with the signal of the intact molecule, distinct information regarding the amount of possible formation of these metabolites is crucial before application in humans. Thus, aims

of the present study were the metabolic characterisation and the comparison of the two A3R PET tracers, [18F]FE@SUPPY and [18F]FE@SUPPY:2.

In detail we aimed for,

(1) the assessment of the *in-vitro* stability of FE@SUPPY and FE@SUPPY:2 against

 Carboxylesterase and the metabolites;

(2) the determination of the extent of metabolisation of [18F]FE@SUPPY and [18F]FE@SUPPY:2 in rodents; and

(3) the comparison of the metabolic behaviour of both tracers.

**Materials and Methods**

*General*

Radioanalytical thinlayer chromatography (radio-TLC) was performed for determination of radiochemical purity using TLC Silicagel 60 $F_{254}$ plates from Merck (Darmstadt, Germany). Analyses of radio-TLC plates were performed using a Canberra-Packard Instant Imager (Perkin Elmer, Watford, UK). Analytical high-performance liquid chromatography (HPLC) system was used for determination of specific radioactivity and identity consisting of a Merck-Hitachi LaChrom pump and UV-detector, as well as a NaI-radiodetector from Berthold Technologies (Bad Wildbach, Germany). The semi-preparative HPLC system (as part of the GE *TRACERlab Fx$_{FN}$* synthesizer) consisted of a Sykam S1021 pump (Sykam GmbH, Eresing, Germany), an UV detector and a radioactivity detector.

Solid phase extraction cartridges (SepPak® C18plus) were purchased from Waters Associates (Milford, USA). Anion exchange cartridges (PS-HCO₃) for [¹⁸F]fluoride fixation were obtained from Macherey-Nagel (Dueringen, Germany). All starting materials for precursor and reference standard syntheses were commercially available and used without further purification. Acetonitrile was purchased from Merck; methanol and carboxylesterase (E-3019) were purchased from Sigma Aldrich (Steinheim, Germany).

*HPLC System1:* Autosampler 1100, quaternary pump 1200 (at a flow rate of 1ml/min) and diode array detector 1100 (248 and 255nm) were purchased from Agilent (Böblingen, Germany). LiChrospher®100 (RP-18 LiChroCART® 125-4mm) and LiChrospher®100 pre-column (RP-18 LiChroCART® 4-4mm) as well as chemicals for mobile phase (0.034M sodium citrate tribasic dihydrate, pH 2.5 and acetonitrile) were purchased from Merck. Mobile phase: citrate buffer/acetonitrile 1:1.

*HPLC System2:* Pump L-6220 (at a flow rate of 2ml/min) and UV-detector L-4000 were purchased from Merck-Hitachi. Radiomatic Flo-One Beta Flow Scintillation Analyzer was purchased from Packard, Radiomatic FlowBeta FSA 150 detector cell from PerkinElmer. Columns (Cromolith® Performance RP-18e 100-4.6mm) and chemicals for mobile phase (60% acetonitrile and 40% water/acetic acid 97.5/2.5, 32mM ammonium acetate, pH 3.5) were purchased from Merck.

*Chemistry and Radiochemistry*

The preparations of the precursors, Tos@SUPPY and Tos@SUPPY:2, as well as the productions of the reference standards FE@SUPPY, FE@SUPPY:2, SUPPY:0, FE@SUPPY:11, FE@SUPPY:21, DFE@SUPPY and DFE@SUPPY:2 were described in detail elsewhere [9, 10, 12, 13] (for chemical structures see figure 1).

The automated preparations of both [18F]fluorinated FE@SUPPY analogues were performed on a GE *TRACERlab Fx$_{FN}$* synthesizer by radiofluorination of the corresponding tosylated precursor in a one-step, one-pot reaction, as already described [5, 9].

*Enzyme reactions*

Experiments (n=3) were performed using several pre-tested concentrations of the two tracers to get reasonable Michaelis-Menten kinetics. For FE@SUPPY concentrations of 20, 50, 100, 200, 350µg/ml and for FE@SUPPY:2 concentrations of 5, 10, 20, 50, 200, 350µg/ml turned out to be most useful. Incubations of the substrates were accomplished with constant quantity of porcine carboxylesterase: 80 I.U. in phosphate buffered saline (PBS) at 37°C. Enzymatic reactions were stopped by adding twice the amount of acetonitrile/methanol (10:1) after 0, 60, 120, 180, 240, 360min, respectively. After centrifugation (10000rpm, 3min) of the reaction mixtures, the obtained supernatant (~80µl) was analyzed by HPLC (injecting volume 20µl; System1).

*Metabolite studies*

*In-vivo* experiments were approved by the Austrian law on animal experiments and followed the protocol established in previous studies of our group [6]. Briefly, 42 male wild type rats (250-300g) were either injected with 17±1MBq of [18F]FE@SUPPY (n=21) or with 14±1MBq of [18F]FE@SUPPY:2 (n=21) through a tail vein. Subsequently, the rats were sacrificed after 2, 5, 10, 15, 30, 60, 120 minutes (n=3).

Blood samples (3ml) were collected from the abdominal aorta in sodium citrate buffered tubes and centrifuged (3000rpm, 5min) to separate cellular components. Sample clean-up was performed by vortexing plasma with the equivalent amount of methanol/acetonitrile (9:1) for 1min and by subsequent two step-centrifugation (3000rpm, 3min and 10000rpm,

3min) to remove precipitated proteins. The obtained supernatants were analyzed by HPLC (System2).

Brains were collected, weighed, homogenized and washed twice with phosphate buffered saline. After centrifugation (15000rpm; 5min), sample clean-up was performed as described for blood samples. Statistical calculations were performed with Microsoft® Excel and Graph Pad Prism®.

**Results**

*Radiochemistry*

The radiopreparations for both A3R radioligands were completed within 70-80min. Starting from 51±25GBq of [$^{18}$F]fluoride, 9.4±3.6GBq ([$^{18}$F]FE@SUPPY) and 5.1±4.2GBq ([$^{18}$F]FE@SUPPY:2) were formulated. Specific radioactivity (determined via radio-HPLC) was 70±26GBq/µmol for [$^{18}$F]FE@SUPPY and 340±140GBq/µmol for [$^{18}$F]FE@SUPPY:2 at the end of synthesis (EOS). Radiochemical purities always exceeded 98%.

*Enzyme reactions*

Results are presented in figure 2. The *in-vitro* assays showed Michaelis-Menten constants ($K_M$) of 20.15µM for FE@SUPPY and 13.11µM for FE@SUPPY:2. The limiting velocities ($V_{Max}$) were 0.035µM/min for FE@SUPPY and 0.015µM/min for FE@SUPPY:2. FE@SUPPY was cleaved to DFE@SUPPY, while FE@SUPPY:2 was cleaved to FE@SUPPY:21 (see figure 1). The HPLC assay was capable to qualitatively and quantitatively separate and resolve the potential metabolites. The detected radioactive metabolites are co-eluting with the corresponding reference standards (see table 1).

*Metabolite studies*

Extent of metabolism of [18F]FE@SUPPY and [18F]FE@SUPPY:2 in blood is presented in figure 3A. Rate of metabolism was different for [18F]FE@SUPPY and [18F]FE@SUPPY:2. 47.7% of [18F]FE@SUPPY were intact 15min after injection compared to 33.1% of [18F]FE@SUPPY:2; 30min p.i. 30.3% of intact [18F]FE@SUPPY were found compared to 15.6% of [18F]FE@SUPPY:2.

The radiolabeled metabolites in brain are presented in figure 3B. The point of time of the first detection of metabolites was different for [18F]FE@SUPPY and [18F]FE@SUPPY:2.

**Discussion**

*General*

It appears undisputed, that there is a demand for a suitable PET-ligand for the A3R both for *in-vitro* and *in-vivo* use. The molecules, based on a diacyl-pyridine structure [18F]FE@SUPPY and [18F]FE@SUPPY:2, and later, xanthine-derivatives (radiolabelled with bromine-76) have been introduced for that purpose [5-7, 9, 10, 12]. All these molecules did not yet find their way into human application. In preclinical experiments with [18F]FE@SUPPY and [18F]FE@SUPPY:2, so far, the results indicate to focus on these molecules [5, 6, 9, 10]: Both automated radiosyntheses were feasible; uptake was found in organs reliably expressing A3R mRNA and first brain autoradiographic slides showed good selectivity and specificity. The uptake pattern of [18F]FE@SUPPY and [18F]FE@SUPPY:2 was similar and comparable to that found by Kiesewetter et al. [7].

To find its way into clinical application a newly developed radiotracer has to show favourable metabolic characteristics: sufficient stability within the time period specified for the application and absence of excessive metabolites in the target tissue.

*Enzyme reactions*

Taking a closer look on the chemical structure of [$^{18}$F]FE@SUPPY and [$^{18}$F]FE@SUPPY:2, it can be expected, that, after passing the blood brain barrier or other tissue membranes, the molecules are cleaved by hydrolase (e.g. carboxylesterase) by forming 2-[$^{18}$F]fluoroethanol and the respective corresponding acids (cf. figure 1). 2-[$^{18}$F]Fluoroethanol would easily diffuse from tissue and would not contribute to receptor signal leading to lower non-specific accumulation compared to tracers keeping their radiolabel to their backbone. To obtain a first estimate of potential *in-vivo* degradation, *in-vitro* enzyme (e.g. CES) reactions can be a helpful tool. It can be derived from figure 2 and table 1, that the degradation paths of enzymatic cleavage of FE@SUPPY and FE@SUPPY:2 are similar: In both cases, cleavage was observed on the carboxylic function while the thiocarboxylic core remained intact. This observation cannot be explained by the fact that carboxylesterases only address carboxylic functions (and not thiocarboxylic cores) - as probably inspired by its name. Since it is well known, that carboxylesterases contribute to cleavage on both ester functions [14], this observation has to be due to different stability properties of the thio- and carboxylic core within our molecules.

*Metabolite studies*

Sometimes, tracers, radiolabelled with fluorine-18 tend to show defluorination. In case of [$^{18}$F]FE@SUPPY and [$^{18}$F]FE@SUPPY:2, the minimum uptake in bone, shown in our precedent biodistribution studies, revealed no separation of [$^{18}$F]fluoride from the parent molecules

[6,10]. In both, blood and brain, one hydrophilic metabolite was detected for [18F]FE@SUPPY and [18F]FE@SUPPY:2. As evident from figure 3A, differences in blood are between the time period of 15 and 30 minutes p.i. In this time period, [18F]FE@SUPPY is more stable (after 15 minutes a factor of 1.42, after 30 minutes a factor of 1.93). This higher stability is in agreement with our *in-vitro* findings (difference in $K_M$: factor 1.54). In brain, we found major differences: [18F]FE@SUPPY:2 formed an early hydrophilic metabolite, whereas metabolism of [18F]FE@SUPPY was not observed before 30 minutes p.i. A possible explanation for these findings could be the differences in metabolic pathways as observed in our previous carboxylesterase experiments.

*Comparison of enzyme reactions and ex-vivo metabolite studies*

Comparing the findings of carboxylesterase experiments with the *ex-vivo* studies, one has to remark, that [18F]FE@SUPPY:2 would be expected to form a radioactive hydrophilic metabolite ([18F]FE@SUPPY:21), potentially interacting with the target. In contrast, from the carboxylesterase path, [18F]FE@SUPPY forms DFE@SUPPY – a non-radioactive metabolite. Hence, from this point of view, [18F]FE@SUPPY, forming no radioactive hydrophilic derivative by CES path, would be favourable for potential applications in the central nervous system.


**Conclusion**

Aim of the present study was the assessment of the *in-vitro* and *in-vivo* stability of [18F]FE@SUPPY and [18F]FE@SUPPY:2. Although being structurally closely related, the way of CES degradation was different. Metabolic characteristics both in rodent blood and brain were different, too: for [18F]FE@SUPPY, brain metabolites were not observed before 30 minutes p.i, and its metabolism in blood was more slowly. Knowing, that metabolism in rats

is several times faster than in human, we conclude that [$^{18}$F]FE@SUPPY should be stable for the typical time span of a clinical investigation. Hence, from a metabolic point of view, for imaging of the density of the A3R one would tend to decide in favour of [$^{18}$F]FE@SUPPY.

## References

[1] Baraldi PG, Cacciari B, Romagnoli R, Merighi S, Varani K, Borea PA et al. $A_3$ adenosine receptor ligands: history and perspectives. Med Res Rev 2000;20:103-28.

[2] Fishman P, Bar-Yehuda S, Madi L, Cohn I. A3 adenosine receptor as a target for cancer therapy. Anticancer Drugs 2002;13:437-43.

[3] Madi L, Ochaion A, Rath-Wolfson L, Bar-Yehuda S, Erlanger A, Ohana G et al. The A3 adenosine receptor is highly expressed in tumor versus normal cells: potential target for tumor growth inhibition. Clin Cancer Res 2004;10:4472-9.

[4] Li AH, Moro S, Forsyth N, Melman N, Ji XD, Jacobson KA. Synthesis, CoMFA analysis, and receptor docking of 3,5-diacyl-2, 4-dialkylpyridine derivatives as selective A3 adenosine receptor antagonists. J Med Chem 1999;42:706-21.

[5] Wadsak W, Mien LK, Shanab K, Weber K, Schmidt B, Sindelar KM et al. Radiosynthesis of the adenosine $A_3$ receptor ligand 5-(2-[$^{18}$F]fluoroethyl)2,4-diethyl-3-(ehtylsulfanylcarbonyl)-6-phenylpyridine-5-carboxylate ([$^{18}$F]FE@SUPPY). Radiochim. Acta 2008;96:119-24.

[6] Wadsak W, Mien LK, Shanab K, Ettlinger DE, Haeusler D, Sindelar K et al. Preparation and first evaluation of [$^{18}$F]FE@SUPPY: a new PET tracer for the adenosine $A_3$ receptor. Nucl Med Biol 2008;35:61-6.

[7] Kiesewetter DO, Lang L, Ma Y, Bhattacharjee AK, Gao ZG, Joshi BV et al. Synthesis and characterization of [$^{76}$Br]-labeled high-affinity A3 adenosine receptor ligands for positron emission tomography. Nucl Med Biol 2009;36:3-10.

[8] Satoh T, Hosokawa M. The mammalian carboxylesterases: from molecules to functions. Annu Rev Pharmacol Toxicol 1998;38:257-88.

[9] Haeusler D, Mitterhauser M, Mien LK, Shanab K, Lanzenberger RR, Schirmer E et al. Radiosynthesis of a novel potential adenosine $A_3$ receptor ligand 5-ethyl 2,4-diethyl-

3-((2-[18F]fluoroethyl) sulfanylcarbonyl)-6-phenylpyridine-5-carboxylate
([$^{18}$F]FE@SUPPY:2). Radiochim Acta 2009;97:753-758.

[10] Mitterhauser M, Haeusler D, Mien LK, Ungersboeck J, Nics L, Lanzenberger RR et al.
Automatisation and first evaluation of [$^{18}$F]FE@SUPPY:2, an alternative PET-Tracer for
the Adenosine A$_3$ Receptor: A Comparison with [$^{18}$F]FE@SUPPY. The Open Nuclear
Medicine Journal 2009;1:15-23.

[11] Azéma L, Lherbet C, Baudoin C, Blonski C. Cell permeation of a Trypanosoma brucei
aldolase inhibitor: Evaluation of different enzyme-labile phosphate protecting
groups. Bioorg Med Chem Lett 2006;16:3440-3.

[12] Shanab K, Wadsak W, Mien LK, Mitterhauser M, Holzer W, Polster V et al. Synthesis of in
vivo metabolites of the new adenosine A3 receptor PET-radiotracer[$^{18}$F]FE@SUPPY.
Heterocycles 2008;75:339-56.

[13] Shanab K. Synthesis of precursors of adenosine A$_3$ receptor PET-tracers: In the nuclear
Medicine`s service (Synthese von Precursoren von A3-Adenosin-Rezeptor PET-
Tracern: Im Dienste der Nuklearmedizin). Wien: Vdm Verlag, 2008.

[14] Stoops JK, Hamilton SE, Zerner B. Carboxylesterases (EC 3.1.1). A comparison of some
kinetic properties of horse, sheep, chicken, pig and ox liver carboxylesterases. Can J
Biochem 1975;53:865-73.

**Figure 1**

**Figure 2**

**A**



FE@SUPPY

$V_{max}$   0.035

$K_M$   20.15

**B**



FE@SUPPY:2

$V_{max}$   0.015

$K_M$   13.11
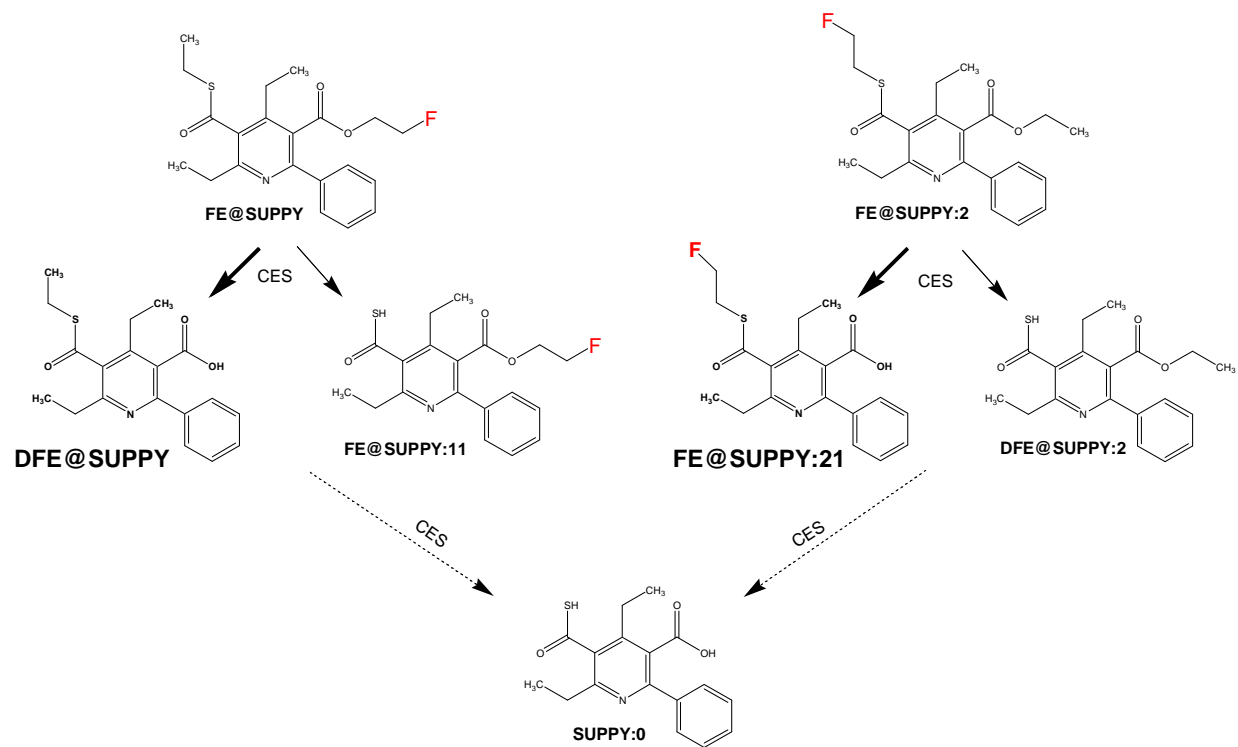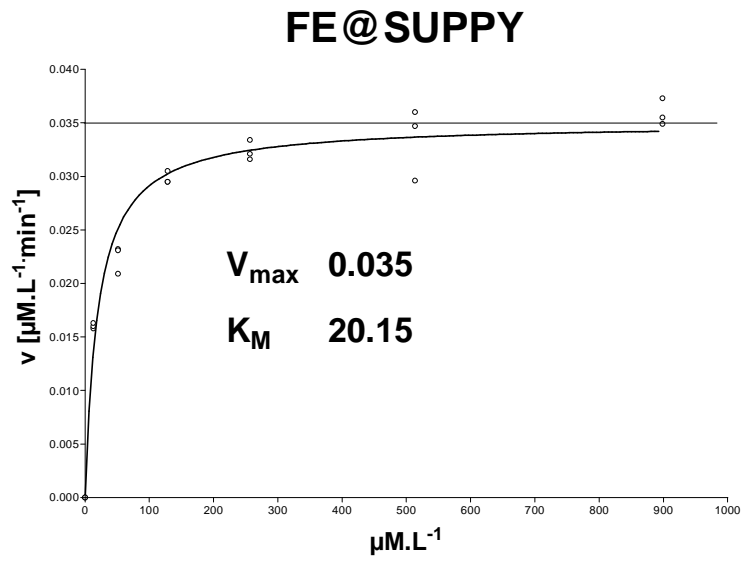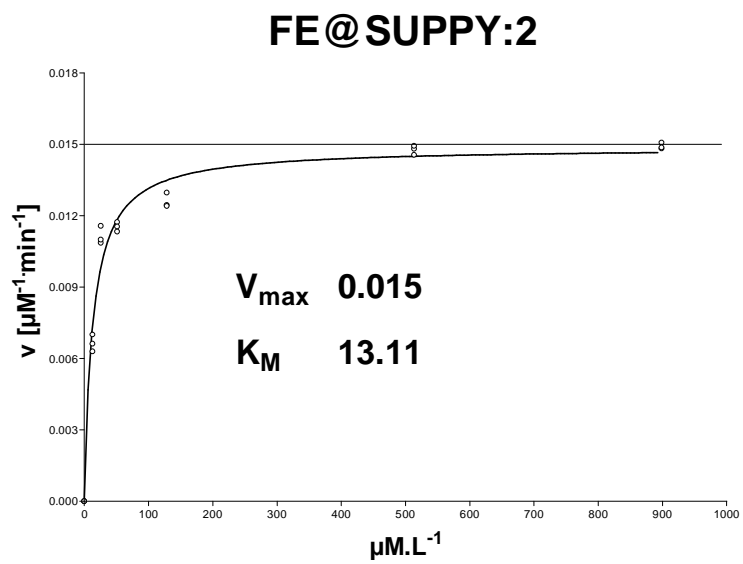
**Figure 3**
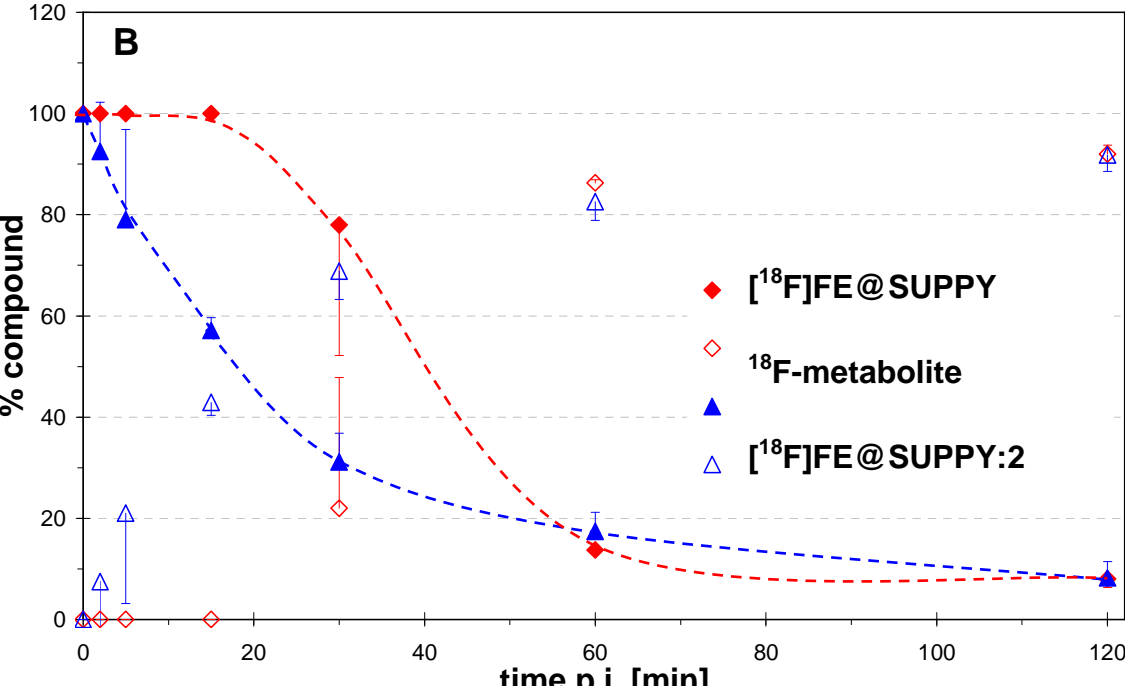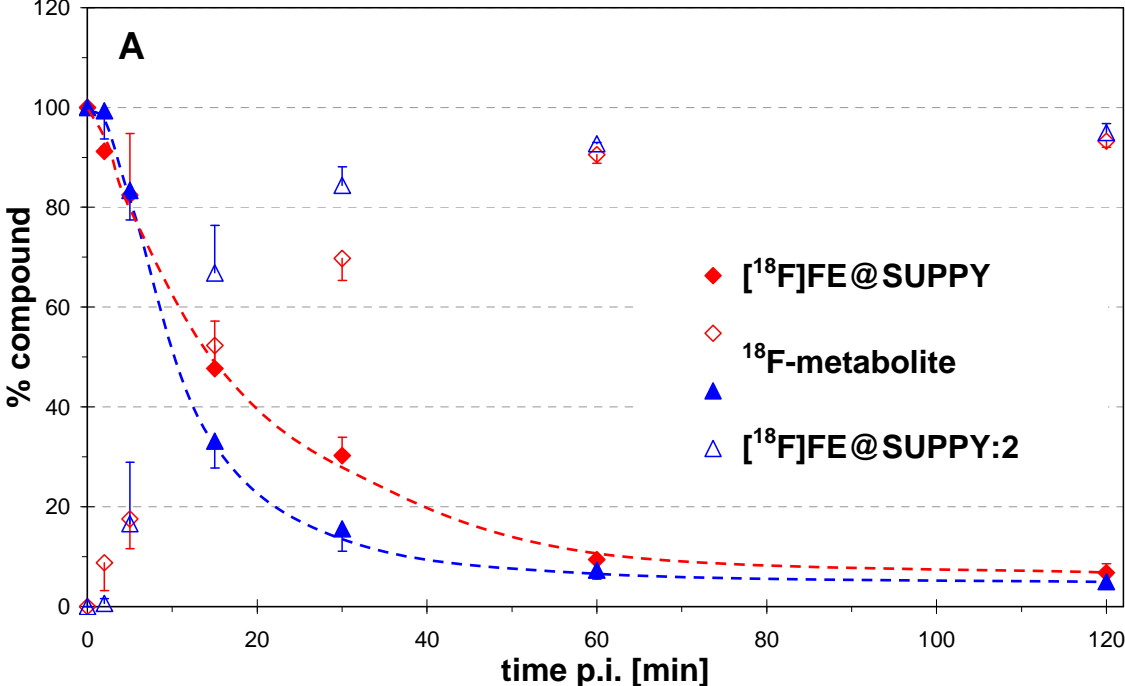
**Table 1**

| A3R<br><br>Ligands | defluoroethylated<br><br>metabolite | fluoroethylated<br><br>metabolite | final expected<br><br>metabolite | found<br><br>metabolite |
|---|---|---|---|---|
| *FE@SUPPY*<br><br>11.03±0.02 | *DFE@SUPPY*<br><br>3.76±0.01 | *FE@SUPPY:11*<br><br>3.16±0.01 | *SUPPY:0*<br><br>9.69±0.02 | *DFE@SUPPY*<br><br>3.78±0.02 |
| *FE@SUPPY:2*<br><br>10.70±0.01 | *DFE@SUPPY:2*<br><br>16.94±0.02 | *FE@SUPPY:21*<br><br>2.86±0.01 | *SUPPY:0*<br><br>9.69±0.02 | *FE@SUPPY:21*<br><br>2.86±0.01 |

**Captions**

**Figure 1:** Potential metabolic pathways of [$^{18}$F]FE@SUPPY and [$^{18}$F]FE@SUPPY:2 cleaved by carboxylesterase (CES). Metabolites found in the CES experiments are in bold letters.

**Figure 2:** Michaelis-Menten kinetics and schematic Lineweaver-Burk illustration of (A) FE@SUPPY and (B) FE@SUPPY:2 – each single point represents the mean value of triplicate analyses. $v_{max}$ is the limiting velocity and $K_M$ is the Michaelis-Menten constant.

**Figure 3:** Scheme showing [$^{18}$F]FE@SUPPY and [$^{18}$F]FE@SUPPY:2 and their respective metabolites

A) in blood

B) in brain

**Table 1:** Retention times [min] of [$^{18}$F]FE@SUPPY and [$^{18}$F]FE@SUPPY:2 and their metabolites. Data represent arithmetic means ± SD.

# METABOLISM AND AUTORADIOGRAPHIC EVALUATION OF [18F]FE@CIT: A COMPARISON WITH [123I]ß-CIT AND [123I]FP-CIT

Authors: Dagmar E Ettlinger[1], **Daniela Haeusler**[1,2], Wolfgang Wadsak[1,3], Friedrich Girschele[1], Karoline M Sindelar[1], Leonhard-Key Mien[1,2,4], Johanna Ungersboeck[1,3], Helmut Viernstein[2], Kurt Kletter[1], Robert Dudczak[1], Markus Mitterhauser[1,2,5,*]

1 Dept of Nuclear Medicine, Medical University of Vienna, Austria

2 Dept of Pharmaceutic Technology and Biopharmaceutics, University of Vienna, Austria

3 Dept of Inorganic Chemistry, University of Vienna, Austria

4 Dept of Psychiatry and Psychotherapy, Medical University of Vienna, Austria

5 Hospital Pharmacy of the General Hospital of Vienna, Austria

**Abstract**

*Purpose:* Since the late 1980s, cocaine analogues based on the phenyltropane structure, such as [11C]CFT and [123I]ß-CIT have been used for the imaging of the dopamine transporter. Fe@CIT (fluoropropyl ester) and FP-CIT (N-fluoropropyl derivative) are further analogues. Aim of this study was to (1) evaluate and compare the metabolic stability of ß-CIT, FP-CIT and FE@CIT against carboxyl esterases and (2) evaluate selectivity of [18F]FE@CIT compared to [123I]ß-CIT and [123I]FP-CIT using autoradiography.

*Methods:* In-vitro enzymatic hydrolysis assays were performed using different concentrations of ß-CIT, FE@CIT and FP-CIT with constant concentrations of carboxyl esterase. Autoradiography was performed on coronal 20 μm rat brain sections incubated with different radioactivity concentrations of [123I]ß-CIT, [123I]FP-CIT or [18F]FE@CIT and additionally with DASB (SERT) and nisoxetine (NET) for blocking experiments.

*Results:* In-vitro assays showed Michaelis-Menten constants of 175 μmol (ß-CIT), 183 μmol (FE@CIT) and 521 μmol (FP-CIT). Limiting velocities were 0.1005 μmol/min (ß-CIT), 0.1418 μmol/min (FE@CIT) and 0.1308 μmol/min (FP-CIT). This indicates a significantly increased stability of FP-CIT, whereas carboxyl esterase stability of ß-CIT and FE@CIT showed no significant difference. Autoradiographic analyses revealed a good correlation between DAT-rich regions and the uptake pattern of FE@CIT. Blocking experiments showed a higher DAT selectivity for [18F]FE@CIT than for the other two tracers.

*Conclusion:* We found, that (1) the metabolic stability of FE@CIT was comparable to that of ß-CIT, whereas FP-CIT showed higher resistance to enzymatic hydrolysis; and (2) the overall uptake pattern of [18F]FE@CIT on brain slices was comparable to that of [123I]ß-CIT and [123I]FPCIT. After blocking of NET and SERT-binding, a significantly higher DAT-selectivity was observed for [18F]FE@CIT. Hence, [18F]FE@CIT may be of interest for further clinical application.

Key words: FE@CIT, DAT, Metabolism, Autoradiography

## Introduction

Alterations in the dopamine transporter (DAT) are associated with a variety of neurological and psychiatric diseases. Hence, the imaging of the DAT is undisputedly valuable for the diagnosis of these diseases. So far, a series of DAT-ligands - both for SPECT and PET - have been investigated with varying specificities and selectivities. [123I]ß-CIT (2ß-carbomethoxy-3ß-(4-[123I]iodophenyl)tropane) and [123I]FP-CIT (N-(3-fluoropropyl)-3ß-(4-[123I]iodophenyl) nortropane-2ß-carboxylic acid methyl ester) have been established for routine SPECT. [11C]PE2I ([O-methyl-11C]N-(3-iodoprop-2E-enyl)-2ß-carbomethoxy-3ß-(4-methylphenyl) nortropane) was so far discussed as the carbon-11 labelled ligand of choice for PET. However, recent data revealed the formation of interfering metabolites and slow kinetics in humans hampering its applicability [1]. Furthermore, no fluorine-18 labelled radioligand has prevailed so far. We recently presented [18F]FE@CIT (2-[18F]fluoroethyl 3ß-(4-iodophenyl)tropane 2ß-carboxylate) which offers favourable binding characteristics compared to FE-CIT, CFT, FECT, FETT, ß-CIT or FP-CIT and PE2I [1-5]. However, the molecules were compared on a cellular level. Another important parameter influencing the suitability of a radioligand is its metabolic behaviour. Therefore, the aim of the present study was the comparative evaluation of (1) the metabolic stability of ß-CIT, FP-CIT and FE@CIT (figure 1) against carboxyl esterases and (2) the autoradiographic binding pattern of [123I]ß-CIT, [123I]FP-CIT and [18F]FE@CIT, respectively.

## Materials and Methods

*Radiochemistry.* [18F]FE@CIT was synthesized by reacting 3-β-(4-Iodophenyl)tropane-2-β-carboxylic acid with 2-bromo-1-[18F]fluoroethane as reported elsewhere [2]. The radiosynthesis evinced radiochemical yields of > 90% (based on [18F]BFE), the specific radioactivity was > 416 GBq/µmol. An average 30 µAh cyclotron irradiation yielded more than 2.5 GBq [18F]FE@CIT. Radiochemical purity of [18F]FE@CIT exceeded 96% and total amounts of radioactivity up to 2.5 GBq were achieved.

*Enzyme reactions.* Experiments were performed in triplicate (n=3), using different amounts of ß-CIT, FE@CIT and FP-CIT (ABX GmbH, Radeberg, Germany; 60, 120, 180, 240 and 360 µmol) with a constant concentration of carboxyl esterase (porcine, E-3019, Sigma-Aldrich,

Steinheim, Germany; 24 Units/mg; 80 I.U., 36°C in 500 µl phosphate buffered saline). The reactions were stopped by adding the double amount of ice-cold methanol at 0, 60, 120, 180, 240, 300 and 360 minutes, respectively. After centrifugation (10000 rpm, 3 min) of the reaction mixtures, the obtained supernatant was subjected to HPLC analysis (Agilent 1100 system, Agilent diode array UV detector at 235 nm and 240 nm and a Raytest NaI Socket; stationary phase: Merck LiChrospher 100 RP-18 column (5 µm, 250 x 4 mm); mobile phase: 63% ammonium acetate buffer (0.03M pH 3.5), 30% acetonitrile and 7% ethanol at a flow rate of 1 ml/min).

*Autoradiography.* In vitro autoradiography was performed on 20 µm coronal brain sections (Interaural 7.12mm, Bregma -1.88mm) from male Wistar rats (30 days, 300 g). Frozen brain slices were thawed in binding buffer (Tris – HCl 50 mM, pH 7.4) and dried. Subsequently, brain sections were incubated with a mixture of 2 nM [123I]ß-CIT, 15 nM [123I]FP-CIT or 2 nM [18F]FE@CIT, respectively, in binding buffer. For blocking experiments 7 nM DASB (3-Amino-4-(2-dimethylaminomethyl-phenylsulfanyl)-benzonitrile; ABX GmbH, Radeberg, Germany) and 10 nM nisoxetine (N-151, Sigma-Aldrich) were added to the incubation mixture. Incubation was performed for 90 min with activities ranging from 10 to 80 kBq/slice. After washing with ice-cold binding buffer and ice-cold water, the dried slices were subjected to imaging. Images were analyzed on a Canberra Packard instant imager (Canberra Packard Perkin Elmer, Waltham, MA, USA). Semi quantitative analysis was performed with two regions of interest (ROIs), one inside (DAT-rich, region 1) and one outside the striatum (DAT-poor, region 2). Correct location of the ROIs was verified by histochemical counterstaining of the vicinal slices. Each obtained value represented the net counts per minute per mm$^2$ for each ROI. Calculated ratios were the quotients of the corresponding region 1 and region 2 for each slice. Thereafter, arithmetic means ± standard deviations were derived for baseline and blocked values.

Statistical calculations were performed with Microsoft® Excel 2000, Microsoft Corporation (2-tailed unpaired t-test) and Michaelis-Menten kinetics (Michaelis-Menten constants, $K_M$, and limiting velocities, $v_{max}$) were calculated with GraphPad Prism® (GraphPad software Inc. San Diego, CA, USA) Version 3.00.

**Results**

*Enzyme reactions.* Results are presented in figure 2. The in-vitro assays showed Michaelis-Menten constants of 175 µmol for ß-CIT, 183 µmol for FE@CIT and 521 µmol for FP-CIT, respectively. The limiting velocities were comparable: 0.1005 µmol/min (ß-CIT), 0.1418 µmol/min (FE@CIT) and 0.1308 µmol/min (FP-CIT), respectively.

*Autoradiography.* Single values of each experiment of the semi quantitative analysis are presented in table 1. Mean values range from 2.0 ± 0.3 (ratio [123I]FP-CIT, blocked) up to 2.4 ± 0.3 (ratio [18F]FE@CIT, baseline) and are also presented in figure 3. Representative autoradiographic images for different amounts of [18F]FE@CIT comprising the ROIs are shown in figure 4.

**Discussion**

*General.* The history of the evaluation and clinical application of DAT-ligands ranges back to the late 1980s [6], and a broad variety of radioligands have been introduced so far for PET and SPECT [7]. DAT-ligands mostly base on a tropane structure and exhibit different affinities for the central monoamine transporters DAT, SERT (serotonin transporter) and NET (norepinephrine transporter). However, for distinct imaging of the DAT, a high affinity for the DAT and selectivity DAT over SERT and DAT over NET is a prerequisite. [18F]FE@CIT, being one of the DAT-ligands displaying highest affinity and selectivity [3] radiolabelled with fluorine-18, has been introduced by our group recently [2]. Since a successful radioligand is characterized by (1) its affinity for the target (pharmacodynamics) and (2) its fate through the organism on its way to the target (pharmacokinetics and metabolism), these characteristics have to be resolved prior to clinical application. Since [123I]ß-CIT and [123I]FP-CIT have found their way into routine clinical practice, we decided to evaluate [18F]FE@CIT in comparison to those well established radioligands.

*Enzyme reactions.* Carboxyl esterases are prominent enzymes in vivo and are widely responsible for phase I metabolism of drugs [9]. Therefore, the estimation of the stability of drugs against these carboxyl esterases is desirable. It is well known, that carboxylesterases from different species show different quantitative behaviour (different Michaelis-Menten

constants with the same substrates) [10]. However, porcine carboxyl esterase used in these experiments – as compared to human carboxyl esterase – shows little qualitative deviation but operates significantly faster. Hosokawa et al found that porcine carboxyl esterases – due to similar catalytic properties of its isoenzymes – proved of value as a good model for human enzymatic hydrolysis [10]. Since we evaluated the stabilities of [123I]ß-CIT, [18F]FE@CIT and [123I]FP-CIT in a comparative manner and bearing short half-lives of positron emitters in mind we chose faster porcine carboxyl esterase for our purposes.

Seibyl et al. showed acid cleavage as a major metabolic route for FP-CIT [11]. The Michaelis-Menten constant represents the dissociation constant (affinity for substrate) of the enzyme-substrate complex. Low values indicate that the enzyme-substrate complex is held together very tightly and rarely dissociates without the substrate first reacting to form product. The method used in the present experiments is a well established tool for the estimation of the stability of drugs against these enzymes [12] already introduced for PET tracers as well [13]. As shown in figure 2, the carboxyl esterase stabilities of [123I]ß-CIT and [18F]FE@CIT are comparable, whereas [123I]FP-CIT displays significantly increased carboxyl esterase stability compared to ß-CIT ($p < 0.01$) and FE@CIT ($p < 0.05$). One explanation could be the fact that in the FP-CIT molecule a more bulky fluoropropyl moiety is attached at the tropane substructure which could obstruct carboxylesterases from approaching to the ester bond. An even bulkier moiety is attached to the tropane in the PE2I structure, but there, it was shown recently that the para-methyl group is the primary target for metabolism (figure 1, number (4)) [1]. Since these radioactive metabolites were also found in brain, kinetic modelling could be complicated. Hence, an optimized DAT-ligand should not carry a methyl group in the para position of the phenyl ring. The method presented here using carboxyl esterases could facilitate the future design of PET tracers carrying ester functions by simply mimicking the main metabolic *in-vivo* route by a fast *in-vitro* method. Comparative knowledge of the metabolic pattern *in-vitro* could influence the schedule of forthcoming animal experiments.

*Autoradiography*. The selectivity of DAT ligands versus SERT and NET is an important prerequisite for clinical appropriateness and "some degree of selectivity could be assumed from ratios of β-CIT and FP-CIT binding sites in the striatum and the cortex" [14]. From the obtained ratios, selectivity DAT/SERT and DAT/NET can be estimated. Amounts of radioactivity were selected in a range from 10 kBq up to 80 kBq per slice to measure the

influence of activity concentration on the binding characteristics. Single values presented in table 1 explicitly exclude that our results are biased by amount of radioactivity. On our semi-quantitative analysis we observed comparable ratios for baseline experiments (see figure 3): Comparing [$^{18}$F]FE@CIT with [$^{123}$I]ß-CIT yielded a p-level of 0.45, comparing [$^{18}$F]FE@CIT with [$^{123}$I]FP-CIT yielded a p-level of 0.83. Based on these findings, selectivity advantages of neither ligand could be predicted. Calculating ratios obtained after blocking NET and SERT, the values of [$^{18}$F]FE@CIT were significantly higher than those of [$^{123}$I]ß-CIT ($p = 0.02$) and [$^{123}$I]FP-CIT ($p = 0.01$). Therefore, our experiments revealed a significantly higher DAT-selectivity of [$^{18}$F]FE@CIT using autoradiography which is in line with the findings presented by Gu et al [3] using an *in-vitro* binding assay. The authors described there a higher affinity of FE@CIT for DAT ($K_i$ 0.93 nM) versus ß-CIT ($K_i$ 1.33 nM) and FP-CIT ($K_i$ 8.29 nM) and a higher DAT/SERT and DAT/NET selectivity for FE@CIT. This higher selectivity of FE@CIT compared to the other DAT-ligands was reproduced by our experiments using semi quantitative autoradiography.

**Conclusion**

We found, that (1) the metabolic stability of FE@CIT was comparable to that of ß-CIT, whereas FP-CIT showed a significantly higher stability against carboxylesterases; and (2) the overall uptake pattern of [$^{18}$F]FE@CIT on native rat brain slices was comparable to that of [$^{123}$I]ß-CIT and [$^{123}$I]FP-CIT. After blocking of NET and SERT-binding, a significantly higher DAT-selectivity was observed for [$^{18}$F]FE@CIT. The chemical structure of [$^{18}$F]FE@CIT avoids the formation of radioactive metabolites passing the blood-brain-barrier. Hence, [$^{18}$F]FE@CIT may be of value for further clinical application.

**Acknowledgements**

**References**

1        Shetty HU, Zoghbi SS, Liow J-S, Ichise M, Hong J, Musachio JL, et al. Identification and regional distribution in rat brain of radiometabolites of the dopamine transporter PET radioligand [11C]PE2I. Eur J Nucl Med 2007; 34:667-78.

2        Mitterhauser M, Wadsak W, Mien LK, Hoepping A, Viernstein H, Dudczak R, et al. Synthesis and Biodistribution of [18F]FE@CIT, a New Potential Tracer for the Dopamine Transporter. Synapse 2005; 55:73-9.

3        Gu X-H, Zong R, Kula NS, Baldessarini RJ, Neumeyer JL. Synthesis and Biological Evaluation of a Series of Novel N- or O-Fluoroalkyl Derivatives of Tropane: Potential Positron Emission Tomography (PET) Imaging Agents for the Dopamine Transporter. Bioorg Med Chem Lett 2001; 11:3049–53.

4        Kula NS, Baldessarini RJ, Tarazi FI, Fisser R, Wang S, Trometer J, et al. [3H]beta-CIT: a radioligand for dopamine transporters in rat brain tissue. Eur J Pharmacol 1999; 385:291-4.

5        Wilson AA, DaSilva JN, Houle S. In vivo evaluation of [11C]- and [18F]-labelled cocaine analogues as potential dopamine transporter ligands for positron emission tomography. Nucl Med Biol 1996; 23:141–6.

6        Aquilonius S-M, Bergstrom K, Eckernäs S-A, Hartvig P, Leenders KL, Lundquist H, et al. In vivo evaluation of striatal dopamine reuptake sites using [11C]nomifensine and positron emission tomography. Acta Neurol Scand 1987; 76:283-7.

7        Kung HF, Kung M-P, Choi SR. Radiopharmaceuticals for single-photon emission computed tomography brain imaging. Sem Nucl Med 2003; 33:2-13.

8        Meyer JH, Ichise M. Modeling of receptor ligand data in PET and SPECT imaging: A review of major approaches. J Neuroimaging 2001; 11:30-9.

9        Potter PM, Wadkins RM. Carboxylesterases--detoxifying enzymes and targets for drug therapy. Curr Med Chem. 2006; 13:1045-54.

10    Hosokawa M, Maki T, Satoh T. Characterisation of molecular species of liver microsomal carboxylesterases of several animal species and humans. Arch Biochem Biophys 1990; 277:219-27

11    Seibyl JP, Marek K, Sheff K, Zoghbi S, Baldwin RM, Charney DS, et al. Iodine-123-beta-CIT and iodine-123-FPCIT SPECT measurement of dopamine transporters in healthy subjects and Parkinson's patients. J Nucl Med 1998; 39:1500-8.

12    Humerickhouse R, Lohrbach K, Li L, Bosron WF, Dolan ME. Characterization of CPT-11 hydrolysis by human liver carboxylesterase isoforms hCE-1 and hCE-2. Cancer Res 2000; 60:1189-92.

13    Ettlinger DE, Wadsak W, Mien LK, Machek M, Wabnegger L, Rendl G, et al. [18F]FETO: metabolic considerations. Eur J Nucl Med Mol Imaging 2006; 33:928-31.

14    Sihver W, Drewes B, Schulze A, Olsson RA, Coenen HH. Evaluation of novel tropane analogues in comparison with the binding characteristics of [18F]FP-CIT and [131I]beta-CIT. Nucl Med Biol 2007; 34:211-9.

**Captions**

*Figure 1.* Chemical structures of (1) ß-CIT, (2) FE@CIT and (3) FP-CIT. Red arrows indicate the ester bond to be cleaved by carboxylesterase, green arrow indicates the found major metabolic route for PE2I.

*Figure 2.* Michaelis-Menten kinetics of (A) FE@CIT, (B) ß-CIT and (C) FP-CIT: Points represent the mean values of triplicate analyses. $v_{max}$ is the limiting velocity and $K_M$ is the Michaelis-Menten constant.

*Figure 3.* Target/non-target binding ratios of native (red bars) and blocked (yellow bars) rat brain slices after semi quantitative autoradiographic analysis (ratio of net counts/$mm^2$). Columns represent arithmetic means, error bars represent standard deviations. Significance levels are indicated by grey brackets.

*Figure 4.* Representative autoradiographic images of [$^{18}$F]FE@CIT comprising the ROIs for semi quantitative analysis. Autoradiographies were developed simultaneously under the same conditions. Colour code represents relative intensity levels as given by the autoradiograph (linear scale).

*Table 1.* Semi quantitative analysis of autoradiographies of [$^{18}$F]FE@CIT, [$^{123}$I]ß-CIT and [$^{123}$I]FP-CIT. Each value represents the net counts per minute per $mm^2$ for each ROI (mean value ± SD). Ratios are the quotients of the corresponding DAT-rich and DAT-poor Regions for each slice.

*Figure 1.* Chemical structures of (1) ß-CIT, (2) FE@CIT, (3) FP-CIT and (4) PE2I. Red arrows indicate the ester bond to be cleaved by carboxylesterase, green arrow indicates the found major metabolic route for PE2I.

*Figure 2.* Michaelis-Menten kinetics of (A) FE@CIT, (B) ß-CIT and (C) FP-CIT: Points represent the mean values of triplicate analyses. $v_{max}$ is the limiting velocity and $K_M$ is the Michaelis-Menten constant.

*Figure 3.* Target/non-target binding ratios of native (red bars) and blocked (yellow bars) rat brain slices after semi quantitative autoradiographic analysis (ratio of net counts/mm$^2$). Columns represent arithmetic means, error bars represent standard deviations. Significance levels are indicated by grey brackets.

*Figure 4.* Representative autoradiographic images of [$^{18}$F]FE@CIT comprising the ROIs for semi quantitative analysis. Autoradiographies were developed simultaneously under the same conditions. Colour code represents relative intensity levels as given by the autoradiograph (linear scale).



| | [$^{18}$F]FE@CIT |
|---|---|
| 10 kBq | |
| 40 kBq | |
| 80 kBq | |

*Table 1.* Semi quantitative analysis of autoradiographies of [$^{18}$F]FE@CIT, [$^{123}$I]ß-CIT and [$^{123}$I]FP-CIT. Each value represents the net counts per minute per mm$^2$ for each ROI (mean value ± SD). Ratios are the quotients of the corresponding DAT-rich and DAT-poor Regions for each slice.

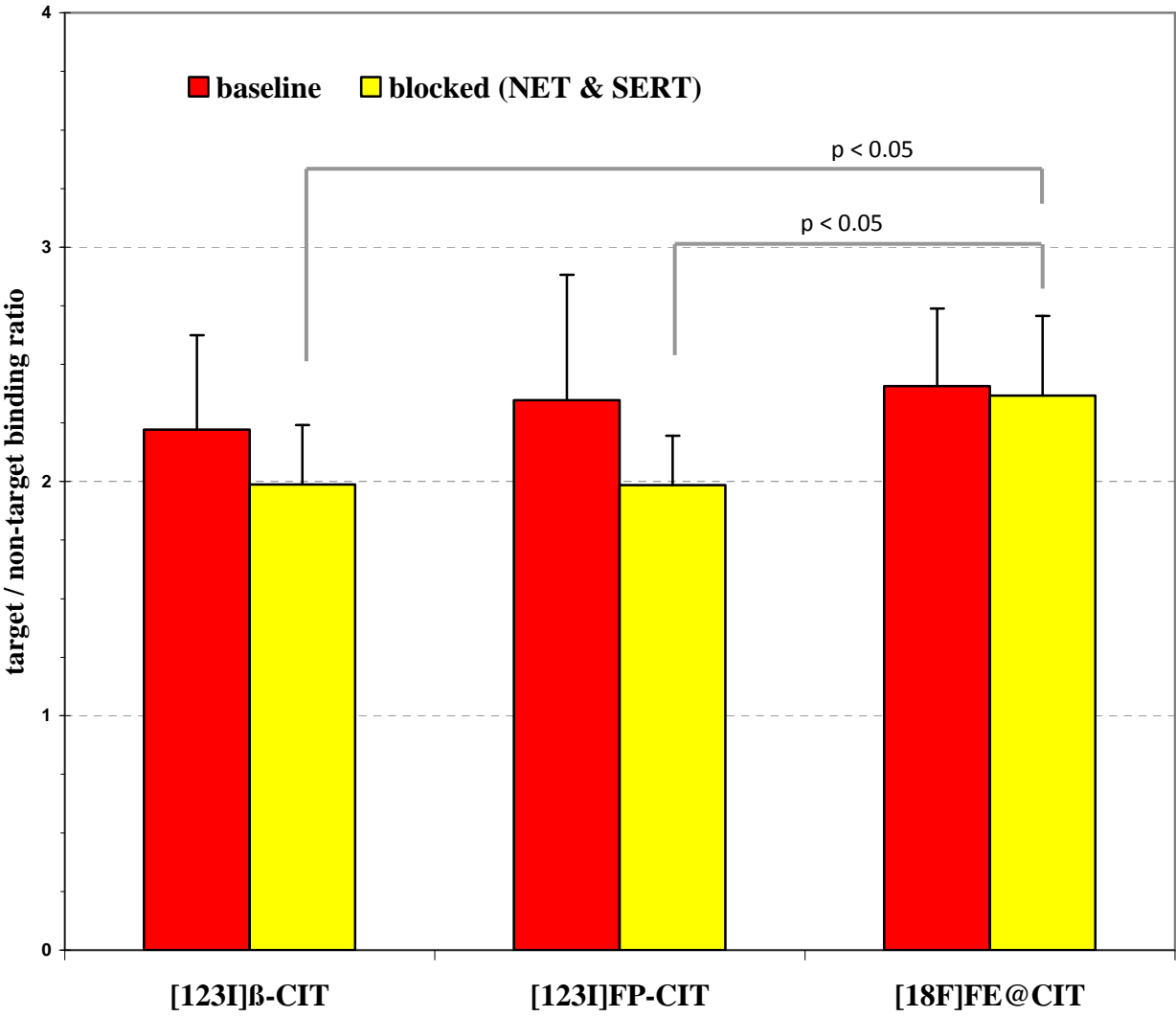| NET CPM/mm$^2$ | | DAT-rich region | | DAT-poor region | | ratio | |
|---|---|---|---|---|---|---|---|
| activity [MBq] | | baseline | blocked | baseline | blocked | baseline | blocked |
| [$^{18}$F]-FE@CIT | 0.01 | 41±4 | 29.5±1.4 | 17.4±5.4 | 11.8±2.6 | 2.4±0.5 | 2.6±0.4 |
| | 0.04 | 166±14 | 91.6±9.7 | 76±11 | 39.3±7.3 | 2.2±0.5 | 2.4±0.2 |
| | 0.08 | 312±24 | 218±24 | 121.2±3.0 | 103±23 | 2.6±0.1 | 2.2±0.5 |
| | | | | | | **mean** | **mean** |
| | | | | | | **2.4 ± 0.3** | **2.4 ±0.3** |
| [$^{123}$I]-ß-CIT | 0.01 | 2.1±0.2 | 1.7±0.6 | 1.2±0.1 | 0.9±0.2 | 1.8±0.1 | 1.9±0.4 |
| | 0.04 | 6.8±0.8 | 4.3±1.0 | 3.2±0.4 | 2.2±0.3 | 2.2±0.4 | 2.0±0.3 |
| | 0.08 | 13.4±1.5 | 11.3±2.1 | 5.1±1.4 | 5.5±1.3 | 2.7±0.5 | 2.1±0.4 |
| | | | | | | **mean** | **mean** |
| | | | | | | **2.2 ± 0.5** | **2.0 ±0.4** |
| [$^{123}$I]-FP-CIT | 0.01 | 1.9±0.9 | 2.4±1.4 | 1.0±0.4 | 1.4±1.1 | 1.8±0.3 | 1.9±0.3 |
| | 0.04 | 10.6±4.9 | 5.2±2.1 | 4.5±2.4 | 2.6±1.0 | 2.5±0.7 | 2.0±0.2 |
| | 0.08 | 17.1±4.8 | 12.2±6.2 | 6.1±1.6 | 6.7±4.5 | 2.8±0.3 | 2.0±0.6 |
| | | | | | | **mean** | **mean** |
| | | | | | | **2.4 ± 0.6** | **2.0 ±0.3** |

# 2.3. DISCUSSION

PET is the first choice technology for the visualization and quantification of receptors and transporters, allowing observation of physiological and pathophysiological conditions on a molecular level. New and innovative PET-radiopharmaceuticals need to be developed, to get further insights into the biochemical mechanisms involved in pathological changes. A suitable PET-tracer requires different parameters as e.g. high affinity and high specificity towards the dedicated target site, low lipophilicity and preferably also low unspecific binding. In addition, the degree of metabolization and degradation of the desired PET-tracer is of highest importance: radioactive metabolites might interfere with the target itself, and would lead to undesirable enhanced binding signal. Moreover, the binding kinetics of the investigated molecule has a major impact on the suitability of the tracer. So, in fact, all these prerequisites have to be considered and validated in the development and evaluation process of new PET-tracers.

Hence, two major tools are crucial in the development process of new PET-tracers:

1) a reliable production method and, even more important, an automated set-up, to assure save and reliable radiochemical preparation of the PET-radiopharmaceutical, and to keep the radiation burden of the operator to a minimum. Moreover, an automated radiosynthesis also serves as a prerequisite for the save and reliable routine production for the preclinical evaluation process, which leads to point 2:

2) proof of tracer suitability (high affinity, high selectivity and specificity, beside low unspecific binding) through preclinical evaluation in an animal model, prior to human application.

### 1) Reliable production method/automatisation:

In the thesis, both radionuclides, C-11 and F-18, were used for the description of the PET-tracer development process: On the one hand, the short half-lived nuclide C-11 (20.3min), which requires quick handling, and an indirect synthetic route using gasous methyliodide, leading to an automated preparation method described in paper 1 ([$^{11}$C]DASB), was used. On the other hand, the longer half-lived nuclide F-18 (109.2min), which allows longer synthetic procedures, including liquid chemistry, was used for the production of [$^{18}$F]FE@SUPPY and [$^{18}$F]FE@SUPPY:2 via direct fluorination methods, and was further used for a fluorination method via synthon ([$^{18}$F]FE@CIT).

### A) [$^{18}$F]FE@SUPPY-derivatives

[$^{18}$F]FE@SUPPY:2, a completely new potential [$^{18}$F]fluoroethylated radiotracer for the A3R, has been successfully prepared (paper 2) and, furthermore, even an automated method for this tracer has been presented in this thesis. [$^{18}$F]FE@SUPPY was introduced as the first A3R PET tracer recently, and the automation of its radiosynthesis was also covered in this thesis. Both automations, and, moreover, also a comparison of the parameters of the two tracers were described in paper 3 in the scientific topic section. In summary, both radiotracers were prepared in a feasible and reliable manner via direct radiofluorination. Automated preparations were performed on a GE TRACERlab FxFN synthesizer module within 70-80 minutes. The radiochemical purities exceeded 97% in accordance with the regulations of the European pharmacopoeia. Sufficient overall yields and radiochemical purity for preclinical and potential future clinical investigations were achieved.

Differences were observed concerning the amount of precursor molecules: [$^{18}$F]FE@SUPPY:2 needed higher amounts (about a double) of precursor, leading to 3-fold lower radiochemical yields, in comparison to [$^{18}$F]FE@SUPPY. Interestingly, specific radioactivity of [$^{18}$F]FE@SUPPY:2 was 5-fold higher than for [$^{18}$F]FE@SUPPY. This fact seems very promising, since for investigations concerning receptors and transporters, high specific radioactivity is important. On the other hand, [$^{18}$F]FE@SUPPY:2 showed sluggish behaviour in the radiochemical preparation procedure, which seems not so favourable.

### B) [$^{18}$F]FE@CIT

Radiochemical preparation of [$^{18}$F]FE@CIT was not yet automated.

*C) [¹¹C]DASB*

Concerning the first manuscript, the radiosynthesis of the innovative SERT PET-tracer [¹¹C]DASB was optimized towards a fully-automated, rapid and simple preparation, in order to provide this tracer for the neuroimaging of SERT-associated psychiatric disorders as e.g. depression. For routine application, the production of a radiotracer has to fulfil more requirements than just high yields and purity, therefore, a fully-automated synthetic procedure was developed, which also reduces the radiation burden for the operator. Although, this method was still prepared in a short overall production time, the failed syntheses rate remained extremely low.

According to the successfull implementation of the fully-automated set-up, clinical and scientific studies were conducted with [¹¹C]DASB at the PET-Center of Vienna in cooperation with the neuroimaging-group of Doz. Lanzenberger. First baseline results revealed, after injected radioactivity between 158 and 510 MBq of [¹¹C]DASB, high serotonin transporter density in the striatum, thalamus, midbrain, raphe region (see figure 38). Medium serotonin transporter levels were found in the cingulate cortex.
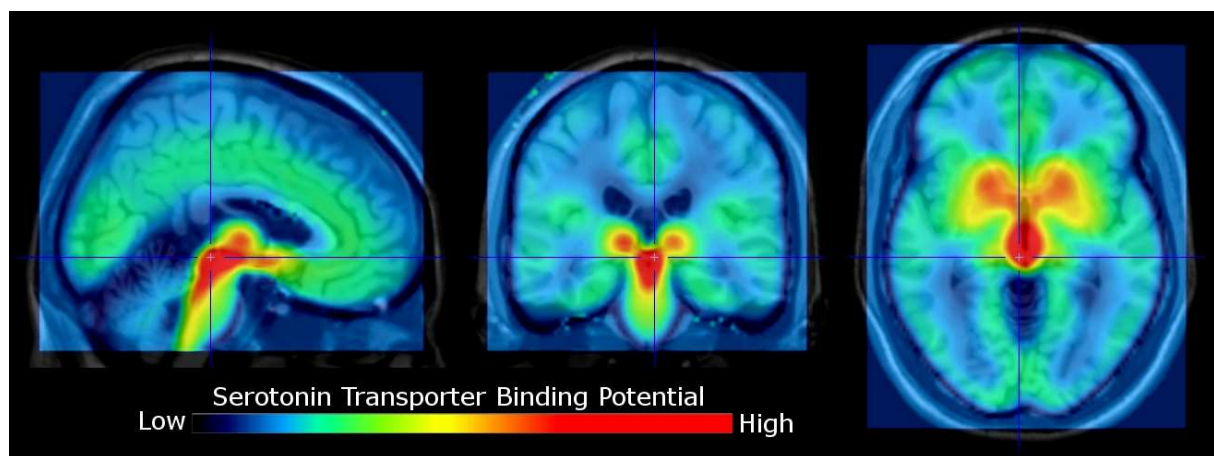


**Figure 38: Distribution of the serotonin transporter in the human brain. Triplanar view (sagittal, coronal, axial sections), the blue cross indicates corresponding slices. The color table indicates the binding potential value.**

First results of a clinical study with [¹¹C]DASB, where depressive patients were treated with SSRIs, are given in figure 39.

It is satisfying to observe that the very methodical approach in the synthesis lab allows for the successful application in a clinical trial. Even more pleasant, if the clinical study allows for general answers in clinical questions.
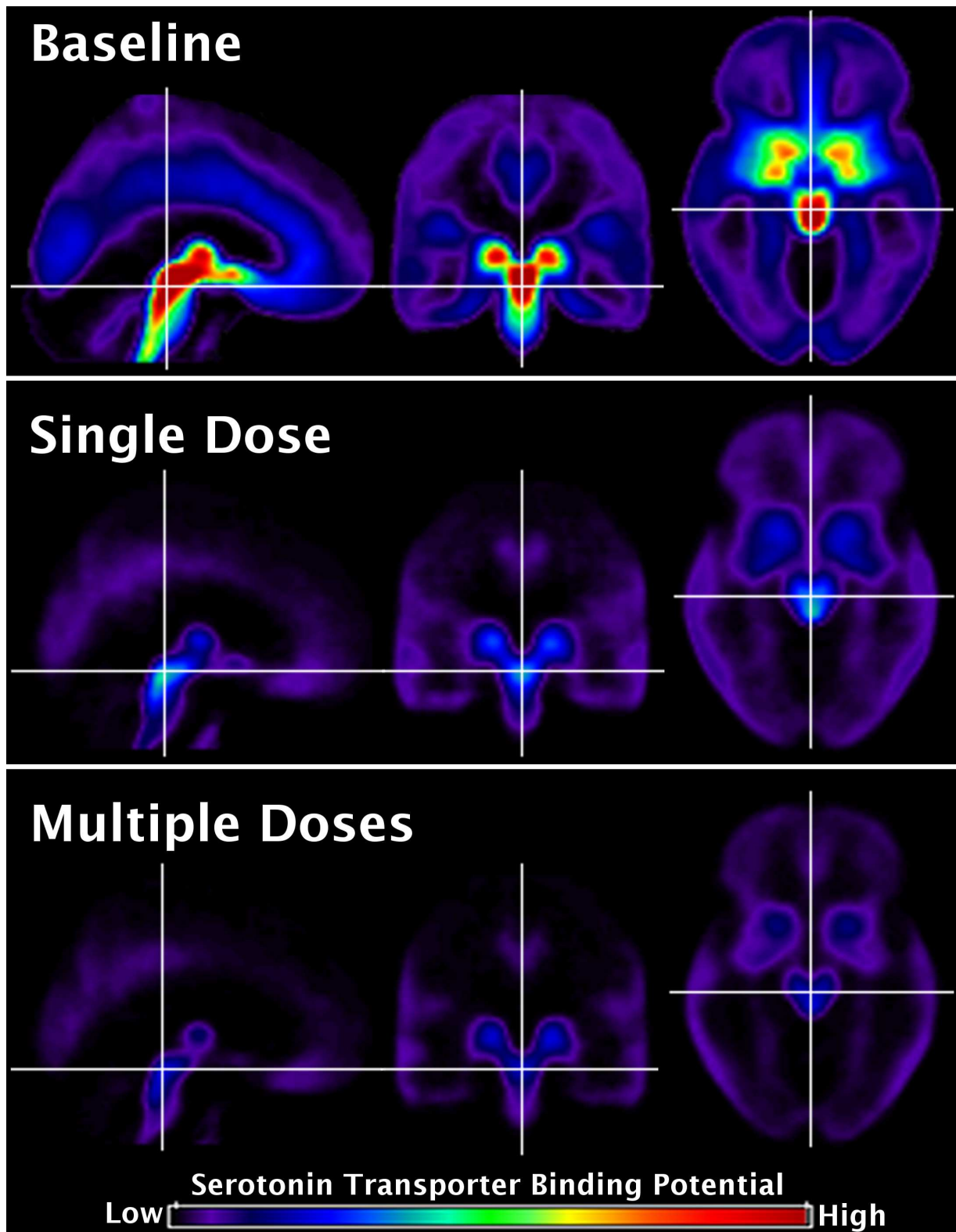
**Figure 39: SERT occupancy during treatment with SSRIs: the SERT binding is given before treatment (baseline), 6 hours after a single therapeutic dose, and after a treatment period of several weeks (multiple doses) in patients suffering from major depression (the parametric data are mean values of 18 patients).**

## 2) Proof of tracer suitability - preclinical evaluation:

### Biodistribution

*A) [$^{18}$F]FE@SUPPY-derivatives*

Highest uptake of [$^{18}$F]FE@SUPPY was found in liver, pronounced uptake in kidney, lung and heart, whereas in brain only intermediate to low uptake was observed. Highest uptake of [$^{18}$F]FE@SUPPY:2 was found in bowels and liver, pronounced uptake in kidney and heart, low uptake in fat, lung, spleen and brain. Biodistribution of these two tracers showed good correlations in brain, muscle and testes. The blood to brain ratio remained stable over time for [$^{18}$F]FE@SUPPY:2 and increased over time for [$^{18}$F]FE@SUPPY.

*B) [$^{18}$F]FE@CIT & C) [$^{11}$C]DASB*

Biodistribution experiments have not been conducted with these two tracers.

### Metabolic stability

*A) [$^{18}$F]FE@SUPPY-derivatives*

Regarding the metabolic characterisation, both [$^{18}$F]FE@SUPPY-derivatives belong to the class of dialkylpyridines, and comprise two ester functions within one molecule. Therefore, carboxylesterases were expected to significantly contribute to cleavage and degradation. The expected increased stability of the derivative [$^{18}$F]FE@SUPPY:2, the isomer with the 18F-label at the thiocarboxylic ester function, was not observed. Both, in in-vitro carboxylesterase studies, as well as in ex-vivo metabolite studies in rat blood and brain, revealed higher stability of [$^{18}$F]FE@SUPPY. In blood, 15 minutes p.i. 50% of [$^{18}$F]FE@SUPPY and 30% of [$^{18}$F]FE@SUPPY:2 were intact; and 30 minutes p.i. 30% of [$^{18}$F]FE@SUPPY and 15% of [$^{18}$F]FE@SUPPY:2 were still intact. In brain an early hydrophilic metabolite was observed for [$^{18}$F]FE@SUPPY:2. For [$^{18}$F]FE@SUPPY a radioactive metabolite in brain was not observed before 30 min p.i. Altough, structurally closely related, the pathway of CES degradation was different for the tracers. Enzyme reaction studies revealed cleavage of FE@SUPPY to DFE@SUPPY, and cleavage of FE@SUPPY:2 to FE@SUPPY:21.

*B) [$^{18}$F]FE@CIT*

In-vitro enzymatic assays revealed comparable stability of FE@CIT and ß-CIT, whereas FP-CIT was significantly more stable.

*C) [$^{11}$C]DASB*

Metabolic stability experiments have not been conducted with this tracer in our group.

**Autoradiographic studies**

*A) [$^{18}$F]FE@SUPPY-Derivatives*

For the autoradiographic studies with the two A3R tracers, a selection of commercially available adenosine receptor ligands was used, as listed in table 3.

| Compound | Receptor-subtype | Ligand | Affinity [nM] | Selectivity | Species |
|---|---|---|---|---|---|
| DPCPX | $A_1$ | Antagonist | Ki=0.46 [152] | 740 fold vs A1 | rat |
| SCH442416 | $A_{2A}$ | Antagonist | Ki=0.048 [153] Ki=0.5 | 23000 fold for hA2A vs hA$_1$ | human rat |
| MRS1754 | $A_{2B}$ | Antagonist | Ki=1.13 [154] | | |
| 2-Cl-IB-Meca | $A_3$ | Agonist | Ki=0.33 [155] | 2500 vs A$_1$ 1400 vs A$_{2A}$ | |
| MRS1523 | $A_3$ | Antagonist | Ki=18.9 [156] Ki=113 | | human rat |
| MRS 1191 | $A_3$ | Antagonist | Ki=31.4 [157] | | rat & human |
| [$^{125}$I]AB-Meca | $A_3$ | Agonist | Kd=0.59 [50] | | human |

**Table 3: Selection of commercially available adenosine receptor ligands**

First preliminary results of the autoradiographic distribution of [$^{18}$F]FE@SUPPY were presented recently[54]. Then, highest binding of [$^{18}$F]FE@SUPPY was then found in nucleus accumbens and caudate putamen and little uptake was observed in cortical regions in rat brain slices. Highly selective binding of [$^{18}$F]FE@SUPPY was shown by displacement of 2-Cl-IB-MECA, a selective blocking agent for the A3R. According to E.E. Bennaroch, the A3R is distributed in hippocampus and cerebellum in low and medium abundance[7], which we could partly confirm in further experiments on rat brain slices, so far (see figure 40, figure 41). Blockings were conducted with the adenosine ligands given in Table 3.
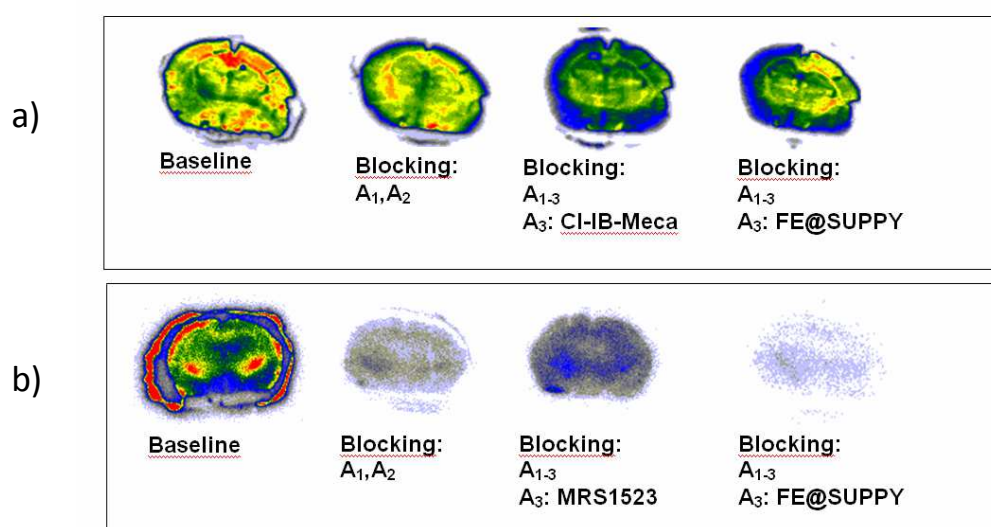


**Figure 40: First autoradiographic results of [$^{18}$F]FE@SUPPY and [$^{125}$I]AB-MECA on rat brain slices:**

**a) shows the distribution of [$^{18}$F]FE@SUPPY in baseline and under blocking conditions**

**b) shows the distribution of [$^{125}$I]AB-MECA in baseline and under blocking conditions**
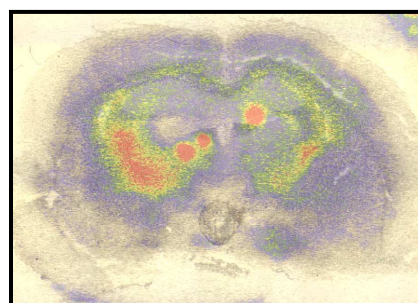


**Figure 41: Fusion of a [$^{125}$I]AB-MECA distribution of the A3R (since blocked with the dedicated A$_1$, A$_{2A}$ and A$_{2B}$ compounds) with the histological picture of a rat brain slice.**

In summary, first findings revealed that FE@SUPPY competed the well known A3R agonist [$^{125}$I]AB-MECA completely, which is not true for the commercially available A3R antagonist MRS1523 (see figure 38b). FE@SUPPY:2 also competed [$^{125}$I]AB-MECA in a comparable range to FE@SUPPY (data not shown). Binding of [$^{18}$F]FE@SUPPY revealed high uptake in the hippocampal formation and was competed with Cl-IB-MECA and FE@SUPPY.

All in all, the two novel [$^{18}$F]labelled ligands for the A3R displayed some very good and important properties as suitable A3R PET-tracers: e.g. high affinity and selectivity. On the other hand, the octanol/water partition coefficient (as a measure of lipophilicity of the tracers), was determined using an HPLC essay based on the work of Donovan and Pescatore[158] and was found to be between 4 and 5 ($_{HPLC}$logP=4 at a pH 7.4; $_c$logP=5.81). This high lipophicity was also reflected in the observed high unspecific binding in a rat model. Hence, the two tracers seem (from the momentary point of view) not to be so favorable to apply them to humans in the future.

But, since the A3R shows large interspecies differences, especially between rodents and human, rats don´t seem to be a very suitable animal model for the examination of A3R studies. It also has to be pointed out that many authors state, one amongst them K.A. Jacobson, that, since the A3R appears only in low densities and in a disease specific manner, it is especially challenging to asses them in-vivo[159]. Moreover, Prof. Schubiger showed in a rat model, that the well known imaging agent [$^{18}$F]FDG, which is widely used for brain imaging of various conditions in humans, didn´t show uptake in the brain of wild-type rats (see figure 42). Since, [$^{18}$F]FE@SUPPY displays much lower affinity towards the rat A3R ($K_i$=600nM) than towards the human A3R subtype ($K_i$=4.2nM), there is still hope and a lot to explore in humanized animal models and e.g. post-mortem human brain slice autoradiography.
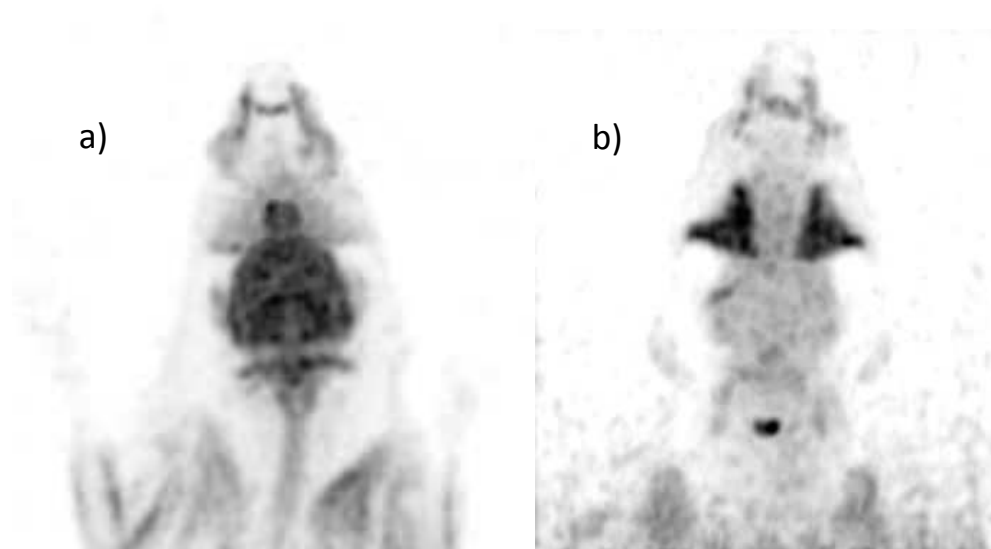
**Figure 42: Stunning observation, that [$^{18}$F]FDG uptake was found in the brain of Wistar rats (a) , but not in the brain of Brown-Norway rats (b).[160]**

*B) [$^{18}$F]FE@CIT*

Baseline uptake of [$^{18}$F]FE@CIT on rat brain slices was comparable with the uptake of [$^{123}$I]ß-CIT and [$^{123}$I]FP-CIT. Under blocking conditions, [$^{18}$F]FE@CIT revealed significant higher DAT-selectivity than the other two tracers. Detailed results of the autoradiographic analyisis of [$^{18}$F]FE@CIT are given in the specific topic section in paper 5. In summary, the high selectivity of [$^{18}$F]FE@CIT over SERT and NET was confirmed in this study, and furthermore, this selectivity was significantly higher than selectivity of the well known tracers [$^{123}$I]ß-CIT and [$^{123}$I]FP-CIT.

*C) [$^{11}$C]DASB*

Autoradiographic experiments have not been conducted with this tracer by our group.

# PART 3

# CONCLUSION
# &
# OUTLOOK

# 3. CONCLUSION AND OUTLOOK

The development and preclinical evaluation of 4 different PET-tracers for 3 targets, the DAT, the SERT and the A3R, respectively, were covered in the present thesis. The presented method for a fast and reliable radiosynthesis of [$^{11}$C]DASB will facilitate further clinical investigations with this tracer. [$^{18}$F]FE@SUPPY:2 was prepared successfully and in a feasible and reliable manner. Preclinical evaluations of the two novel [$^{18}$F]labelled ligands for the A3R were conducted and the evinced parameters allowed a first estimate upon their suitability as A3R PET-tracers. [$^{18}$F]FE@CIT was successfully evaluated in terms of metabolic stability against CES and autoradiographic distribution on rat brain slices.

*Future implementations and investigations*

[$^{11}$C]DASB will be rapidly prepared according to the presented method in the first manuscript, and is currently used for neuroimaging of the 5-HTT in scientific and clinical psychiatric trials with special interest in e.g. patients with attention-deficit hyperactivity disorder (ADHD) and serotonin transporter changes in steroid hormone treatment (e.g. high-level long-term administration of opposite sex steroid hormones in transsexuals).

Regarding the results of the manuscripts 2-4, [$^{18}$F]FE@SUPPY and [$^{18}$F]FE@SUPPY:2 served as PET-tracers for the A3R and revealed valuable results for ongoing in-vitro studies concerning the visualization and quantification of the A3R. From the present point of view, a clinical application of these two PET-tracers in humans cannot be seen. However, results are only evinced from rodents and due to the large interspecies differences of the A3R (especially between human and rats), there is a lot left to discover in e.g. post mortem human tissue slices or other humanized models.

Future emphasis will be on the reduction of the high lipophilicity of our title compounds: more hydrophilic structural analogues, [$^{18}$F]FE@SUPPY:11 and [$^{18}$F]FE@SUPPY:21, are at the present in radiochemical preparation and will come into the preclinical evaluation process as soon as possible. Simultaneously we are working on improvements of the radiosyntheses via microfluidics and on improvements of the autoradiographic and micro-PET experiments.

Based on the results of the fifth paper, we aim for the future diagnostic application of [$^{18}$F]FE@CIT in humans with neurological and psychiatric diseases caused by changes in the dopaminergic system (e.g. Parkinson's disease, depression, drug abuse). The broad field of application of this tracer and its excellent DAT over SERT selectivity will provide an essential benefit for patients and medical research focused on drug development in this field.

# PART 4

# APPENDIX

# 4. APPENDIX

## 4.1. CURRICULUM VITAE

**Mag. pharm. Daniela Häusler**

**Personal Information**

*Nationality:* Austria

*Date & Place of Birth:* 04.12.1982, Vienna

*Email:* daniela.haeusler@meduniwien.ac.at

**Education**

| | |
|---|---|
| *2006-2010* | PhD-thesis, University of Vienna & Medical University of Vienna |
| *2000-2006* | Study of Pharmacy at the University of Vienna; passed with distinction |
| *1992-2000* | High School "Realgymnasium Perchtoldsdorf", diploma passed with distinction |
| *1988-1992* | Elementary School, Vienna |

**Internships and professional experience**

| | |
|---|---|
| *2009* | tutor for "Pharmazeutisches Grundpraktikum" at the Department of Pharmaceutical Technology and Biopharmaceutics, Vienna |
| *2007* | Introductory Course in Laboratory Animal Science, Veterinary Medicine of Vienna |
| | Practical training at the Institute of Brain Research, University of Vienna |
| *2003* | Clinical traineeship in acupuncture at the Chinese-Japan Friendship Hospital, Beijing, China |
| *2001-2005* | Practical training at the Pharmacy "Birkenapotheke", Vienna |
| *1998-2006* | Sports trainer at the "Sport Union Perchtodsdorf" and "VHS Liesing" |

**Scholarship**

| | |
|---|---|
| *2007-2009* | DOC-fFORTE, Austrian Academy of Sciences |

**Award**

*2009*        4th THP award of the Austrian Society of Nuclear Medicine and Molecular Imaging for Basic Sciences in the field of nuclear medicine

**Memberships**

European Association of Nuclear Medicine (EANM)

Österreichische Gesellschaft für Nuklearmedizin (OGN)

**Practical supervision of diploma theses:**

Practical supervision of the diploma thesis of Ms. Hoda El Samahi for the study project "Biopharmazeutische Aspekte bei der Evaluierung von FE@SUPPY", of the diploma thesis of Ms. Stefanie Pupeter for the study project "Zell-Bindungsstudien zur präklinischen Evaluierung von PET-Tracern am Beispiel des Adenosin A3 Rezeptor Liganden $^{18}$F-FE@SUPPY"and of the diploma thesis of Ms. Elisabeth Szerencsics for the study project "Präklinische Evaluierungen von [$^{18}$F]FE@SUPPY and [$^{18}$F]FE@SUPPY:2 anhand von Autoradiographien".

**Personal Interests**

Kundalini-Yoga, Dancing, Swimming, Rock climbing, Sailing, Kayaking, Skiing

**Scientific publications**

*Peer reviewed research articles:*

**D. Haeusler,** L.Nics, L.-K. Mien, J. Ungersboeck, R. R. Lanzenberger, K.Shanab, K. M. Sindelar, H. Viernstein, K.-H.Wagner, R. Dudczak, K.Kletter, W.Wadsak, M.Mitterhauser. [$^{18}$F] FE@SUPPY and [$^{18}$F]FE@SUPPY:2 - Metabolic considerations. *Nucl Med Biol* **2010,** in press

**D. Haeusler**, M. Mitterhauser, L.-K. Mien, K. Shanab, R. R. Lanzenberger, E. Schirmer, J. Ungersboeck, L. Nics, H. Spreitzer, H. Viernstein, R. Dudczak, K. Kletter, W. Wadsak. Radiosynthesis of a novel potential adenosine A3 receptor ligand 5-ethyl 2,4-diethyl-3-((2-[$^{18}$F]fluoroethyl) sulfanylcarbonyl)-6-phenylpyridine-5-carboxylate ([$^{18}$F]FE@SUPPY:2). *Radiochim Acta* **2009**; 97: 753-758

**D. Haeusler**, L.-K. Mien, L. Nics, J. Ungersboeck, C. Philippe, R.R. Lanzenberger, K. Kletter, R. Dudczak, M. Mitterhauser, W. Wadsak. Simple and rapid preparation of [$^{11}$C]DASB with high quality and reliability for routine applications. *Appl Radiat Isot* **2009** Mar; 67: 1654-1660

M. Mitterhauser, **D. Haeusler**, L.-K. Mien, J. Ungersboeck, L. Nics, R. R. Lanzenberger, K. Sindelar, H. Viernstein, R. Dudczak, K. Kletter, H. Spreitzer, W. Wadsak. Automatisation and first evaluation of [$^{18}$F]FE@SUPPY:2, an alternative PET-Tracer for the Adenosine A$_3$ Receptor: A Comparison with [$^{18}$F]FE@SUPPY. *TO Nucl Med J* **2009** May;1: 15-23

D. E. Ettlinger, **D. Haeusler**, W. Wadsak, F. Girschele, K. M. Sindelar, L. K. Mien, J. Ungersböck, H. Viernstein, K. Kletter, R. Dudczak, M. Mitterhauser. Metabolism and Autoradiographic Evaluation of [$^{18}$F]FE@CIT: A Comparison with [$^{123}$I]ß-ⵍCIT and [$^{123}$I]FP-CIT. *Nucl Med Biol* **2008** May;35(4):475-9.

Wadsak W., Mien L. K., Shanab K., Weber K., Schmidt B., Sindelar K.M., Ettlinger D.E., **Haeusler D.**, Spreitzer H., Keppler B.K., Viernstein H., Dudczak R., Kletter K., Mitterhauser M. The radiosynthesis of the adenosine A3 receptor ligand 5-(2-[$^{18}$F]fluoroethyl) 2,4-diethyl-3-(ethylsulfanylcarbonyl)-6-phenylpyridine-5-carboxylate ([$^{18}$F]FE@SUPPY). *Radiochim Acta* **2008**;96:119-24.

W. Wadsak, L. K. Mien, K. Shanab, D. E. Ettlinger, **D. Haeusler**, K. Sindelar, R. R. Lanzenberger, H. Spreitzer, H. Viernstein, B. K. Keppler, R. Dudczak, K. Kletter, M. Mitterhauser. Preparation and first evaluation of [$^{18}$F]FE@SUPPY: a new PET-Tracer for the Adenosine A$_3$ Receptor. *Nucl Med Biol.* **2008** Jan;35(1):61-6

Toegel S., Wadsak W., Mien L.K., Viernstein H., Kluger R., Eidherr H., **Haeusler D.**, Kletter K., Dudczak R., Mitterhauser M. Preparation and pre-vivo evaluation of no-carrier-added, carrier-added and cross-complexed [$^{68}$Ga]-EDTMP formulations. *Eur. J. Pharm. Biopharm.* **2008** Feb;68(2):406-12

Wadsak W., Mien L.K., Ettlinger D.E., Eidherr H., **Haeusler D.**, Sindelar K.M., Keppler B.K., Dudczak R., Kletter K., Mitterhauser M. [$^{18}$F]Fluoroethylations: Different strategies for the rapid translation of [$^{11}$C]methylated Radiotracers. *Nucl Med Biol* **2007**;34:1019-28.

Wadsak W., Mien L.K., Ettlinger D. E., Lanzenberger R. R., **Haeusler D.**, Dudczak R., Kletter K., Mitterhauser M. Simple and fully automated preparation of [carbonyl-$^{11}$C]WAY-100635. *Radiochim Acta* **2007**; 95:417-422.

*Oral presentations :*

**D.Haeusler**, L.K.Mien, L.. Nics, J. Ungersboeck, W. Wadsak, C. Kuntner, T. Wanek, R. R. Lanzenberger, H. Viernstein, R. Dudczak, K. Kletter, M. Mitterhauser. The adenosine A3 receptor PET-tracers, [$^{18}$F]FE@SUPPY and [$^{18}$F]FE@SUPPY:2 –the story goes on! *Nuklearmedizin* **2009**; 48: 215-242, S. A142

**D. Haeusler**, L.K. Mien, L. Nics, J. Ungersboeck, W. Wadsak, F. Girschele, C. Kuntner, T. Wanek, R. R. Lanzenberger, H. Viernstein, R. Dudczak, K. Kletter, M. Mitterhauser. [$^{18}$F]FE@SUPPY – the first PET tracer for the Adenosine A$_3$ receptor. *Eur J Nucl Med* **2009,** in press

**D. Haeusler,** K.M. Sindelar, L-K. Mien, J. Ungersboeck, L. Nics, F. Girschele, C. Kuntner, T. Wanek, H. Viernstein, R. Duczak, K. Kletter, W. Wadsak, M. Mitterhauser. [$^{18}$F]FE@SUPPY:2 - *ex-vivo* Metaboliten. *Nuklearmedizin* **2008**; 47: 225-274, S. A152

**D. Haeusler**, W. Wadsak, L.K. Mien, D.E. Ettlinger, K.M. Sindelar, R.R. Lanzenberger, C. Kuntner, H. Viernstein, R. Dudczak, K. Kletter, M. Mitterhauser. In vivo and in vitro evaluation of [$^{18}$F]FE@SUPPY. *Nuklearmedizin* **2007**; 46:233-301, S. A148

# 4.2. REFERENCES

[1] Poulsen SA. Quinn RJ. Adenosine receptors: New opportunities for Future Drugs. **1998** *Bioorg Med Chem*.6:619-641.

[2] Müller CE., Scior T. Adenosine receptors and their modulators. **1993** *Pharma Acta Helv.* 68:77-111

[3] George SR. Twenty Questions. **2004** *Nature drug discovery*; 3:577-626.

[4] Morris AJ. Malbon CC. Physiological Regulation of G Protein-Linked Signaling. **1999** *Physiol. Rev;* 79:1373-1430.

[5] Armstrong JM. et al. Gene dose effect reveals no Gs-coupled A2A adenosine receptor reserve in murine T-lymphocytes: Studies of cells from A2A-receptor-gene-deficient mice. **2001** *Biochem J;* 354(Pt.1):123-130.

[6] http://phylogenomics.berkeley.edu/AnimalProteome/gpcr_banner.jpg (28.01.2010)

[7] Benarroch EE. Adenosine and its receptors: Multiple modulatory functions and potential therapeutic targets for neurologic disease. **2008** *Neurology;* 70:231-236.

[8] Fredholm BB. et al. Structure and function of adenosine receptors and their genes. **2000** *Arch Pharmacol;* 326:364-374.

[9] Klotz KN. Adenosine receptors and their ligands. **2000** *Arch Pharmacol;* 362:382-391.

[10] Zhao Z et al. Characterisation of the mouse A3 adenosine receptor gene: exon/intron organization and promotor activiy. **1999** *Genomics;* 57:152-155.

[11] Fredholm BB. et al. Nomenclature and classification of purinoceptors. **1994** *Pharmacol Rev;* 46:143-156.

[12] Fredholm BB. et al. Towards a revised nomenclature for P1 and P2 receptors. **1997** *Trends Pharmacol Sci;* 18:79-82.

[13] Fredholm B.B. et al. International Union of Pharmacology.XXV.Nomenclature and Classification of Adenosine Receptors. **2001** *Pharmacol Rev*; 53:527-552.

[14] Drury AN., Szent-Györgyi A. The physiological activity of adenine compounds with especial reference to their action upon the mammalian heart. **1929** *J Physiol*; 68:213-237.

[15] Sattin A., Rall TW. The effect of adenosine and adenine nucleotides on the cyclic adenosine 3`, 5`-phosphate content of guinea pig cerebral cortex slices. **1970** *Mol Pharmacol;* 6:13-23.

[16] Ralevic V, Burnstock G. Receptors for purines and pyrimidines. **1998** *Pharmacol Rev;* 50:413-492.

[17] Wilson CN., Mustafa SJ. Adenosine receptors in health and disease. Handbook of experimental Pharmacology 193. **2009** *Springer-Verlag Berlin Heidelberg; 1-24.*

[18] Fredholm BB. et al. Actions of caffeine in the brain with special reference to factors that contribute to its widespread use. **1999** *Pharm Rev;* 51:83-133.

[19] Mobbs C. Caffeine and the adenosine receptor: Genetics trumps pharmacology in understanding pharmacology. **2005** *Cellscience*; 2:1-6.

[20] Dunwiddie TV., Masino SA. The role and regulation of adenosine in the central nervous system. **2001** *Annu Rev Neurosci;* 24: 31-55.

[21] Cerqueira MD. Advances in pharmacologic agents imaging new A2A receptor agonists. **2006** *Curr Cardiol Rep;* 8:119-122.

[22] Jacobson KA., Gao ZG. Adenosine receptors as therapeutic targets. **2006** *Nature rev drug discovery;* 5: 247-264.

[23] Meyerhof W. et al. Molecular cloningof a novel putative G-protein coupled receptor expressed during rat spermiogenesis. **1991** *FEBS Lett;* 284:162-172.

[24] Linden J. et al. Molecular cloning and functional expression of a sheep A3 adenosine receptor with widespread tissue distribution. **1993** *Mol Pharmacol;* 44:524-532.

[25] Sajjadi FG., Firestein GS. cDNA cloning and sequence analysis of the human A3 adenosine receptor. **1993** *Biochim Biophys Acta;* 1179:105-107.

[26] Salvatore CA. et al. Molebular imaging and characterization of the human A3 adenosine receptor. **1993** *Proc Natl Acad Sci USA;* 90:10365-10369.

[27] Monitto CL. et al. Localization of the A3 adenosine receptor gene (ADORA3) to human chromosome 1p. **1995** *Genomics;* 26:637-638.

[28] Atkinson MR. et al. Cloning, characterisation and chromosomal assignment of the human adenosine A3 receptor (ADORA3) gene. **1997** *Neuroscience Research;* 29:73-79.

[29] www.ncbi.nlm.gov/nuccore/

NC_000001.10?from=112021939&to=112110628&strand=true&report=graph (28.01.2010)

[30] Gessi S. et al. Pharmacological and biochemical characterization of $A_3$ adenosine receptors in Jurkat T cells. **2001** *Br J Pharmacol*; 134:116-26.

[31] Merighi S. et al. Pharmacological and biochemical characterization of adenosine receptors in the human malignant melanoma A375. **2001** *Br J Pharmacol*; 134:1215-26.

[32] Suh BC. et al. Pharmacological characterization of adenosine receptors in PGT-beta mouse pineal gland tumour cells. **2001** *Br J Pharmacol*; 134:132-42.

[33] Gessi S. et al. $A_3$ adenosine receptors in human neutrophils and promyelocytic HL60 cells: a pharmacological and biochemical study. **2002** *Mol Pharmacol*; 61:415-24.

[34] Fishman P. et al. $A_3$ adenosine receptor as a target for cancer therapy. **2002** *Anticancer Drugs*; 13:1-8.

[35] Fishman P. et al. Targeting the $A_3$ adenosine receptor for cancer therapy: inhibition of prostate carcinoma cell growth by A3AR agonist. **2003** *Anticancer Res*; 23:2077-83.

[36] Christofi FL. et al. Differential gene expression of adenosine $A_1$, $A_{2A}$, $A_{2B}$, and $A_3$ receptors in the human enteric nervous system. **2001** *J Comp Neurol*; 439:46-64.

[37] Fishman P. et al. $A_3$ adenosine receptor as a target for cancer therapy. **2002** *Anticancer Drugs*; 13:1-8.

[38] Liang BT., Jacobson K. A. A Physiological role of the adenosine $A_3$ receptor: Sustained cardioprotection. **1998** *Proc Natl Acad Sci U.S.A.*; 95:6995-6999.

[39] von Lubitz DK.et al. Stimulation of adenosine $A_3$ receptors in cerebral ischemia. Neuronal death, recovery, or both? **1999** *Ann. N.Y. Acad. Sci.*; 890:93-106.

[40] Avila MY. et al. Knockout of $A_3$ adenosine receptors reduces mouse intraocular pressure. *Invest.* **2002** *Opthalmol. Visual Sci.*; 43:3021-3026.

[41] von Lubitz DK. et al. Right thing at a wrong time? Adenosine $A_3$ receptors and cerebroprotection in stroke. **2001** *Ann N Y Acad Sci.*; 939:85-96.

[42] Laudadio MA., Psarrapoulou. The $A_3$ receptor agonist 2-Cl-IB-MECA facilitates epileptiform discharges in the CA3 area of immature rat hippocampal slices. **2004** *Epilepsy Res*; 59:83-94.

[43] Lopes LV. et al. Adenosine A$_3$ receptors are located in neurons of the rat hippocampus. **2003** *Neuroreport.*; 26:1645-8.

[44] Okada M. et al. Effects of adenosine receptor subtypes on hippocampal extracellular serotonin level and serotonin reuptake activity. **1997** *J Neurochem;* 69:2581-8.

[45] Sawynok J. Adenosine receptor activation and nociception. **1998** *Eur J Pharmacol*; 347:1-11.

[46] Zhu CB. et al. Adenosine receptor, protein kinase G, and p38 mitogen-activated protein kinase-dependent up-regulation of serotonin transporters involves both transporter trafficking and activation. **2004** *Mol Pharmacol.*; 65:1462-74.

[47] Di Chiara G. Dopamine in the CNS II. Handbook of experimental pharmacology 154/II. **2002** *SpringerVerlag Berlin Heidelberg New York;* 135-150.

[48] Macek TA. et al. Protein kinase C and A3 adenosine receptor activation inhibit presynaptic metabotropic glutamate receptor (mGluR) function and uncouple mGluRs from GTP-binding proteins. **1998** *J Neurosci.*; 18:6138-46.

[49] Baraldi PG. et al. Adenosine receptor antagonists: Translating medicinal chemistry and pharmacology into clinical utility. **2008** *Chem Rev;* 108:238-263.

[50] Olah ME. et al. ^{125}I-4-Aminobenzyl-5´-N-methylcarboxamidoadenosine, a high affinity radioligand for the rat A$_3$ adenosine receptor. **1994** *Mol Pharmacol;* 45:978-982.

[51] Varani K. et al. [^{3}H]MRE 3008F20: A novel antaonist radioligand for the pharmacological and biochemcial characterisation of human A$_3$ adenosine receptors. **2000** *Mol Pharmacol;* 57:968-975.

[52] Li AH. et al. Synthesis, CoMFA analysis, and receptor docking of 3,5-diacyl-2, 4-dialkylpyridine derivatives as selective A$_3$ adenosine receptor antagonists. **1999** *J Med Chem;* 42:706-21.

[53] Wadsak W. et al. The radiosynthesis of the adenosine A3 receptor ligand 5-(2-[^{18}F]fluoroethyl)2,4-diethyl-3-(ethylsulfanylcarbonyl)-6-phenylpyridine-5-carboxylate ([^{18}F]FE@SUPPY). **2008** *Radiochim Acta*; 96:119-24.

[54] Wadsak W. et al. Preparation and first evaluation of [^{18}F]FE@SUPPY: a new PET-Tracer for the Adenosine A$_3$ Receptor. **2008** *Nucl Med Biol;* 35:61-6.

[55] Beuming T. et al. The binding sites for cocaine and dopamine in the dopamine overlap. **2008** *Nature Neuroscience;* 11:780–789.

[56] Shih MC. et al. Parkinson´s disease and dopamine transporter neuroimaging- a critical review. **2006** *Sao Paulo Med J;* 124: 168-75.

[57] Asanuma K. et al. Assessment of disease progression in parkinsonism. **2004** *J Neurol*; 251 Suppl 7:vII4-8.

[58] Brooks DJ. et al. Assessment of neuroimaging techniques as biomarkers of the progression of Parkinson's disease. **2003** *Exp Neurol*; 184 Suppl 1:S68-79.

[59] Pirker W. Correlation of dopamine transporter imaging with parkinsonian motor handicap: how close is it? **2003** *Mov Disord*; 18 Suppl 7:S43-51.

[60] Meyer JH. et al. Lower dopamine transporter binding potential in striatum during depression. **2001** *Neuroreport*; 12:4121-4125.

[61] Logan J. et al. Concentration and occupancy of dopamine transporters in cocaine abusers with [11C]cocaine and PET. **1997** *Synapse;* 27: 347-356.

[62] Piccini PP. Dopamine transporter: basic aspects and neuroimaging. **2003** *Mov Disord;* 18 Suppl 7:S3-8.

[63] Wilcox KM. et al. Self-administration of cocaine and the cocaine analog RTI-113: relationship to dopamine transporter occupancy determined by PET neuroimaging in rhesus monkeys. **2002** *Synapse;* 43:78-85.

[64] Fowler JS. et al. [$^{11}$C]Cocaine: PET studies of cocaine pharmacokinetics, dopamine transporter availability and dopamine transporter occupancy. **2001** *Nucl Med Biol;* 28:561-572.

[65] Tupala E. et al. Dopamine D$_2$ receptors and transporters in type 1 and 2 alcoholics measured with human whole hemisphere autoradiography. **2003** *Hum Brain Mapp*; 20:91-102.

[66] Volkow ND. et al. Mechanism of action of methylphenidate: insights from PET imaging studies. **2002** *J Atten Disord*; 6 Suppl 1:S31-43.

[67] Volkow ND. et al. Relationship between blockade of dopamine transporters by oral methylphenidate and the increases in extracellular dopamine: therapeutic implications. **2002** *Synapse*; 43:181-187.

[68] Learned-Coughlin SM. et al. In vivo activity of bupropion at the human dopamine transporter as measured by positron emission tomography. **2003** *Biol Psychiatry*; 54:800-805.

[69] Wilson AA. et al. [$^{18}$F]fluoroalkyl analogues of the potent 5-HT$_{1A}$ antagonist WAY 100635: Radiosyntheses and *in vivo* evaluation **1996** *Nucl Med Biol;* 23:487–490.

[70] Lundkvist C. et al. [$^{18}$F]β-CIT-FP is superior to [$^{11}$C]β-CIT-FP for quantitation of the dopamine transporter **1997** *Nucl Med Biol;* 24:621-627.

[71] Wilson AA. et al. Synthesis of two radiofluorinated cocaine analogues using distilled 2-[$^{18}$F]fluoroethyl bromide **1993** *Appl Radiat Isot*; 46:765-770.

[72] Gu X-H. et al. Synthesis and biological evaluation of a series of novel N- or O-fluoroalkyl derivatives of tropane: potential positron emission tomography (PET) imaging agents for the dopamine transporter. **2001** Bioorg Med Chem Lett; 11:3049-3053.

[73] Günther I. et al. [$^{125}$I]ß-CIT-FE and [$^{125}$I]ß-CIT-FP are superior to [$^{125}$I]ß-CIT for dopamine transporter visualization: autoradiographic evaluation in the human brain. **1997** *Nucl Med Biol;* 24:629-634.

[74] Kula NS. et al. [$^{3}$H]beta-CIT: a radioligand for dopamine transporters in rat brain tissue **1999** *Eur J Pharmacol*; 385:291-4.

[75] Lavalaye J. et al. **[**$^{123}$I]FP-CIT binding in rat brain after acute and sub-chronic administration of dopaminergic medication. **2000** *Eur J Nucl Med*; 27:346-349.

[76] Bergström KA. et al. The Metabolite Pattern of [$^{123}$I]ß-CIT Determined with a Gradient HPLC Method. **1995** *Nucl Med Biol*; 22:971-976.

[77] Chaly T. et al. Radiosynthesis of [$^{18}$F] N-3-Fluoropropyl-2-ß-Carbomethoxy-3-ß-(4-Iodophenyl) Nortropane and the First Human Study with Positron Emission Tomography. **1996** Nucl Med Biol; 23:999-1004.

[78] Coenen HH. et al. N.c.a. radiosynthesis of [$^{123,124}$I]ß-CIT, plasma analysis and pharmacokinetic studies with SPECT and PET. **1995** *Nucl Med Biol*; 22:977-984.

[79] Mitterhauser M. et al. In vivo and in vitro evaluation of [$^{18}$F]FETO with respect to the adrenocortical and GABAergic system in rats. **2003** *Eur J Nucl Med Mol Imaging*; 30:1398-1401.

[80] Mitterhauser M. et al. Biological evaluation of 2´-[$^{18}$F]fluoro flumazenil ([$^{18}$F]FFMZ), a potential GABA receptor ligand for PET. **2004** *Nucl Med Biol*; 31:291-295.

[81] Mitterhauser M. et al. Synthesis and Biodistribution of [$^{18}$F]FE@CIT, a new potential tracer for the Dopamine Transporter. **2005** *Synapse*, 55:73-79.

[82] Emond P. et al. PE2I: a radiopharmaceutical for in vivo exploration of the dopamine transporter. **2008** *CNS Neurosci Ther;* 14:47-64.

[83] Shih MC. et al. Parkinson´s desease and dopamine transporter neuroimaging- a critical review. **2006** *Sao Paulo Med J;* 124:168-75.

[84] Pavese N., Brooks DJ. Imaging neurodegeneration in Parkinson´s disease. **2009** *Biochim Biophys Acta;* 1972:722-729.

[85] De Bruyne S. et al. Synthesis, radiosynthesis and in vivo evaluation of [$^{123}$I]-4-(2-(bis(4-fluorophenyl)methoxy)ethyl)-1-(4-iodobenzyl)piperidine as a selective tracer for imaging the dopamine transporter. **2009** *J Labelled Comp Radiopharm;* 52:304-311.

[86] Frazer A., Hensler JG. "Chapter 13: Serotonin Receptors". From: Siegel GJ et al (eds) Basic Neurochemistry: Molecular, Cellular, and Medical Aspects. **1999** Philadelphia: Lippincott-Raven. pp. 263–292.

[87] Murphy DL., Lesch K-P. Targeting the murine serotonin transporter: insights into human neurobiology. **2008** *Nature Review Neuroscience*; 9:85-96.

[88] Akimova E. et al. The serotonin-1A receptor in anxiety disorders. **2009** *Biol Psychiatry*;66(7):627-635.

[89] Hurlemann R. et al. 5-HT2A receptor density is decreased in the at-risk mental state. **2008** *Psychopharmacology*;195(4):579-590.

[90] Joyce J N. et al. Serotonin uptake sites and serotonin receptors are altered in the limbic system of schizophrenics. **1993** *Neuropsychopharmacol;* 4:315-36.

[91] Ichimiya T. et al. Serotonin transporter binding in patients with mood disorders: a PET study with [$^{11}$C](+)McN5652. **2002** *Biol Psychiatry;* 9:715-22.

[92] Owens MJ. et al. Role of serotonin in the pathophysiology of depression: focus on the serotonin transporter. **1994** *Clin Chem;* 2:288-95.

[93] Meyer J H. et al. Occupancy of serotonin transporters by paroxetine and citalopram during treatment of depression: a [$^{11}$C]DASB PET imaging study. **2001** *Am J Psychiatry;* 11: 1843-9.

[94] Reivich M. et al. PET brain imaging with [$^{11}$C](+)McN5652 shows increased serotonin transporter availability in major depression. **2004** *J Affect Disord;* 2: 321-7.

[95] Meyer JH. et al. Brain serotonin transporter binding potential measured with carbon 11-labeled DASB positron emission tomography: effects of major depressive episodes and severity of dysfunctional attitudes. **2004** *Arch Gen Psychiatry*; 12:1271-9.

[96] Parsey RV. et al. Lower serotonin transporter binding potential in the human brain during major depressive episodes. **2006** *Am J Psychiatry;* 1:52-8.

[97] Jarret ME. et al. Relationship of SERT polymorphisms to depressive and anxiety symtoms in irritable bowel syndrome. **2007** *Biol Res Nurs;* 2:161-9.

[98] Suehiro M. et al. A PET radiotracer for studying serotonin uptake sites: carbon-11-McN-5652Z. **1993** *J Nucl Med;* 1:120-7.

[99] Wilson A A. et al. Novel radiotracers for imaging the serotonin transporter by positron emission tomography: synthesis, radiosynthesis, and in vitro and ex vivo evaluation of (11)C-labeled 2-(phenylthio)araalkylamines. **2000** *J Med Chem;* 16:3103-10.

[100] Tarkiainen J. et al. Carbon-11 labelling of MADAM in two different positions: a highly selective PET radioligand for the serotonin transporter. **2001** *J Labelled Cpd Radiopharm;* 44:113–120.

[101] Solbach C. et al. Determination of reaction parameters for the synthesis of the serotonin transporter ligand [$^{11}$C]DASB: Application to a remotely controlled high yield synthesis. **2004** *Radiochim Acta*;92: 341-344.

[102] Meyer JH. et al. Brain serotonin transporter binding potential measured with carbon 11-labeled DASB positron emission tomography: effects of major depressive episodes and severity of dysfunctional attitudes. **2004** *Arch Gen Psychiatry;* 12:1271-9.

[103] Meyer JH. et al. Serotonin transporter occupancy of five selective serotonin reuptake inhibitors at different doses: an [$^{11}$C]DASB positron emission tomography study. **2004** *Am J Psychiatry;* 5:826-35.

[104] Meyer JH. et al. Occupancy of serotonin transporters by paroxetine and citalopram during treatment of depression: a [$^{11}$C]DASB PET imaging study. **2001** *Am J Psychiatry;* 11:1843-9.

[105] Parsey RV. et al. Metabolite considerations in the in vivo quantification of serotonin transporters using 11C-DASB and PET in humans. **2006** *J Nucl Med;* 11:1796-802.

[106] Parsey RV. et al. Lower serotonin transporter binding potential in the human brain during major depressive episodes. **2006** *Am J Psychiatry;* 1:52-8.

[107] Schonbachler R. et al. Synthesis and 11C-Radiolabelling of a Tropane Derivative Lacking the 2beta-Ester Group: a Potential PET Tracer for the Dopamine Transporter. **1999** *J Labelled* Cpd Radiopharm; 42:447-456

[108] Larsen P. et al. Synthesis of [$^{11}$C]iodomethane by iodination of [$^{11}$C]methane. **1997** *Appl Radiat Isot;* 48:153-157.

[109] van Dort ME, Tluczek L. Synthesis and carbon-11 labeling of the stereoisomers of *meta*-hydroxyephedrine (HED) and *meta*-hydroxypseudoephedrine (HPED) **2000** *J Label Cpd Radiopharm;* 43(6): 603-612.

[110] Langer O, Gulyás B. et al. Radiochemical labelling *of* the dopamine D3 receptor ligand RGH-1756. **2000** *J Label Cpd Radiopharm;* 43:1069 - 1074.

[111] Coenen HH.et al. Preparation of N.C.A. [$^{18}$F]-CH$_2$BrF via aminopolyether supported nucleophilic substitution. **1986** *J Label Compd Radiopharm;* 23:587.

[112] Bergman J. et al. Automated synthesis and purification of [$^{18}$F]bromofluoromethane at high specific radioactivity **2001** *Appl Rad Isot;* 54: 927-933.

[113] Zheng L, Berridge MS. Synthesis of [$^{18}$F]fluoromethyl iodide, a synthetic precursor for fluoromethylation of radiopharmaceuticals **2000** *Appl Rad Isot;* 52:55-61.

[114] Elsinga PH. et al. Synthesis and evaluation of [$^{18}$F]fluoroethyl SA4503 and SA5845 as PET ligands for the sigma receptor. **2001** *J Label Compd Radiopharm*; 44:S4 (poster session).

[115] Block D. et al. N.c.a. 18F-fluoroacylation via fluorocarboxylic acid esters. **1987**(1988) *J Label Compd Radiopharm;* 25:185–200.

[116] Skaddan MB.et al. Synthesis, [18F]labelling, and biological evaluation of piperidyl and pyrrolidyl benzylates as in vivo ligands for muscarinic acetylcholine receptors. **2000** *J Med Chem;* 43: 4552-62.

[117] Oh SJ.et al. Re-evaluation of 3-bromopropyltriflate as the precursor in the preparation of 3-[18F]fluoropropylbromide. **1999** *Appl Rad Isot;* 51:293-97.

[118] Lundkvist C. et al. [18F]beta-CIT-FP is superior to [11C]beta-CIT-FP for quantitation of the dopamine transporter. **1997** *Nucl Med Biol;* 24:621-7.

[119] Chesis PL, Welsh MJ. Comparison of bromo- and iodoalkytriflates for 18F-labelling of amines. **1990** *Appl Rad Isot;* 41: 259-265.

[120] S. Zijlstra, T.J. de Groot, L.P. Kok, G.M. Visser and W. Vaalburg, *N*-[18F]-Fluoroalkylation of noraporphines: microwave versus thermal treatment, *Eur J Morphol* **33** (1995), pp. 154–157

[121] de Groot TJ. et al. 1-[18F]Fluoro-2-propanol-*p*-toluenesulfonate: a synthon for the preparation of *N*-([18F]fluoroisopropyl)amines **. 1992** *Appl Rad Isot*; 43:1335-1339.

[122] Goodman MM. et al. 18F-labeled FECNT: a selective radioligand for PET imaging of brain dopamine transporters **2000** *Nucl Med Biol*; 27:1-12.

[123] Gründer G. et al. [18F]Fluoroflumazenil: a novel tracer for PET imaging of human benzodiazepine receptors. **2001** *Eur J Nucl Med*; 28:1463-1470.

[124] Satyamurthy N. et al. (2′-[18F]fluoroethyl)spiperone, a potent dopamine antagonist: Synthesis, structural analysis and in-vivo utilization in humans. **1990** *Appl Radiat Isot;* 41:113-129.

[125] Satyamurthy N. et al. No-carrier-added 3-(2′-[18F]fluoroethyl)spiperone, a new dopamine receptor-binding tracer for positron emission tomography **1986** *Nucl Med Biol;* 13:617-624

[126] Chi DY. et al. Synthesis of no-carrier-added N-([18F]fluoroalkyl)spiperone derivatives. **1986** *Int J Rad Appl Instr Part A*; 37:1173-1180.

[127] Zijlstra S. et al. Synthesis and in vivo distribution in the rat of several fluorine-18 labelled N-fluoroalkylaporphines. **1993** *Appl Radiat Isot;* 44:651-658.

[128] Wester HJ. et al. 6-O-(2-[18F]Fluoroethyl)-6-O-Desmethyldiprenorphine ([18F]DPN): Synthesis, biologic evaluation, and comparison with [11C]DPN in humans. **2000** *J Nucl Med;* 41:1279-1286.

[129] Hamacher K, Coenen HH. Efficient routine production of the 18F-labelled amino acid O-(2-[18F]fluoroethyl)-L-tyrosine. **2002** *Appl Radiat Isot;* 57:853-856.

[130] Suehiro M. et al. Radiosynthesis and biodistribution of the S-[18F]fluoroethyl analog of McN5652. **1996** *Nucl Med Biol*; 23:407-412.

[131] Tang G. et al. Pharmacokinetics and radiation dosimetry estimation of O-(2-[18F]fluoroethyl)-L-tyrosine as oncologic PET tracer. **2003** *Appl Radiat Isot;* 58: 219-225.

[132] Chin FT. et al. Syntheses and applications of three 18F-fluoroalkylating agents in a commercial automated radiosynthesis apparatus **2003** *J Label Compd Radiopharm*; 46:S172.

[133] Skaddan MB.et al. Synthesis, [18F]labelling, and biological evaluation of piperidyl and pyrrolidyl benzylates as in vivo ligands for muscarinic acetylcholine receptors. **2000** *J Med Chem;* 43:4552-62.

[134] Zhang MR. et al. How to increase the reactivity of [$^{18}$F]fluoroethylbromide: [$^{18}$F]fluoroethylation of amine, phenol and amide functional groups with [$^{18}$F]FEtBr, [18F]FEtBr/NaI and [$^{18}$F]FetOTf. **2003** *J Label Comp Radiopharm;* 46: 587-598.

[135] Schirrmacher R. et al. Syntheses of novel N-([$^{18}$F]fluoroalkyl)-N-nitroso-4-methyl-benzenesulfonamides and decomposition studies of corresponding 19F-and bromo-analogues: potential new compounds for the 18F-labelling of radiopharmaceuticals. **2003** *J Label Compd Radiopharm;* 46: 959-977.

[136] Lu SY. et al. Efficient O- and N-(fluoroethylations) with NCA [$^{18}$F]fluoroethyl tosylate under microwave-enhanced conditions. **2004** *J Label Compd Radiopharm;* 47: 289-297.

[137] Comagic S. et al. Efficient synthesis of 2-bromo-1-[18F]fluoroethane and its application in the automated preparation of 18F-fluoroethylated compounds. **2002** *Appl Radiat Isot;* 56: 847-851.

[138] Zhang MR. et al. Development of an automated system for synthesizing 18F-labelled compounds using [18F]fluoroethylbromide as a synthetic precursor. **2002** *Appl Radiat Isot;* 57:335-342.

[139] Wadsak w. et al. [$^{18}$F]-fluoroethylations: different strategies for the rapid translation of $^{11}$C-methylated radiotracers. **2007** *Nucl Med Biol;* 34:1019-1028.

[140] http://www.abx.de/ (ABX Radeberg, Germany)

[141] Shanab K. et al. Synthesis of in vivo metabolites of the new adenosine A3 receptor PET-radiotracer [$^{18}$F]FE@SUPPY. **2008** *Heterocycles;* 75:77-86.

[142] http://www.abx.de/ (ABX Radeberg, Germany)

[143] Wadsak W. et al. Radiosynthesis of the adenosine A$_3$ receptor ligand 5-(2-[$^{18}$F]fluoroethyl)2,4-diethyl-3-(ehtylsulfanylcarbonyl)-6-phenylpyridine-5-carboxylate ([$^{18}$F]FE@SUPPY). **2008** *Radiochim. Acta;* 96:119-24 .

[144] Radiopharmaceutical Preparations (Radiopharmaceutica, 5.0/0125). In: European Pharmacopoeia (Europäisches Arzneibuch). 5th edition (5. Ausgabe Grundwerk), official Austrian version. **2005b** *Vienna:Verlag Österreich GmbH*; p.823-831.

[145] Bergström M. et al. Autoradiography with Positron Emitting Isotopes in Postitron Emission Tomography Tracer Discovery. **2003** *Mol Imag Biol;* 3(6):390-396.

[146] Mitterhauser M. et al. Synthesis and biodistribution of [18F]FE@CIT, a potential tracer for the dopamine transporter. **2005** *Synapse;* 55:73-79

[147] Mitterhauser M. et al. In vivo and in vitro evaluation of [$^{18}$F]FETO with respect to the adrenocortical and GABAergic system in rats. 2003 Eur J Nuc Med Mol Imaging; 30:1398-1401.

[148] Pawelke B. Metabolite analysis in positron emission tomography studies: examples from food sciences. **2005** *Amino Acids;* 29:377-388.

[149] Ishiwata et al. Metabolite analysis of [$^{11}$C]flumazenil in human plasma: assessment as the standardized value for quantitative PET studies. **1998** *Ann Nucl Med*; 12:55-59.

[150] Picture taken from a presentation of Dr. M. Berger

[151] Pictures taken from a presentation of Dr. M. Berger

[152] Bruns RF. et al. Binding of the A1-selective adenosine antagonist 8-cyclopentyl-1,3-dipropylxanthine to rat brain membranes. **1987** *Arch Pharmacol;* 335(1):59-63.

[153] Toddle et al. Design, radiosynthesis, and biodistribution of a new potent and selective ligand for in vivo imaging of the adenosine A$_{2A}$ receptor system using positron emission tomography. **2000** *J Med Chem;* 43:4359.

[154] Kim Y-C. et al. Anilide derivatives o fan 8-Phenylxanthine carboxylic congener are highly potent and selective antagonists at human A$_{2B}$ adenosine receptors. **2000** *J Med Chem;* 43: 1165-1172.

[155] Kim H.O. et al. 2-Substitution of *N*$^6$-benzyladenosine-5´-uronamides enhances selectivity for A$_3$ adenosine receptors. **1994** *J Med Chem*; 37:3614–3621.

[156] Li AH. et al. Structure-activity relatonships and molecular modeling of 3,5-diacyl-2,4-dialkylpyridine derivatives as selective A3 adenosine receptor antagonists. **1998** *J Med Chem;* 41:3186-3201.

[157] Jiang JL. et al. 6-phenyl-1,4-dihydropyridine derivatives as potent and selective A3 adenosine receptor antagonists. **1996** *J Med Chem;* 39:4667-4675.

[158] Donovan SF, Pescatore MC. Method for measuring the logarithm of the octanol-water partition coefficient by using short octadecyl-poly(vinyl alcohol) high-performance liquid chromatography columns. **2002** *J Chromatogr A;* 952:47-61.

[159] Wilson CN., Mustafa SJ. Adenosine receptors in health and disease. Handbook of experimental Pharmacology 193. **2009** *Springer-Verlag Berlin Heidelberg;* 635.

[160] Picture thankfully received from Prof. Schubiger